Frontiers in Numerical Relativity

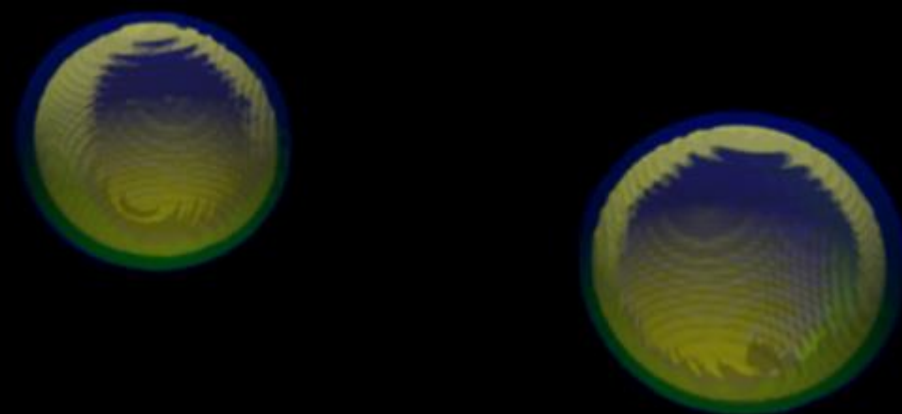

Kenta Kiuchi (AEI/YITP)

Max-Planck-Institut für Gravitationsphysik
Albert-Einstein-Institut

YITP
YUKAWA INSTITUTE FOR THEORETICAL PHYSICS

Outline

Part I

▶Introduction : What are gravitational waves ? What do(did) they tell us ?

Part II

▶ Frontiers in Numerical relativity simulations of binary neutron star mergers

Part III

▶ Frontiers in Numerical relativity simulations of black hole - neutron star binary mergers

Introduction before 2015

What are gravitational waves ?

Ripples of the spacetime predicted by Einstein almost 100 yr ago.

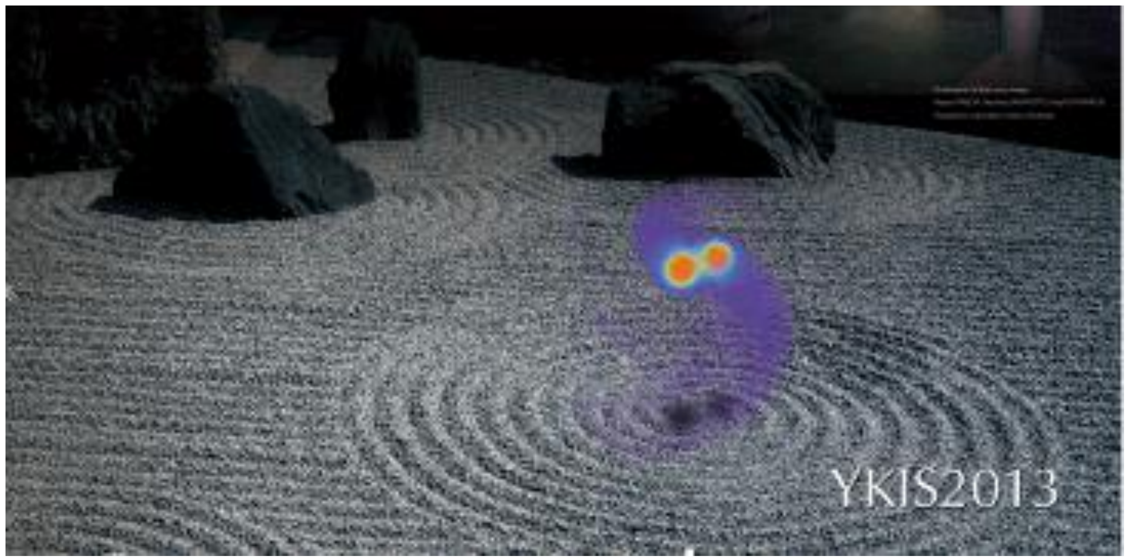

© YKIS2013 poster, the rock garden in a temple in Kyoto

They could see a region which is opaque for the EM signal.

Indirect evidence of GW

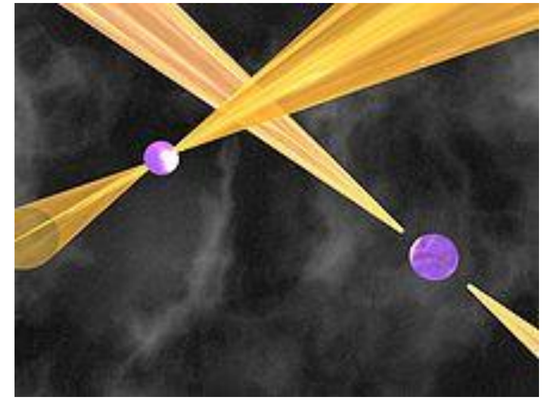

Image of the binary pulsar

Russell Alan Hulse 1950～ Joseph Hooton Taylor, Jr.、1941～

Hulse and Taylor have found the binary pulsar PSRB1913+16 in the Arecibo observatory in 1974.

⇒ The orbital period gets shorter in time.

It implies the energy is radiated from the system.

Indirect evidence of GW

GR predicts the GW with which the energy is carries away.

The shift of the orbital period of 1913+16

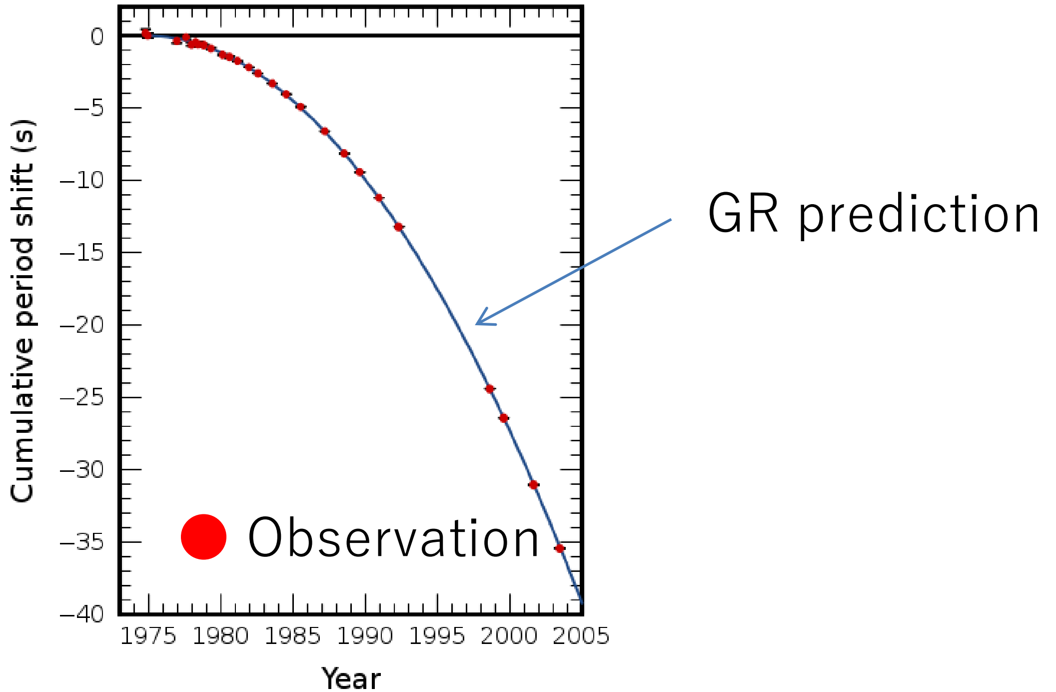

The GR prediction agrees with the observation within 1 %.
⇒ Hulse and Taylor have gotten the Nobel Prize in 1993.

Their work is recognized as the indirect evidence of GW.

Toward direct detections

$h_c \sim 10^{-22}$ ～Size of H atom / the distance from Earth to Sun

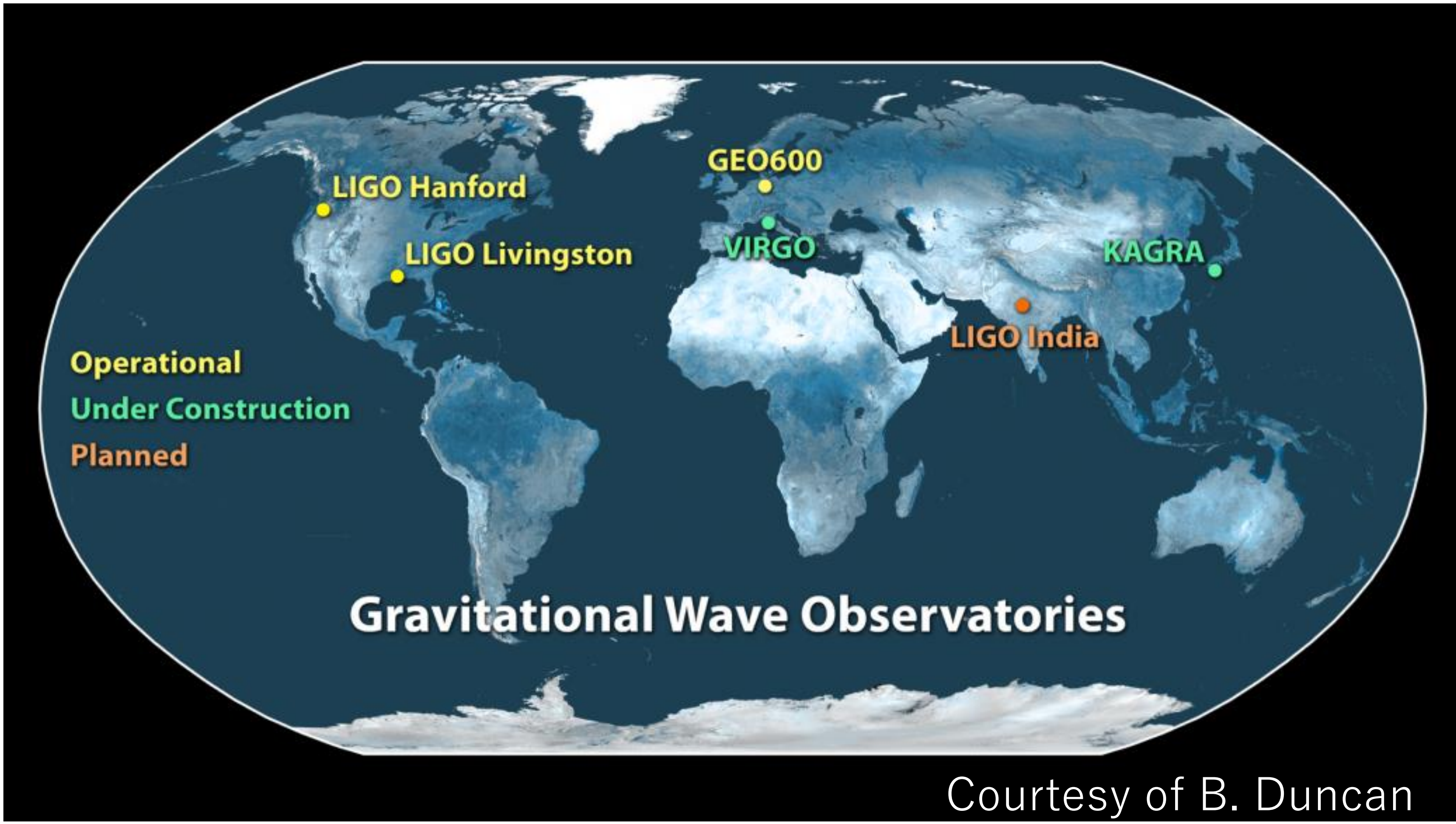

Introduction after 2015

The first direct observation was done!

GW150914 (Abbott et al. 16)

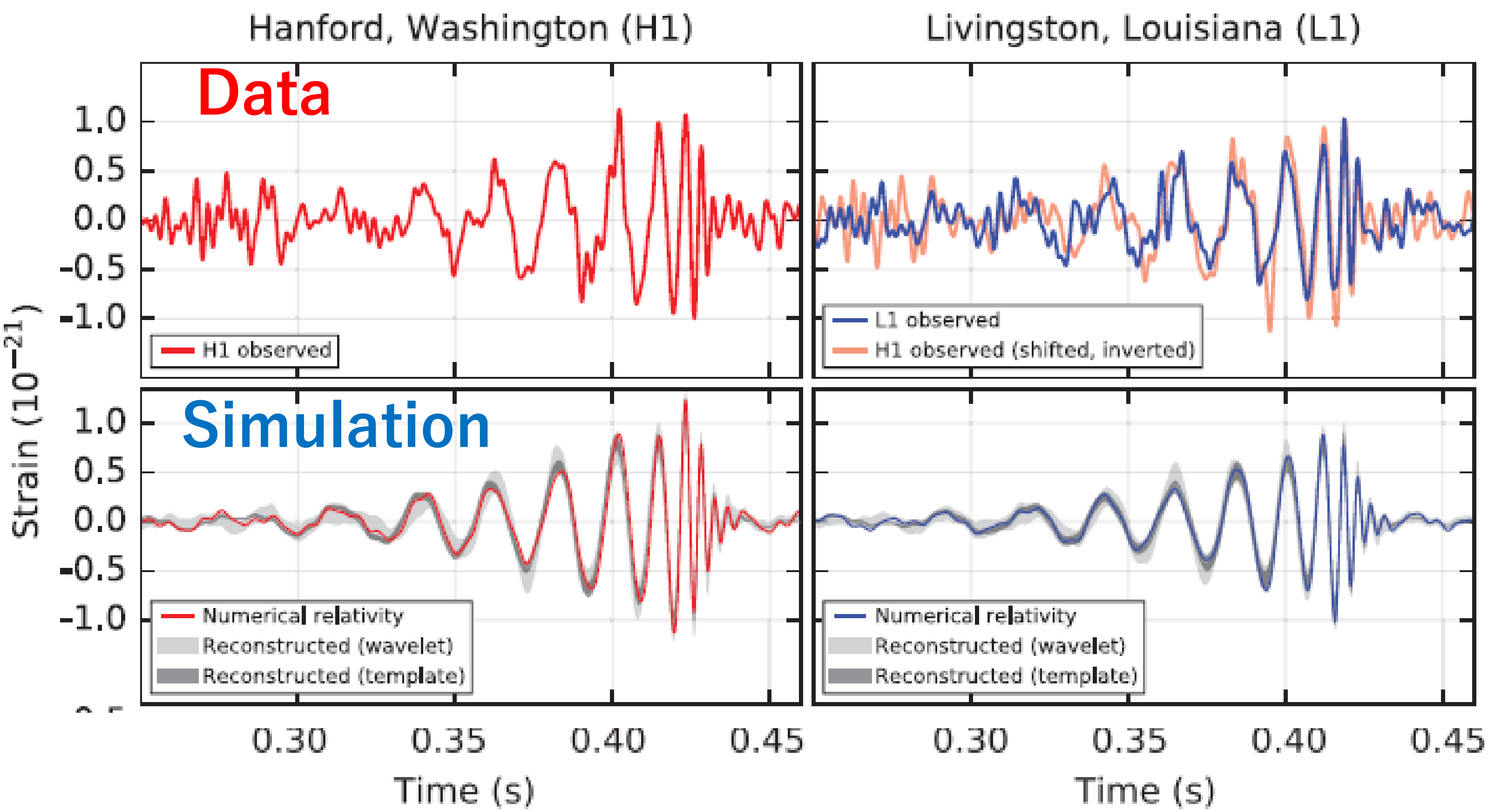

- Black hole-black hole binary of $36M_\odot$-$29M_\odot$
- Luminosity distance is $410^{+160}{}_{-180}$ Mpc
- Final object is the Kerr Black hole with $\chi=0.67$

The 2nd event

GW151226 (Abbott et al. 16)

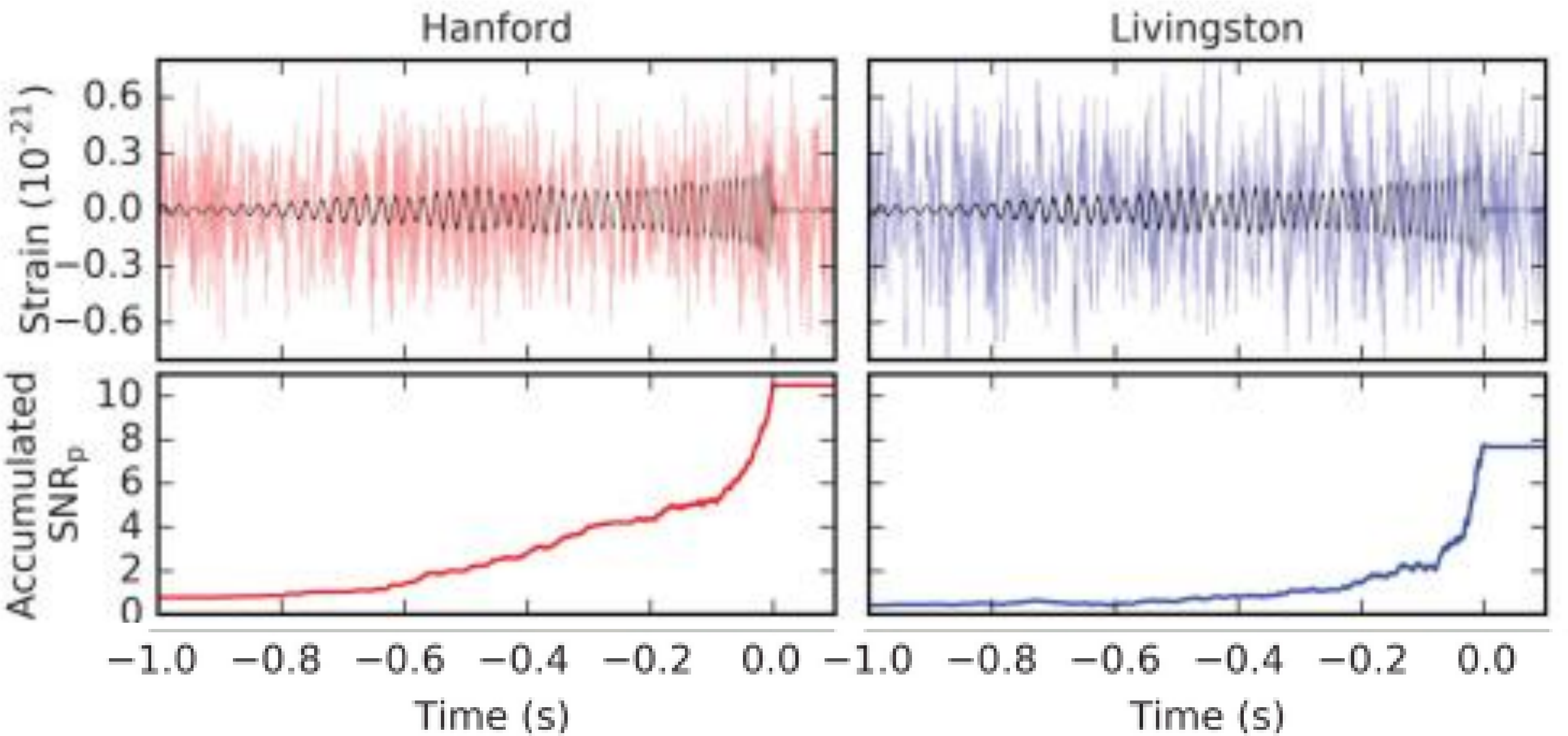

- ▶ Black hole-black hole binary of $14M_{\odot}$-$7M_{\odot}$
- ▶ Luminosity distance is 440^{+180}_{-190} Mpc
- ▶ Final object is the Kerr Black hole with $\chi = 0.74$

The 3rd event

GW170104 (Abbott et al. 17)

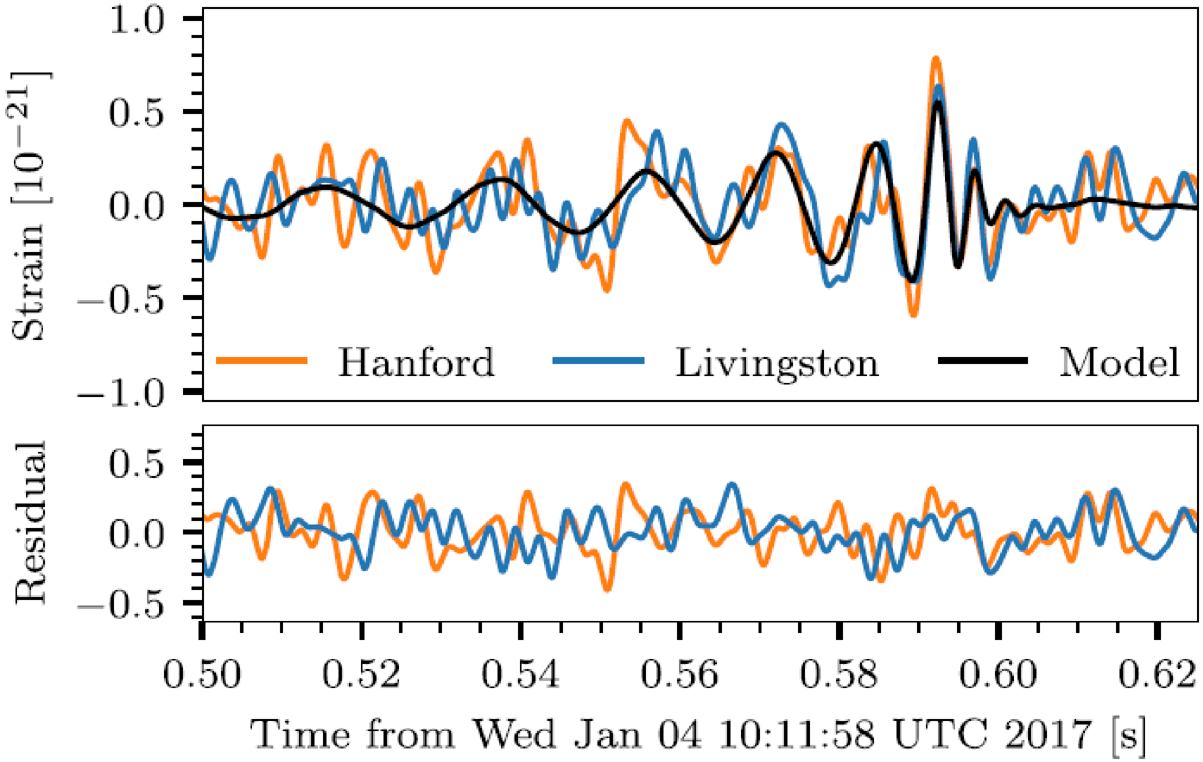

- ▶ Black hole-black hole binary of $31M_\odot$ - $19M_\odot$

The 4th event

GW170814 (Abbott et al. 17)

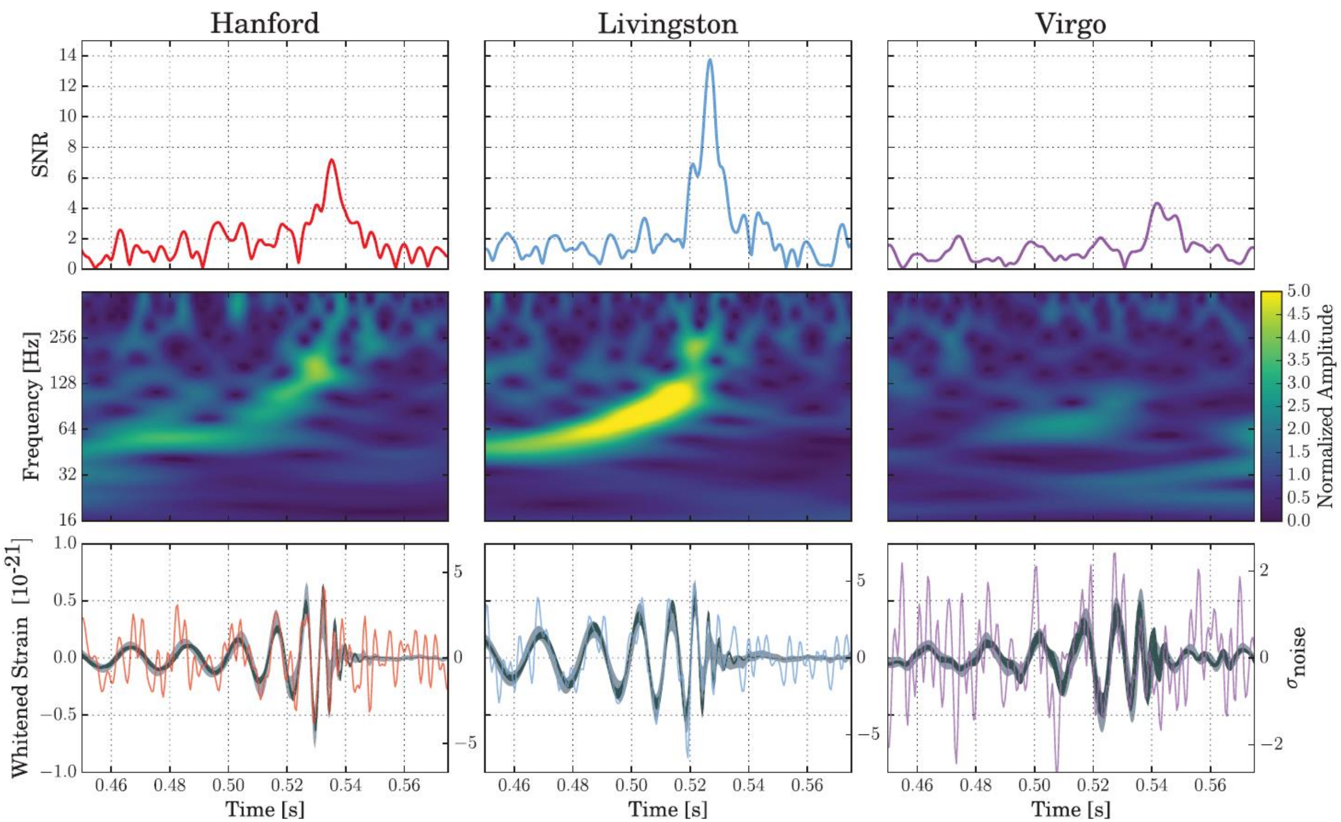

▶ Black hole-black hole binary of $31M_\odot$ - $25M_\odot$

▶ First detection done by three detectors.

Triangulation indeed works!

The 5th event

GW170608 (Abbott et al. 17)

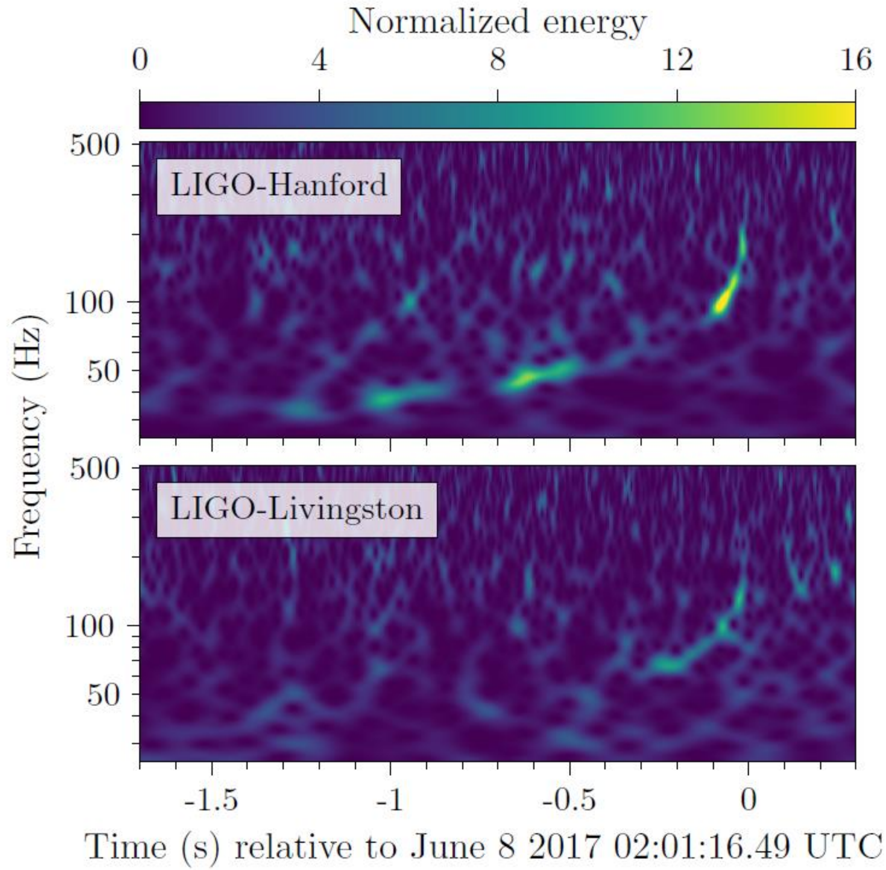

▶ Black hole-black hole binary of $12M_{\odot}$ - $7M_{\odot}$

Black Hole Binaries exist in the nature!

Multiple detections by LIGO+VIRGO

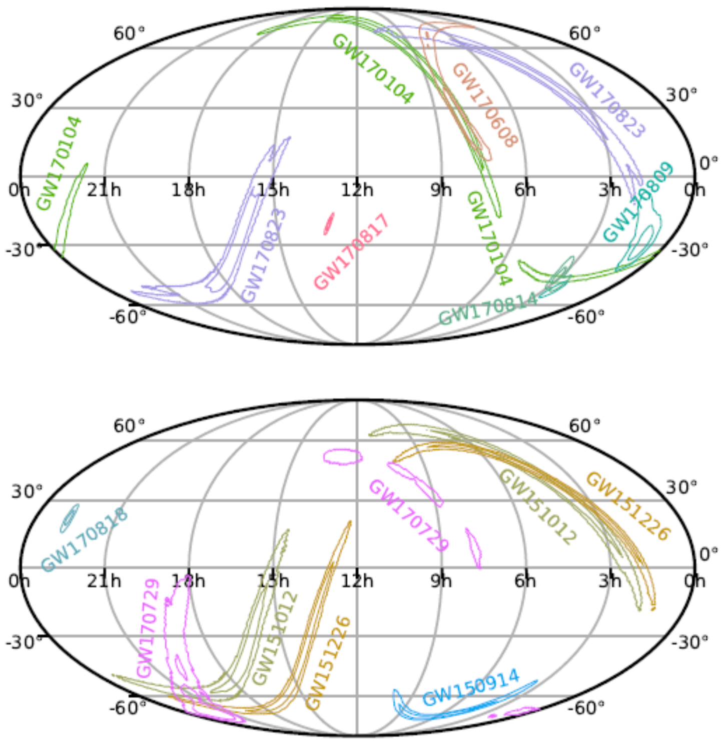

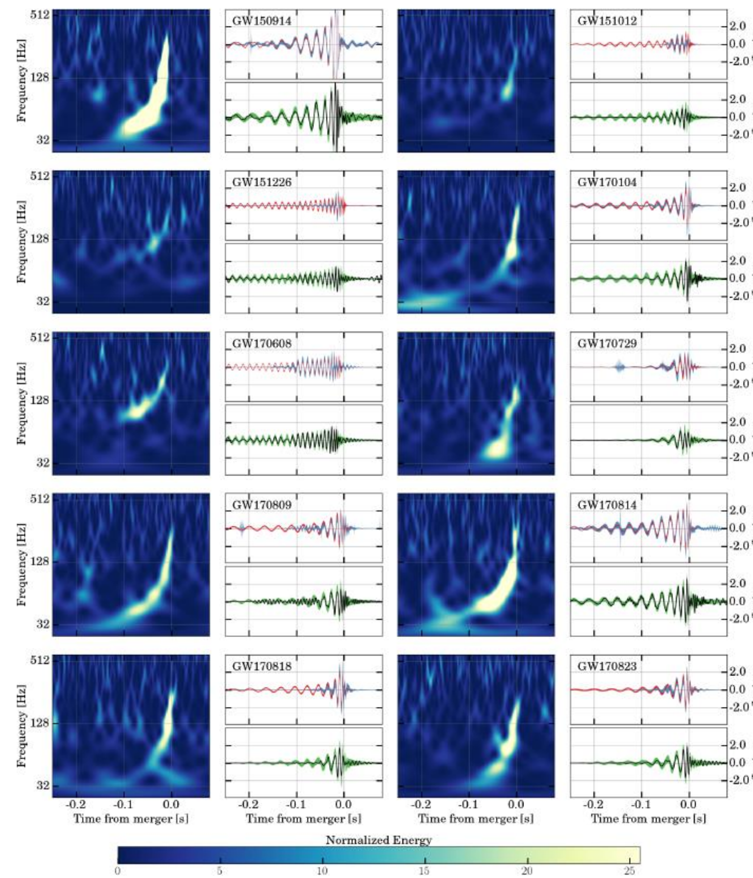

▶ 10 direct detections and one candidate: All the events are a BH-BH merger

▶ Event rate is 9.7-101 $Gpc^{-3}\ yr^{-1}$

The Nobel Prize in Physics 2017

GW170817 as a BNS merger event

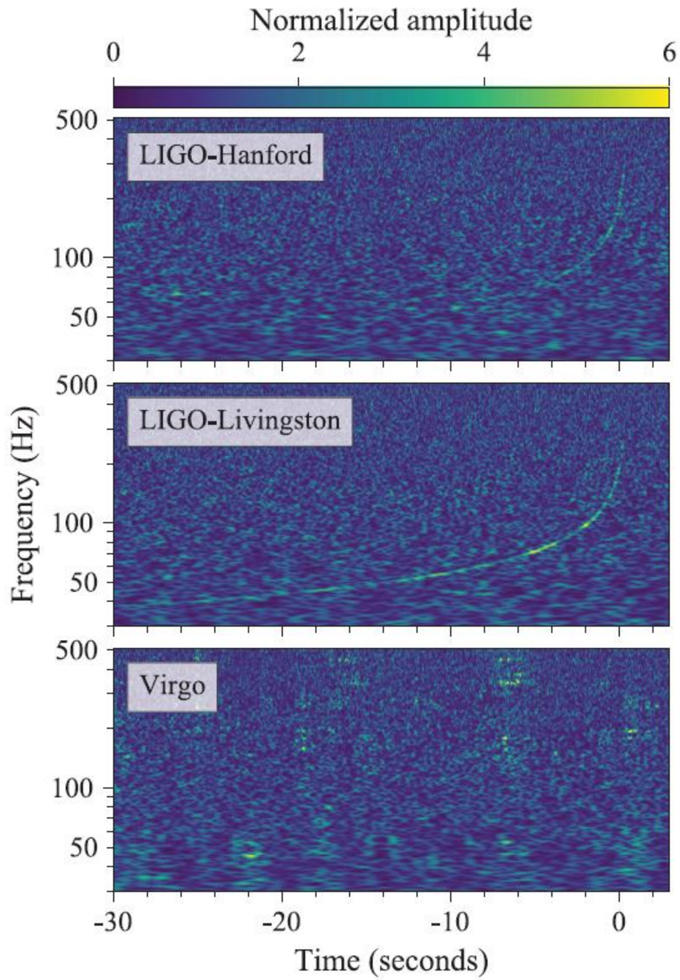

Sky map by LIGO + VIRGO

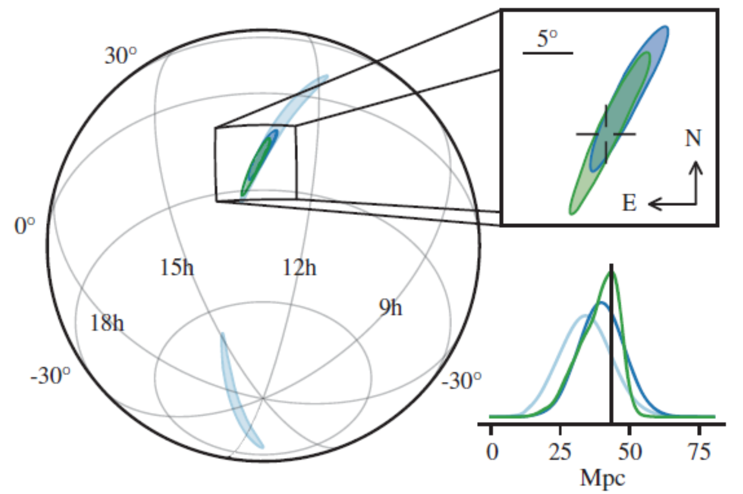

LSC-Virgo collaboration
PRL 2017

▶ Aug. 17th 2017, 74 sec. signals detected by LIGO-Hanford.
▶ S/N is 32.4 !

Real Multimessenger Astronomy Era

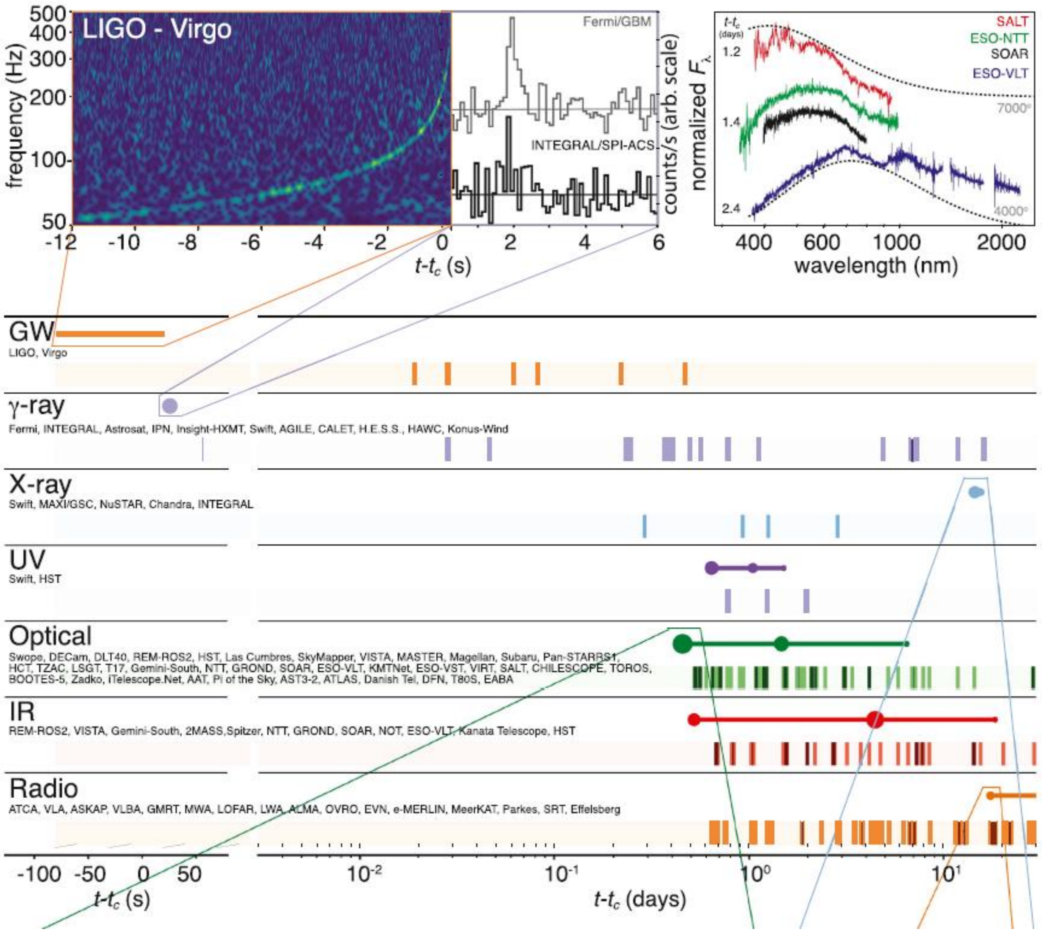

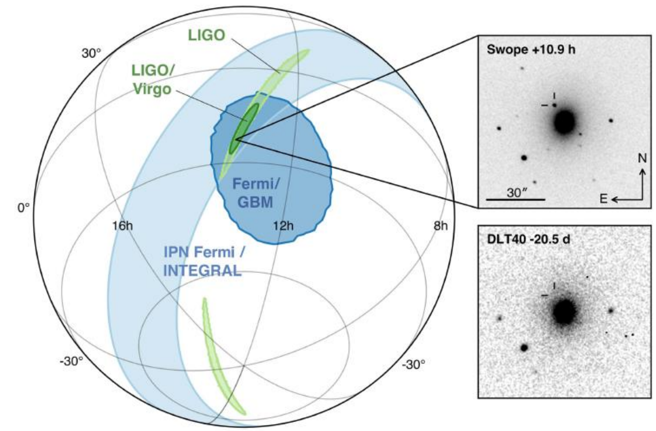

LSC-Virgo collaboration
APJ 848, L12, 2017

- GW ⇒ γ-ray ⇒ UV, Optical, IR ⇒ X-ray ⇒ Radio
- Host galaxy (NGC4993) was identified by the optical telescope (SSS17A)

Source properties of GW170817

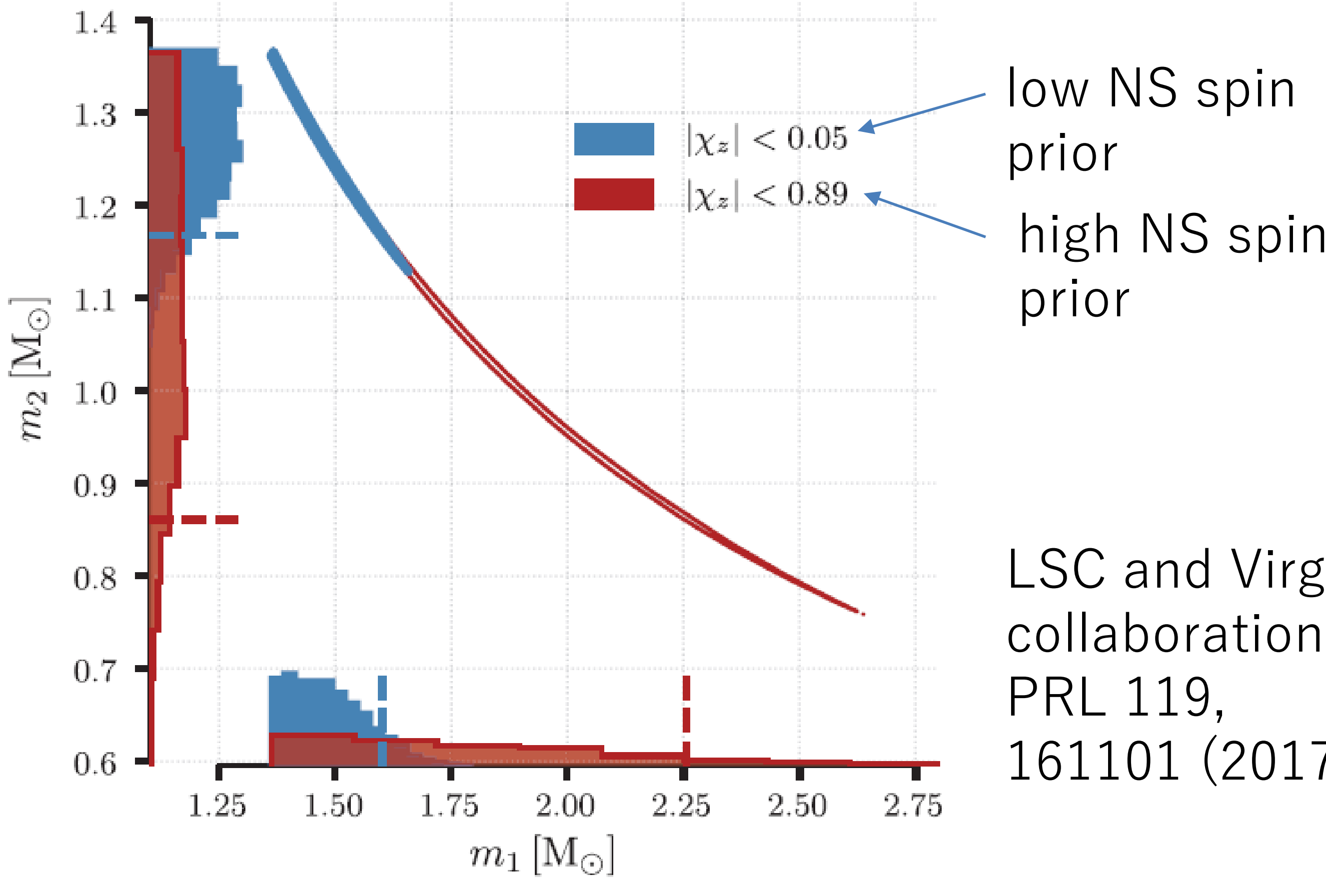

LSC and Virgo collaboration PRL 119, 161101 (2017)

- Mass measurement of NSs.

m_1: 1.36-1.60 $M_\odot$, m_2 : 1.17-1.36 $M_\odot$ (low spin prior)

m_1: 1.36-2.26 $M_\odot$, m_2 : 0.86-1.36 $M_\odot$ (high spin prior)

- Luminosity distance is 40^{+8}_{-14} Mpc

Tidal deformability measurement of NSs

LSC and Virgo collaboration PRL 119, 161101 (2017)

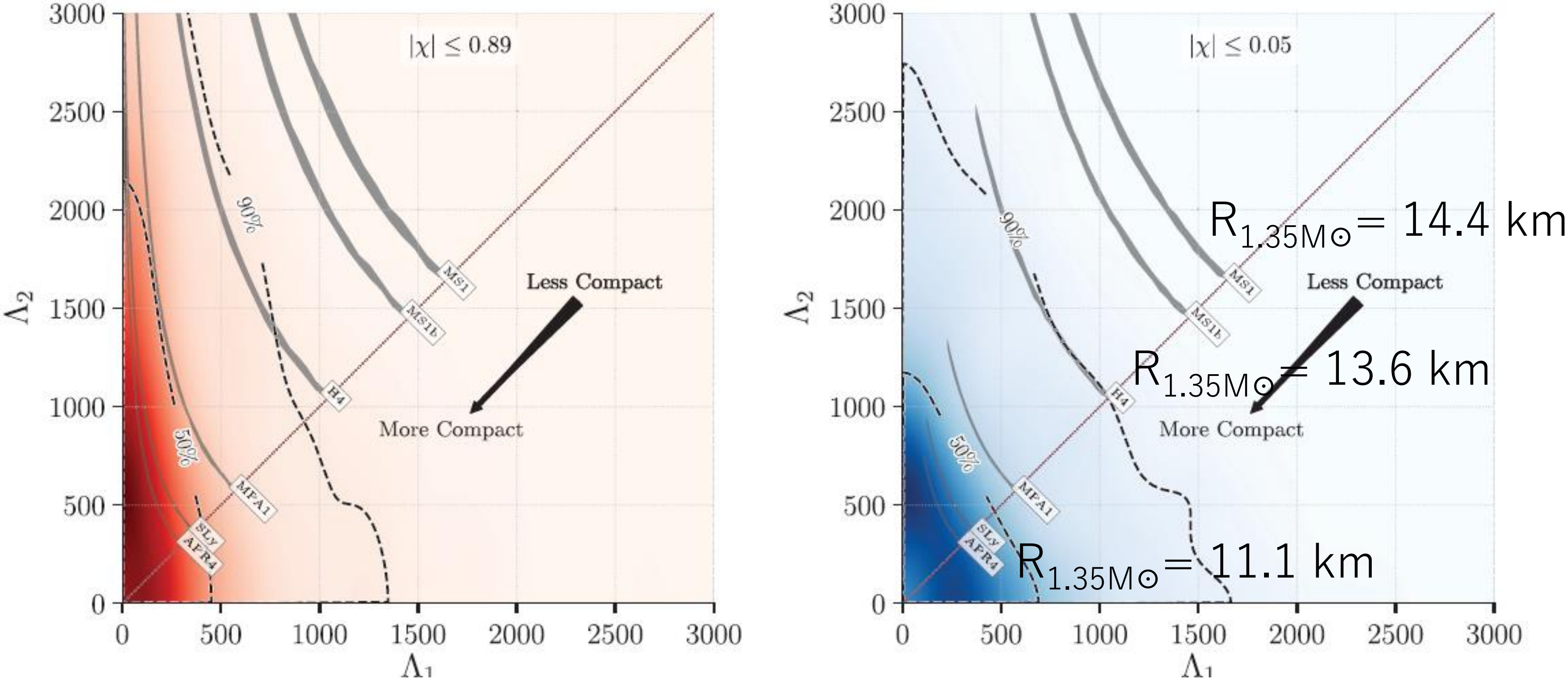

▶ Tidal deformation Λ is related to a NS radius ⇒ Information of the NS equation of state.

▶ Soft EOS is favored ($\Lambda \leq 800$)

Detection of GRB170817A

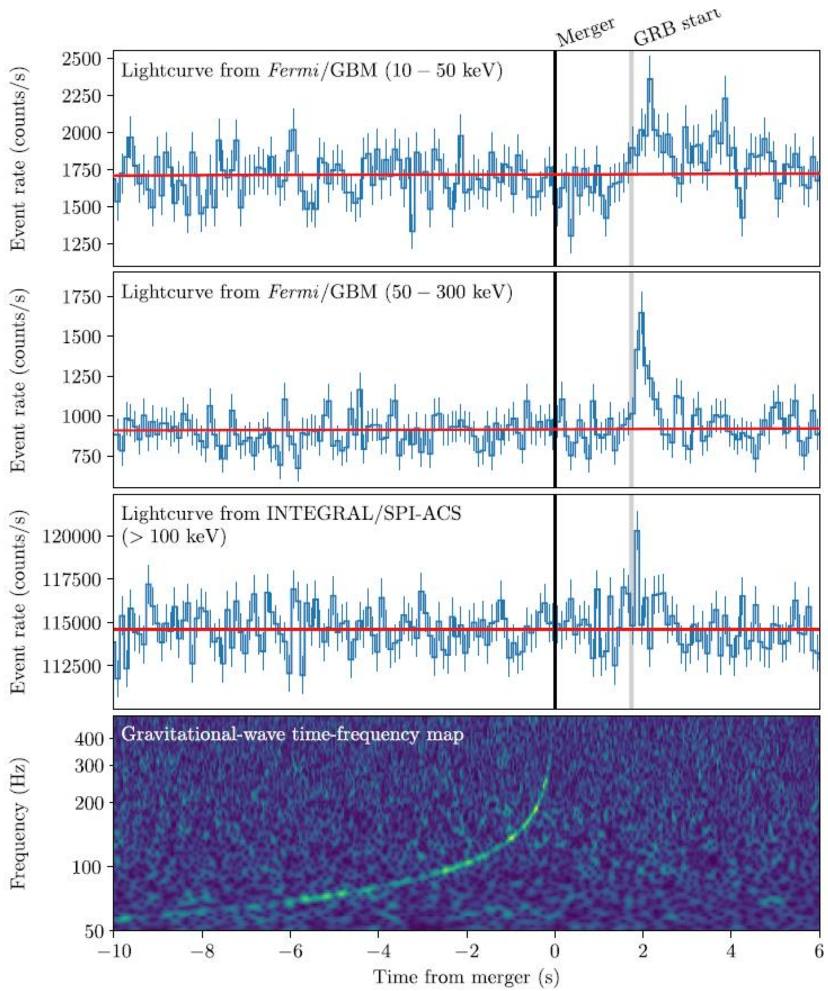

- $T_{90} = 2.0 \mp 0.5$ s, $T_0 = 1.7$s
- $E_{iso} \sim 5 \times 10^{46}$ erg (too dim)

Detected UV-Optical-Infrared emission

Arcavi et al. Nature 24291, 2017

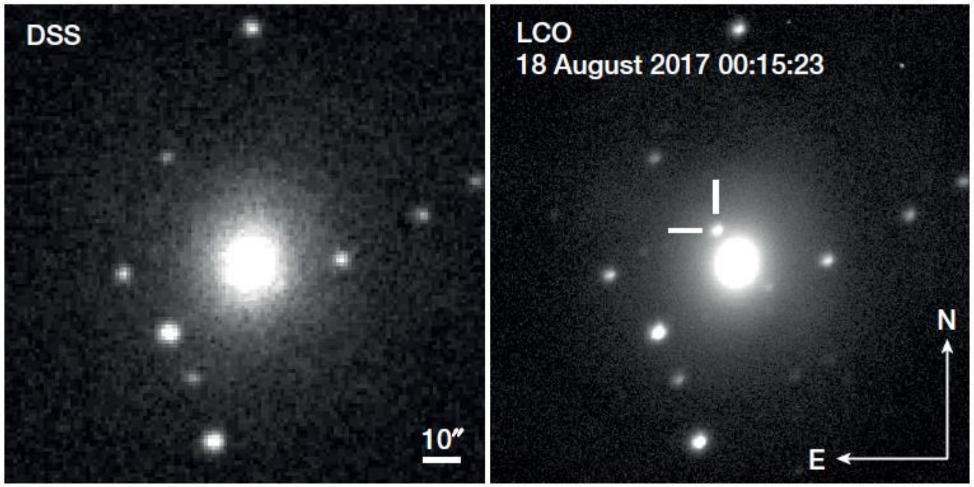

Drout et al. Science (aaq0049) 2017

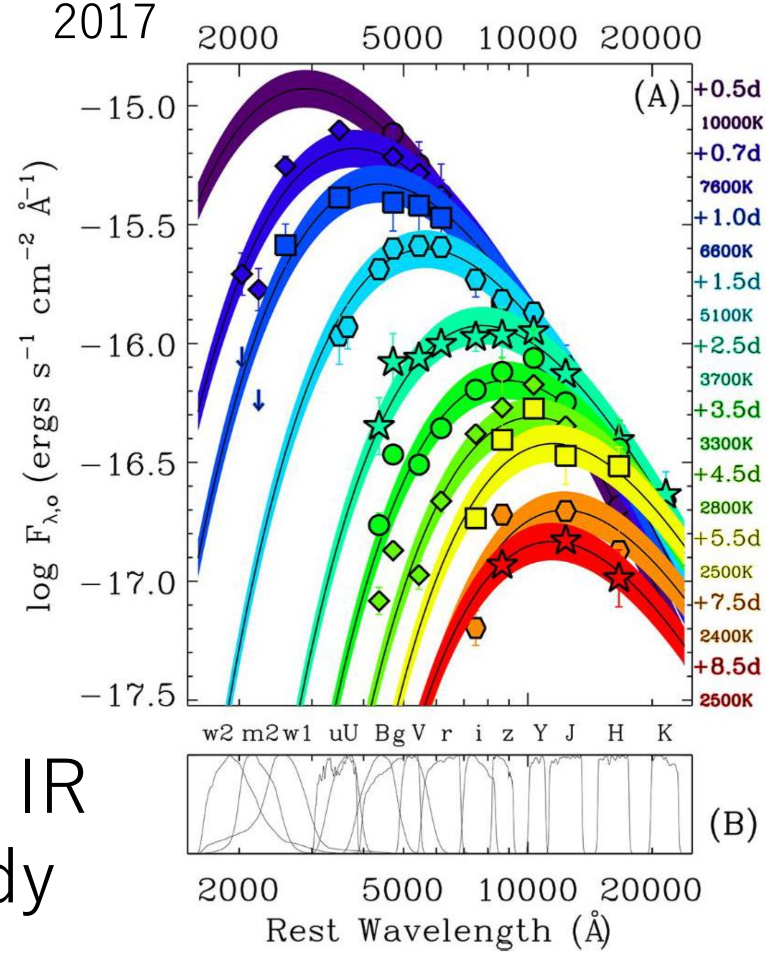

UV Optical IR

- Rapid reddening from UV to IR
- Spectrum is quasi-black body
- Long-duration IR component & short-duration UV-Optical component

About 160 days observation @ Radio, X-ray observation after the merger

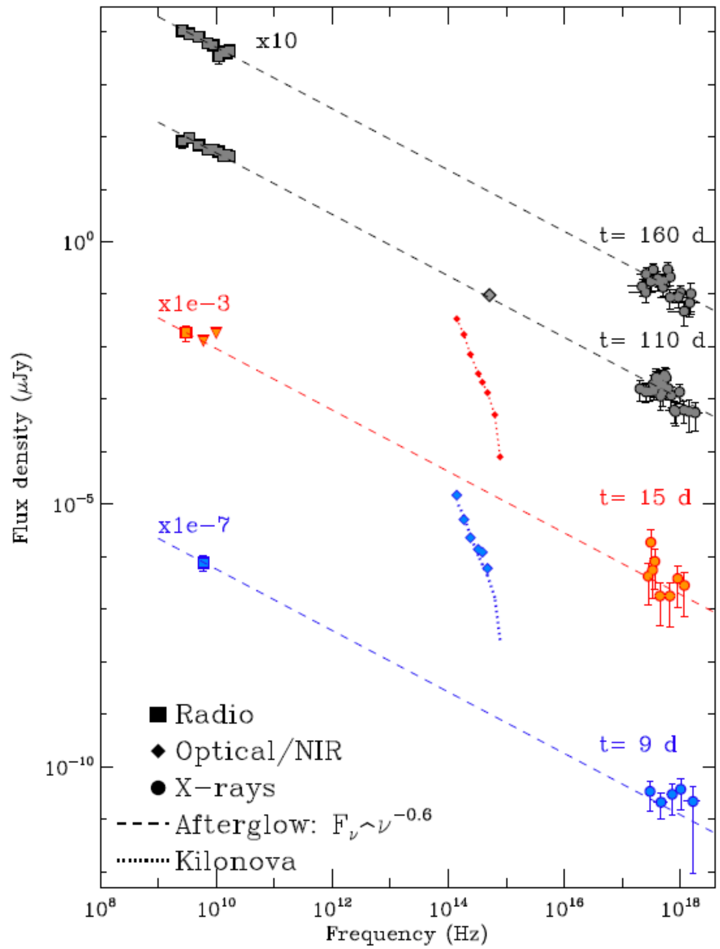

Margutti et al. 18
Mooley et al. 17
Troja et al. 17
Hallnan et al. 17

▶ Structured Jet (Margutti et al. 17, Gottleb et al. 17)

Superluminal motion of GW170817

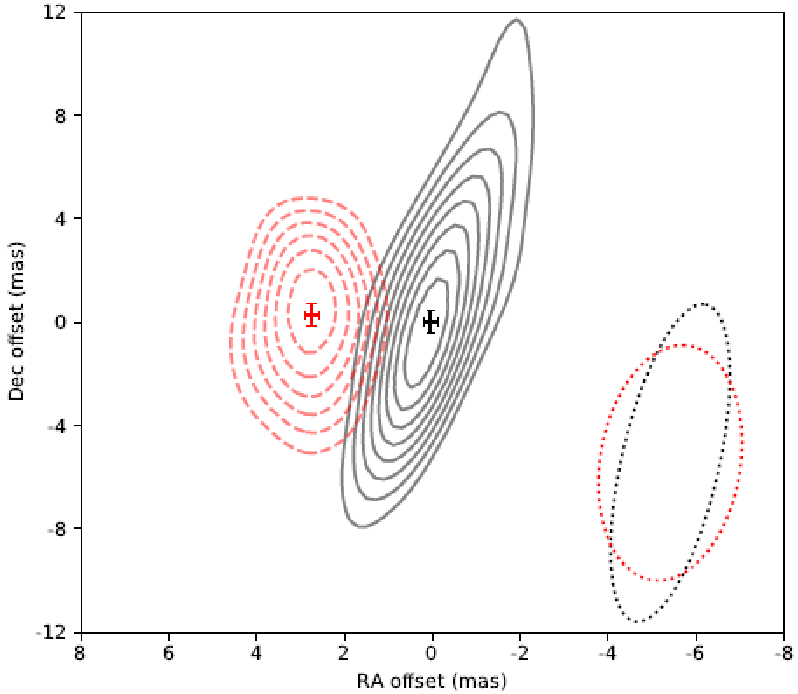

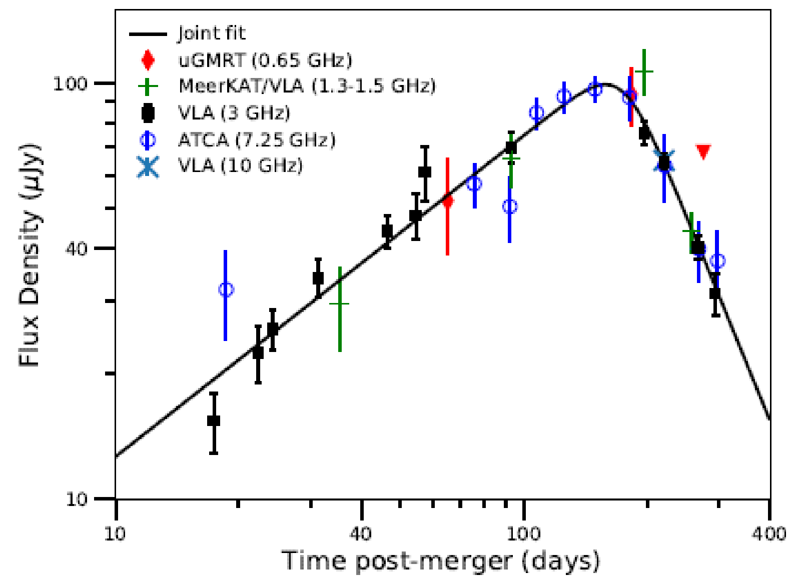

Mooley et al. 18a, b

▶ Superluminal motion of the source image in radio
▶ Light curve fitting suggests a sharp decline at 170 days after the merger
⇒ Strong suggestion of the relativistic jet

Science target of compact binary mergers

Exploring the theory of gravity

▶GW150914 etc. is consistent with GR prediction
(Abott et al. 16, 18)

But, it does not imply that GR is the theory of gravity in a strong gravitational field.

cf. Quasi normal mode from a merger remnant of BBH could prove the theory of gravity (Nakano et al. 16)

Science target of compact binary mergers

<u>Exploring the Equation of State (EOS) of NS matter</u>

NS interior state is poorly known

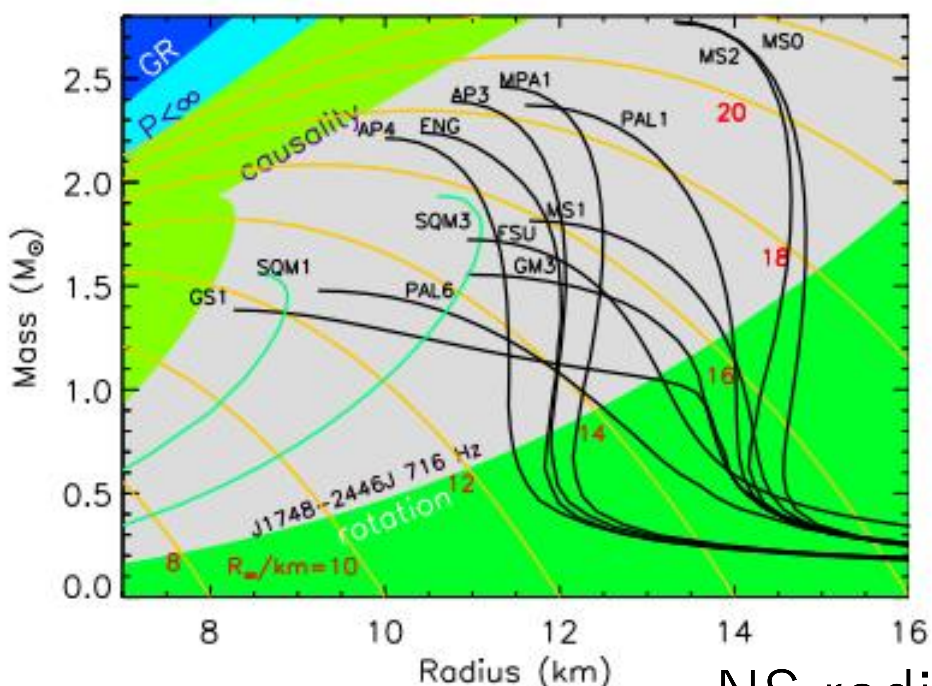

▶ Extraction of the information of NS mass and radius imprinted in merger waveforms ⇒ The EOS of NS matter (Flanagan & Hinderer 08 etc.)

Science target of compact binary mergers

Mystery of the central engine of Short-hard Gamma Ray Burst

- $E_{iso,\gamma} \sim 10^{49}$-$10^{51}$ g cm^2 s^{-2}, Duration ~ 0.1-2 s

They release the huge energy in a short time scale ⇒ A compact object could drive them.

Light curve of GRB

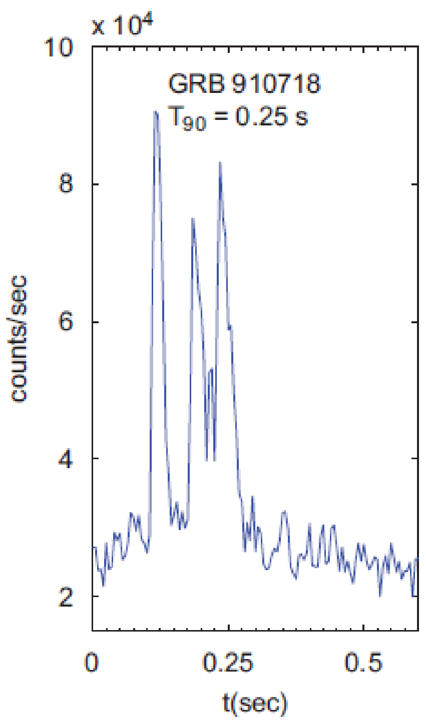

Image of GRB

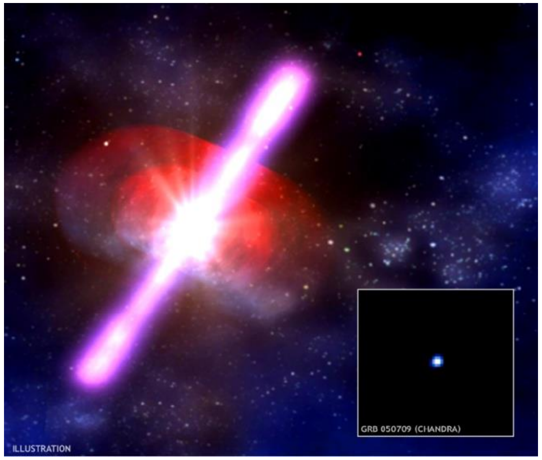

Black-hole – Torus ?

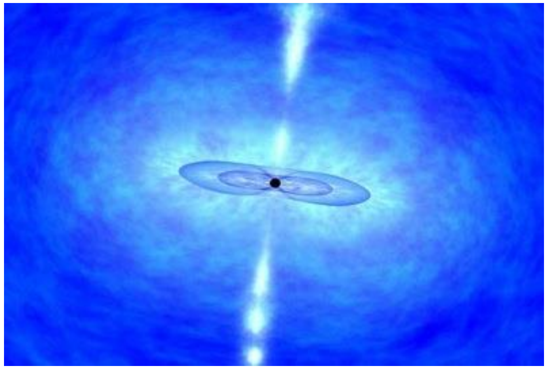

NS-NS or BH-NS merger could drive the GRBs.

Science target of compact binary mergers

Origin of heavy elements in the Universe

Nucleosynthesis by rapid neutron capture process

⇒ Mystery of the nucleosynthesis site

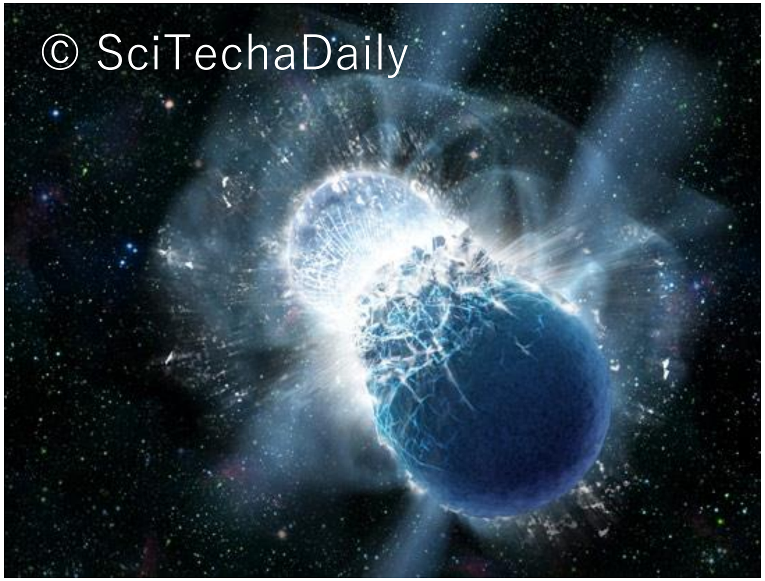

▶NS-NS/BH-NS merger⇒Mass ejection of the neutron rich matter⇒R-process nucleosynthesis (Lattimer & Schramm 76, Wanajo et al. 14)

Science target of compact binary mergers

Electromagnetic counterpart of GW sources

Sky map of LIGO events

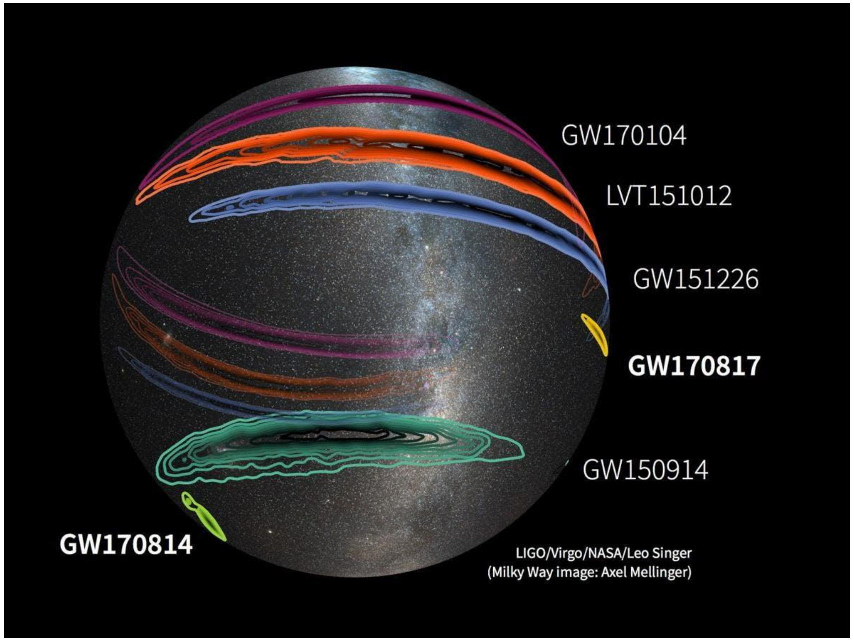

▶ Sky localization is not good by LIGO, c.f., 620 sq deg. for GW150914 ⇒ Hard to identify the host galaxy

▶ Simultaneous detections of EM signal is necessary

▶ Radio active decay of the R-process elements (Li & Paczynski 98)

GRB130603B as a macronova/kilonova event ?

(Berger et al.13, Tanvir et al. 13)

9 days after the burst

30 days after the burst

Optical

NIR

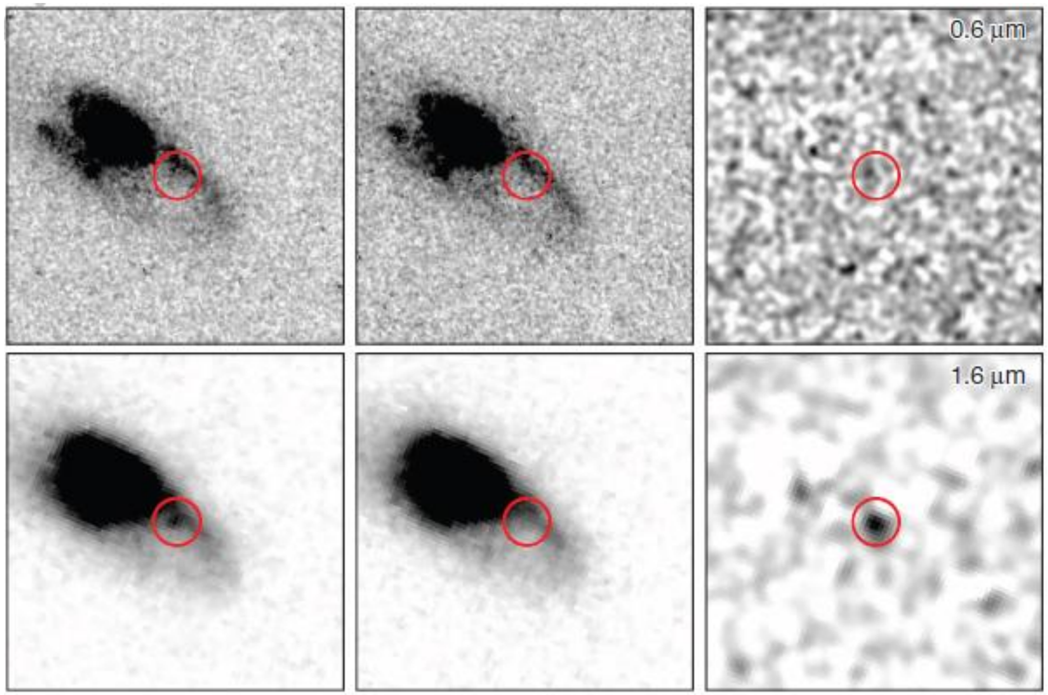

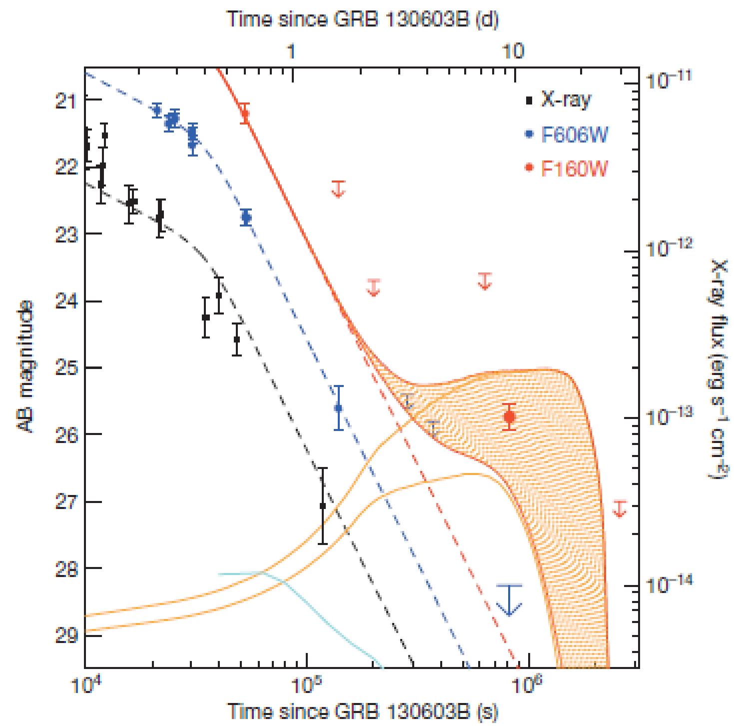

Point source in NIR, not in optical band ⇒ Transient point source in NIR

Basics of numerical relativity

A step toward the physical modeling of compact binary mergers

Numerical Relativity ; Including the basic interactions,

- Gravity (General Relativity)
- Strong interaction (Nuclear matter)
- Weak interaction (Neutrino)
- Electromagnetic force (Magnetic field, cf. NS B-field $10^{11\text{-}15}$ G)

in self-consistent way to figure out high energy astrophysical phenomena in strong gravitational field.

Einstein equations

$$R_{\mu\nu}(\partial^2 g_{\mu\nu}, \partial g_{\mu\nu}) - \frac{1}{2} g_{\mu\nu} R = \frac{8\pi \mathrm{G}}{\mathrm{c}^4} T_{\mu\nu}$$

Conservation laws

$$\nabla_\mu T^{\mu\nu} = 0, \quad T^{\mu\nu} = T^{\mu\nu}_{(\mathrm{fluid})} + T^{\mu\nu}_{(\mathrm{rad})} + T^{\mu\nu}_{(\mathrm{EM})} \qquad \nabla_a F^{ab} = -4\pi j^b,$$

$$\nabla_\mu J^\mu = 0, \quad J^\mu = n_{(\mathrm{baryon})} u^\mu, \; n_{(\mathrm{lepton})} u^\mu, \; \mathrm{etc} \qquad \nabla_{[a} F_{bc]} = 0$$

Equation of state (Closure relation)

$$P = P(\rho, T, Y_{\mathrm{e}})$$

Current status of Numerical Relativity

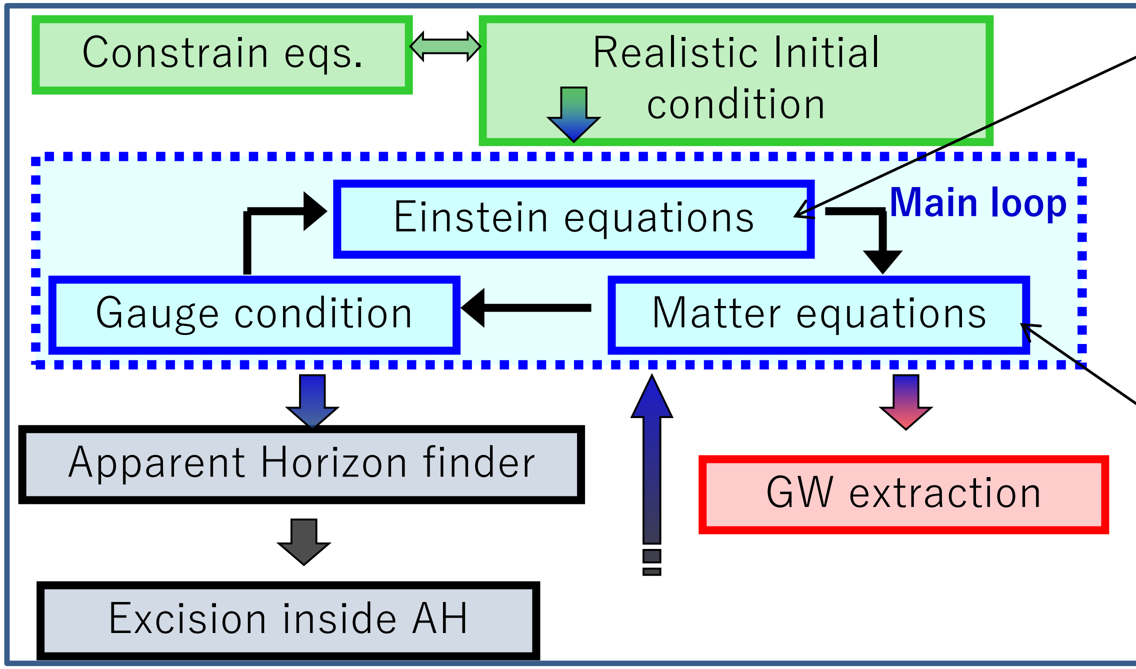

BSSN formulation

(Shibata & Nakamura 95, Baumgrte-Shapiro 99)
cf. Generalized harmonics formulation (Caltech-Cornell-CITA), Fully constraint scheme (Meudon-Valencia)

- G R H D
- G R MH D
- G R R H D
- G R R M H D

Slide courtesy of Sekiguchi

General Relativistic Magneo Hydro Dynamics (GRMHD)

- Formulation by Shibata-Sekiguchi, and Duez et al. (Shibata & Sekiguchi 05, Duez+ 05)

General Relativistic Radiation Hydrodynamics (GRRHD)

- General Relativistic Leakage scheme (Sekiguchi 10)
- Truncated Momentum formalism (Thorne 81, Shibata, KK + 10, Shibata-Sekiguchi 11, Kuroda+12, O'Connor & Ott 13)

Ingredients for numerical relativity

▶ Solver for Einstein’s equation : Formulation for a stable simulation

▶ Solver for relativistic (magneto-)hydrodynamics : Shock capturing scheme

▶ Gauge condition : Choose time and space coordinate

▶ Realistic initial condition : It should be satisfied the constraint equations

▶ Black hole horizon finder : Apparent horizon or Event horizon

▶ Gravitational Wave Extraction : Newman-Penrose or Gauge invariant perturbation

▶ Mesh refinement technique : Adaptive or Fixed mesh refinement

History of Numerical Relativity

Formulation problem of Einstein equation

- 3+ 1 decomposition of Arnowit-Deser-Misner (Intrinsically unstable)
- Shibata-Nakamura formulation（Nakamura et al. 87, Shibata-Nakamura 95、Baumgarte-Shapiro 99)

B(aumgarte)-S(hapiro)-S(hibata)-N(akamura) formulation

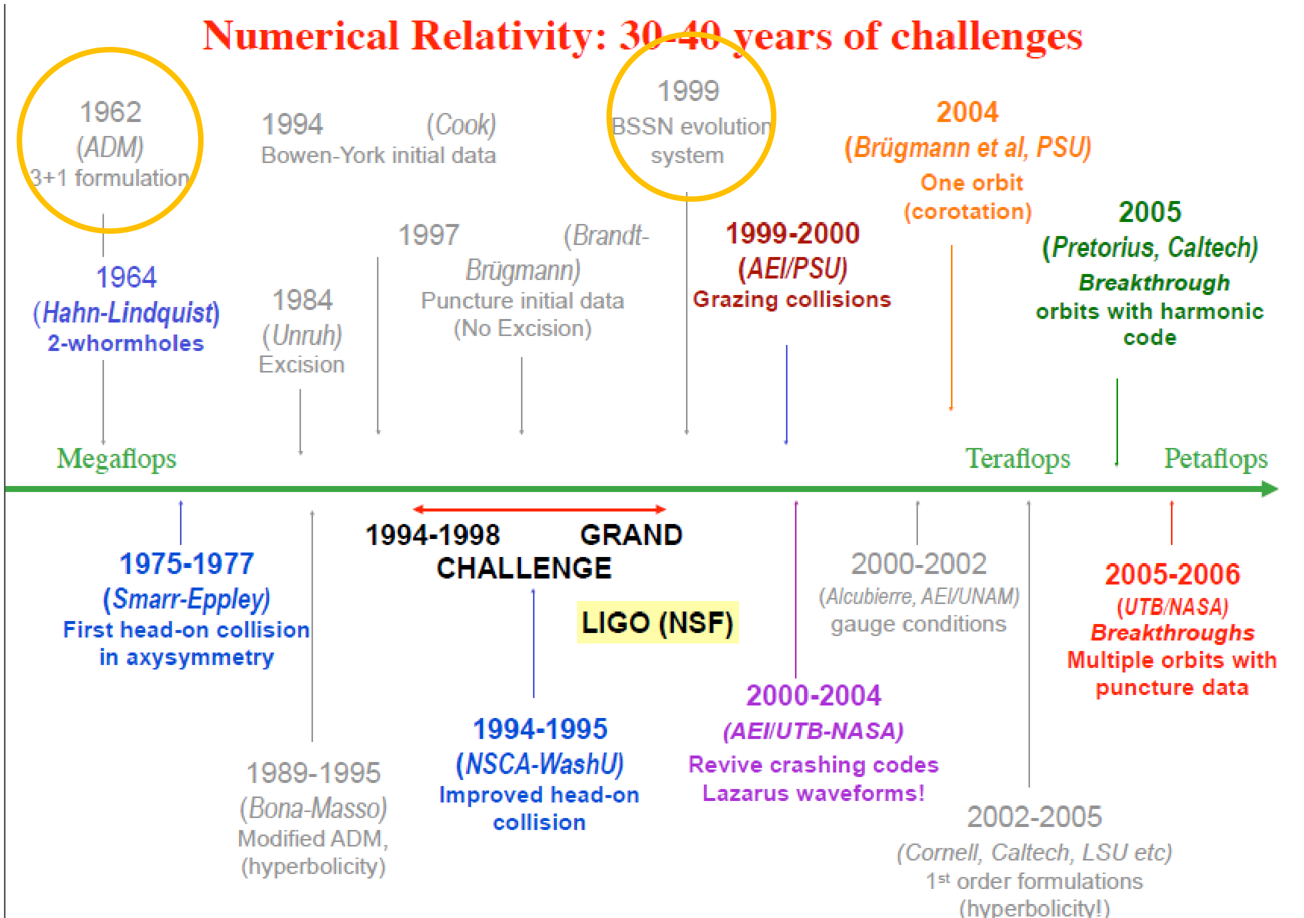

Slide courtesy Carlos Lousto

History of Numerical Relativity

Long-term simulation of binary BH

- Pioneering simulation by F. Pretorius (Excision technique of BH interior)
- BSSN-puncture method (Campanelli et al.06, Baker et al. 06)

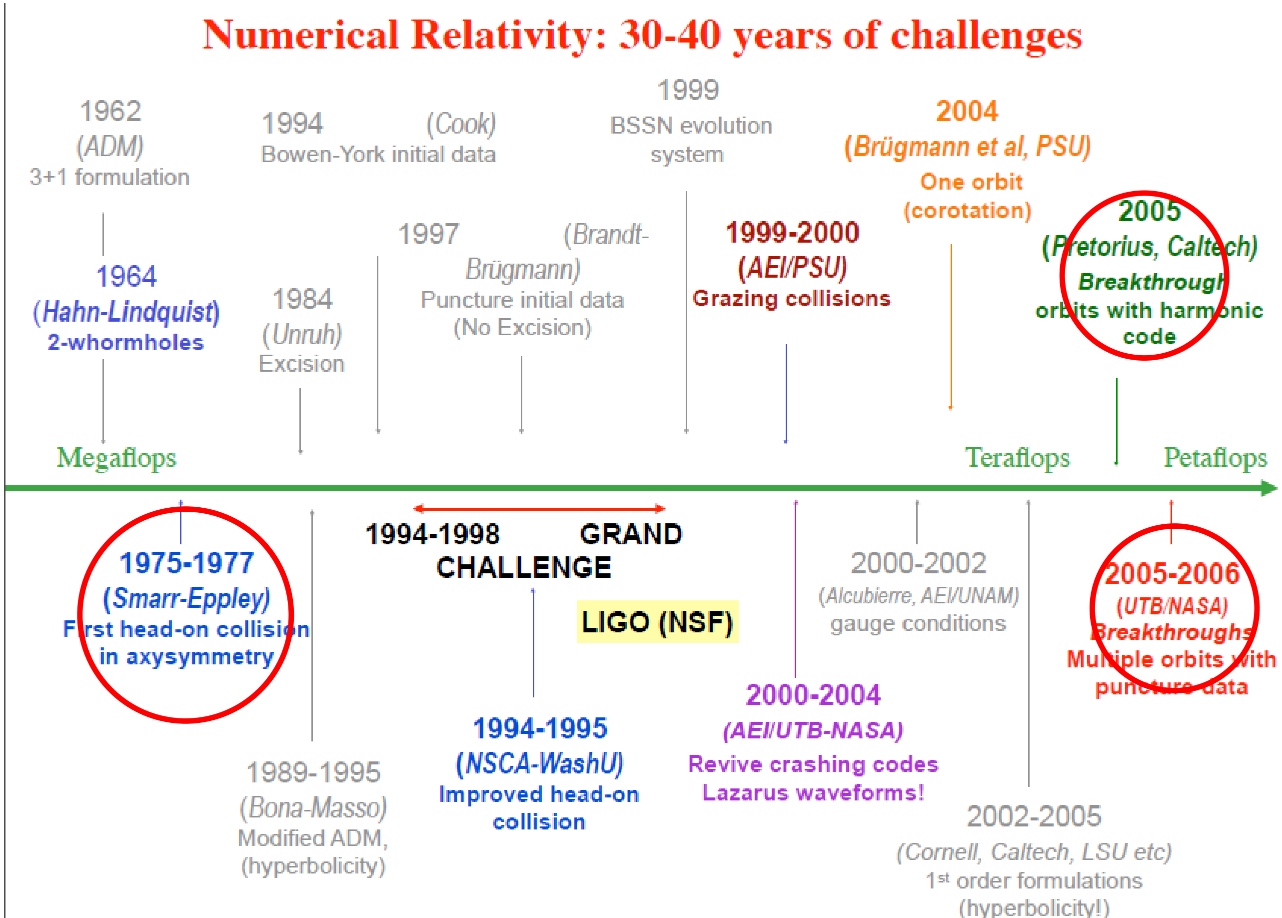

Slide courtesy Carlos Lousto

Other ingredients

- Gauge condition suitable for simulation
- Realistic initial condition

3+1 formalism

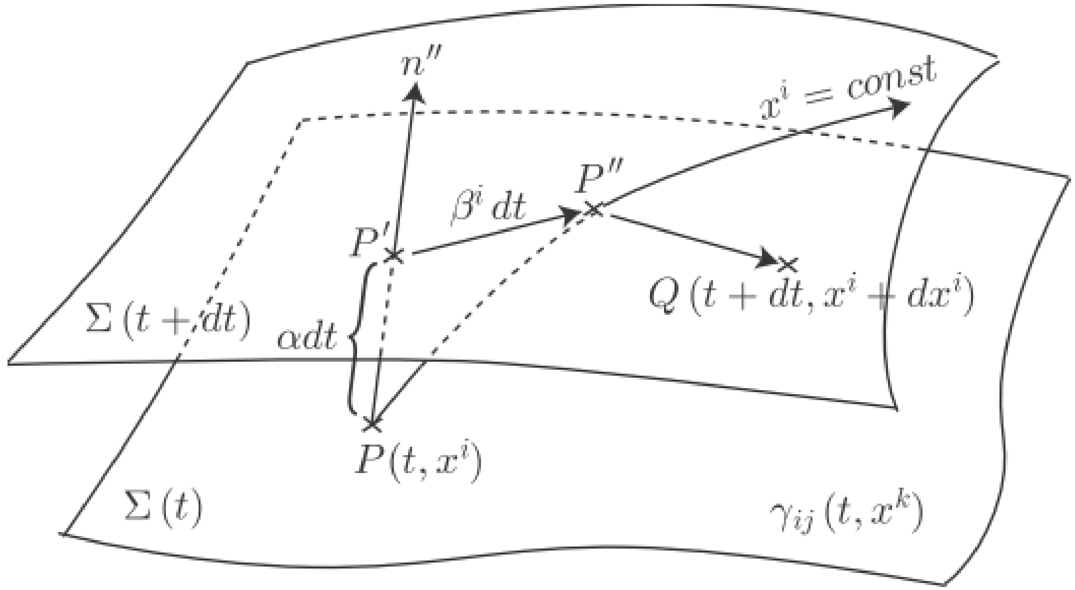

n^a : unit normal vector to the hypersurface $n_a n^a = -1$

γ_{ab} : 3 metric on the hypersurface

$$\gamma_{ab} = g_{ab} + n_a n_b$$

This tensor is a projection tensor on the hyepersurface;

$$n_a \gamma^a{}_b = 0 \Rightarrow \gamma^a{}_b V^b = 0$$

for any spatial vectors on the hypersurface.

3+1 formalism

Introduce a global time function t s.t. a time-like vector field which is the tangent to the time axis;

$$t^a = (\partial/\partial_t)^a \Rightarrow t^a \nabla_a t = t^t = 1$$

Let's define the lapse function and shift vector as

$$\alpha \equiv -t^a n_a, \ \beta^a = t^b {\gamma_b}^a$$

$$\Rightarrow t^a = \alpha n^a + \beta^a$$

Components of the unit vector is

$$n_\alpha = (-\alpha, 0, 0, 0), n^\alpha = (1/\alpha, \beta^i/\alpha)$$

Pythagoros theorem tells you

$$ds^2 = (-\alpha^2 + \beta^i \beta_i) dt^2 + 2\beta_i dt dx^i + \gamma_{ij} dx^i dx^j$$

3+1 formalism

Covariant derivative w.r.t the 3-metric

$$D_a T^{bc\cdots} = \gamma^{\mu}{}_{a}\gamma^{b}{}_{\nu}\gamma^{c}{}_{\alpha}\cdots\nabla_{\mu}T^{\nu\alpha\cdots}$$

Extrinsic curvature

$$K_{ab} \equiv -\gamma_a{}^c \nabla_c n_b = -\frac{1}{2}\pounds_n \gamma_{ab}$$
$$\Rightarrow \partial_t \gamma_{ij} = -2\alpha K_{ij} + 2D_{(i}\beta_{j)}$$

Extrinsic curvature is a measure of the bending of the hypersurface.

$$u^a K_{ab} = -u^c \nabla_c n_b$$

u^a is a spatial vector field tangent to a geodesic on the spatial hypersurface.

3+1 formalism

Gauss equation

$$R_{abcd} = \gamma_a{}^e \gamma_b{}^f \gamma_c{}^g \gamma_d{}^h R^{(4)}_{efgh} + K_{ad}K_{bc} - K_{ac}K_{bd}$$

Codazzi equation

$$D_a K_{bc} - D_b K_{ac} = -\gamma_a{}^d \gamma_b{}^e \gamma_c{}^f R^{(4)}_{defg} n^g$$

Decomposition of the stress-energy tensor

$$T_{ab} = \rho_h n_a n_b + 2J_{(a} n_{b)} + S_{ab},$$

$$\rho_h \equiv T_{ab} n^a n^b,\ J_a \equiv -T_{bc} n^b \gamma^c{}_a,\ S_{ab} \equiv T_{cd} \gamma^c{}_a \gamma^d{}_b$$

3+1 formalism

Contraction of the Gauss equation gives

$$R_{ac} = \gamma_a{}^e \gamma_c{}^h (R^{(4)}_{eh} + R^{(4)}_{ebhd} n^b n^d) + K_{ab} K_c{}^b - K_{ac} K$$

$$R = R^{(4)} + 2R^{(4)}_{bd} n^b n^d + K_{ab} K^{ab} - K^2 = 2G_{ab} n^a n^b + K_{ab} K^{ab} - K^2$$

Projection of the Einstein's equation (1)

$$G_{ab} n^a n^b = 8\pi T_{ab} n^a n^b$$

$$R - K_{ab} K^{ab} + K^2 = 16\pi \rho_h$$

This is the Hamiltonian constraint equation.

Note that it does not contain the time derivative of 3 metric and extrinsic curvature.

3+1 formalism

Contraction of the Codazzi equation gives you

$$D_a K_b{}^a - D_b K = -\gamma_b{}^e (g^{df} + n^d n^f) R^{(4)}_{defg} n^g$$
$$= -\gamma_b{}^e R^{(4)}_{eg} n^g$$

Projection of the Einstein's equation (2)

$$G_{cd} \gamma^c{}_a n^d = 8\pi T_{cd} \gamma_a{}^c n^d$$
$$\Rightarrow D_a K^a{}_b - D_b K = 8\pi J_b$$

This is the momentum constraint equation.

Note that it does not contain the time derivative of 3 metric and extrinsic curvature.

3+1 formalism

Projection of the Einstein's equation (3)

$$G_{\mu\nu}\gamma^{\mu}_{j}\gamma^{\nu}{}_{i} = 8\pi T_{\mu\nu}\gamma^{\mu}{}_{j}\gamma^{\nu}{}_{i}$$

$$\Rightarrow \partial_t K_{ij} = \alpha({}^{(3)}R_{ij} + KK_{ij}) - 2\alpha K_{il}K^{l}{}_{j}$$

$$- 8\pi\alpha(S_{ij} + \frac{1}{2}\gamma_{ij}(\rho_H - S^{l}{}_{l}) - D_i D_j \alpha$$

$$+ D_j\beta^m K_{mi} + D_i\beta^m K_{mj} + \beta^m D_m K_{ij}$$

This is the evolution equation and the equation for the extrinsic curvature is recognized as the time evolution for 3 metrics.

$$\partial_t \gamma_{ij} = -2\alpha K_{ij} + 2D_{(i}\beta_{j)}$$

3+1 formalism

But, the ADM formalism was unstable numerically.
Linear GW propagation cannot be evolved for the long time.
Numerically-induced constraint violation mode grows in time.

Baumgarte-Shapiro-Shibata-Nakamura-puncture formulation

▶ Conformal decomposition

$$\gamma_{ij} = W^{-3}\tilde{\gamma}_{ij},\ W = \exp(-2\phi),\ \det(\tilde{\gamma}_{ij}) = 1$$

$$K_{ij} = W^{-3}\tilde{A}_{ij} - \frac{1}{3}\gamma_{ij}K,\ K = \mathrm{trace}(K_{ij})$$

▶ Introducing new auxiliary variable

$$F_i = \delta^{jk}\partial_j\tilde{\gamma}_{ik} \text{ or } \tilde{\Gamma}^i = -D_j\tilde{\gamma}^{ij}$$

Baumgarte-Shapiro-Shibata-Nakamura-puncture formulation

▶ Rewriting a part of the Ricci tensor with F_i

$$R_{ij} = \tilde{R}_{ij} + R^{W}_{ij}$$

$$\Rightarrow \tilde{R}_{ij} = -\frac{1}{2}\tilde{\gamma}^{kl}[\partial_k\partial_l\tilde{\gamma}_{ij} - \underline{\partial_i\partial_k\tilde{\gamma}_{jl}} - \underline{\partial_j\partial_k\tilde{\gamma}_{il}}] + \cdots$$

$$\partial_j F_i \,\&\, \partial_i F_j$$

▶ Rewriting the equation for F_i with the momentum constraint

Baumgarte-Shapiro-Shibata-Nakamura-puncture formulation

$$(\partial_t - \beta^l \partial_l)\tilde{\gamma}_{ij} = -2\alpha \tilde{A}_{ij} + \tilde{\gamma}_{ik}\partial_j \beta^k + \tilde{\gamma}_{jk}\partial_k \beta^k - \frac{2}{3}\tilde{\gamma}_{ij}\partial_k \beta^k$$

$$(\partial_t - \beta^l \partial_l)\tilde{A}_{ij} = [\alpha W^2 (R_{ij} - \frac{1}{3}\gamma_{ij} R^k{}_k)$$

$$- W^2 (D_i D_j \alpha - \frac{1}{3}\gamma_{ij} D^k D_k \alpha)] + \alpha (K \tilde{A}_{ij} - 2\tilde{A}_{ik}\tilde{A}^k_j)$$

$$+ \partial_i \beta^k \tilde{A}_{kj} + \partial_j \beta^k \tilde{A}_{ki} - \frac{2}{3}\partial_k \beta^k \tilde{A}_{ij}$$

$$- 8\pi\alpha W^2 (S_{ij} - \frac{1}{3} S^k{}_k)$$

$$(\partial_t - \beta^l \partial_l) W = \frac{1}{3} W (\alpha K - \partial_k \beta^k)$$

$$(\partial_t - \beta^l \partial_l) K = \alpha [\tilde{A}_{ij}\tilde{A}^{ij} + \frac{1}{3}K^2]$$

$$- W^2 (\tilde{D}^i \tilde{D}_i \alpha - \frac{\partial_i W}{W}\tilde{\gamma}^{ij}\partial_j \alpha) + 4\pi\alpha (\rho_H + S^k{}_k)$$

$$(\partial_t - \beta^l \partial_l) F_i = 2\alpha [(\tilde{\gamma}^{kj} - \eta^{kj})\partial_j \tilde{A}_{ik} + \partial_j \tilde{\gamma}^{kj}\tilde{A}_{ik}$$

$$- \frac{1}{2}\tilde{\gamma}^{jl}\partial_i \tilde{A}_{jl} - \frac{3\partial_i W}{W} - \frac{2}{3}\partial_i K] - 2\eta^{jk}\partial_j \alpha \partial_k \tilde{A}_{ik}$$

$$+ \eta^{jl}\partial_j \beta^k \partial_k \tilde{\gamma}_{il} + \eta^{jk}(\partial_j \tilde{\gamma}_{il}\partial_k \beta^l + \partial_i \tilde{\gamma}_{jl}\partial_k \beta^l - \frac{2}{3}\tilde{\gamma}_{ij}\partial_l \beta^l)$$

$$- 16\pi\alpha J_i$$

Baumgarte-Shapiro-Shibata-Nakamura-puncture formulation

Gauge condition

$$(\partial_t - \beta^l \partial_l)\alpha = -2\alpha K$$

$$\partial_t \beta^i = \tilde{\gamma}^{ij}(F_j + \Delta t \partial_t F_j)$$

These gauges satisfy desired properties such as

- ▶ Singularity avoidance
- ▶ Suppression of the spatial distortion

Simulating a black hole spacetime is feasible !

Current status of Numerical Relativity

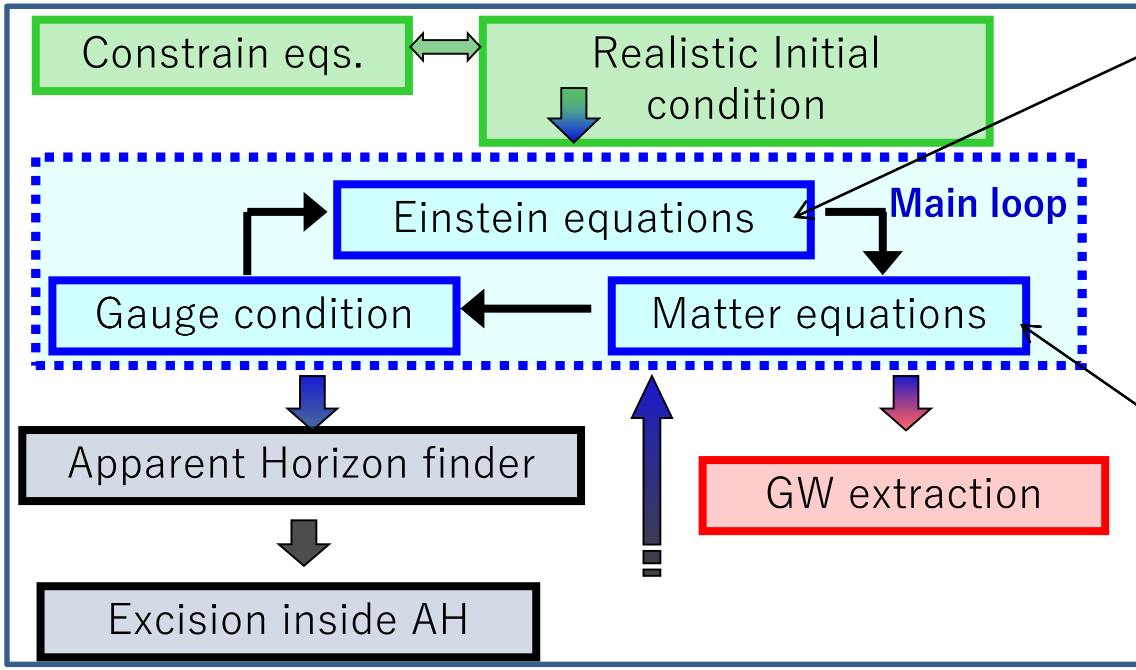

BSSN formulation
(Shibata & Nakamura 95, Baumgrte-Shapiro 99)
cf. Generalized harmonics formulation (Caltech-Cornell-CITA), Fully constraint scheme (Meudon-Valencia)

- G R H D
- G R MH D
- G R R H D
- G R R M H D

Slide courtesy of Sekiguchi

General Relativistic Magneo Hydro Dynamics (GRMHD)

- Formulation by Shibata-Sekiguchi, and Duez et al. (Shibata & Sekiguchi 05, Duez+ 05)

General Relativistic Radiation Hydrodynamics (GRRHD)

- General Relativistic Leakage scheme (Sekiguchi 10)
- Truncated Momentum formalism (Thorne 81, Shibata, KK + 10, Shibata-Sekiguchi 11, Kuroda+12, O'Connor & Ott 13)

Relativistic hydrodynamics

$$\gamma_i{}^{\mu}\nabla_{\nu}T^{\nu}{}_{\mu}=0 \text{ (Relativistic Euler eq.)}$$

$$n^{\mu}\nabla_{\nu}T^{\nu}{}_{\mu}=0 \text{ (Energy eq.)}$$

$$\Rightarrow \partial_t S_k+\partial_j(\alpha\sqrt{\gamma}S^j{}_k-\beta^j S_k)=-S_0\partial_k\alpha+S_i\partial_k\beta^i$$

$$-\frac{1}{2}\alpha\sqrt{\gamma}S_{ij}\partial_k\gamma^{ij}$$

$$\partial_t S_0+\partial_i(-S_0\beta^i+\alpha S^i)=\alpha\sqrt{\gamma}S^{ij}K_{ij}-S_iD^i\alpha$$

where

$$S_k=-\sqrt{\gamma}T_{\mu\nu}n^{\mu}\gamma^{\nu}{}_k=\sqrt{\gamma}\rho whu_i$$

$$S_0=\sqrt{\gamma}T_{\mu\nu}n^{\mu}n^{\nu}=\sqrt{\gamma}(\rho hw^2-P)$$

$$P=P(\rho,\epsilon),\ w=-n_{\mu}u^{\mu},h=1+\epsilon+\frac{P}{\rho}$$

$$S_{ij}=\rho hu_iu_j+P\gamma_{ij}$$

$$\nabla_{\mu}(\rho u^{\mu})=0,\ \text{(Continuity eq.)}$$

$$\Rightarrow \partial_t(\rho\sqrt{-g}u^t)+\partial_i(\rho\sqrt{-g}u^i)=0$$

Extension to relativistic magnetohydrodynamics

Maxwell eq.

$$\nabla_a F^{ab} = -4\pi j^b,$$
$$\nabla_{[a} F_{bc]} = 0$$

Stress energy tensor of the EM field

$$T^{(EM)}_{ab} = \frac{1}{4\pi}(F_{ac}F_b{}^c - \frac{1}{4}g_{ab}F_{cd}F^{cd})$$

3+1 decomposition

$$F^{ab} = n^a E^b - n^b E^a + \epsilon^{abc}B_c,\ E^a = F^{ab}n_b,\ B^a = \frac{1}{2}\epsilon^{abc}F_{bc}$$

The Ohm's law

$$j^a + (j^b u_b)u^a = \sigma_c F^{ab}u_b, \quad \sigma_c : \text{conductivity}$$
$$j^a = \rho_e n^a + \gamma^a{}_b j^b$$

Extension to relativistic magnetohydrodynamics

Constraint eq.

$$n^b\nabla_a F^{ab} \Rightarrow \partial_k(\sqrt{\gamma}E^k) = 4\pi\sqrt{\gamma}\rho_e \text{ (Gauss' law)}$$

$$\epsilon^{abc}\nabla_{[a}F_{bc]} \Rightarrow \partial_k(\sqrt{\gamma}B^k) = 0 \text{ (no mopole constraint)}$$

Evolution eq.

$$\partial_t(\sqrt{\gamma}E^i) = -\partial_k\{\sqrt{\gamma}(\beta^i E^k - \beta^k E^i + \alpha\epsilon^{kij}B_j\}$$

$$-4\pi\sqrt{\gamma}(\alpha\gamma^i{}_a j^a - \rho_e\beta^i) \text{ (Ampére-Maxwell's law)}$$

$$\partial_t(\sqrt{\gamma}B^i) = -\partial_k\{\sqrt{\gamma}(\beta^i B^k - \beta^k B^i - \alpha\epsilon^{kij}E_j)\} \text{ (Faraday's law)}$$

Continuity eq.

$$\nabla_a j^a = 0 \Rightarrow \partial_t(\sqrt{\gamma}\rho_e) + \partial_k(\mathcal{J}^k - \sqrt{\gamma}\rho_e\beta^k) = 0$$

$$\mathcal{J}^k = (v^i + \beta^i)\sqrt{\gamma}\rho_e + \sigma_c\sqrt{\gamma}[-(v^i + \beta^i)E^j u_j + \alpha(wE^i + \epsilon^{ijk}u_j B_k)]$$

Extension to relativistic magnetohydrodynamics

Ideal MHD approximation

$$F^{ab}u_b = 0 \text{ (Electric field in the fluid-rest frame vanishes)}$$

$$\Rightarrow F^{ab} = u_d \epsilon^{dabc} b_c,\ b^a : \text{Magnetic-field in the fluid-rest frame}$$

$$\Rightarrow E^i = -\frac{1}{\omega}\epsilon^{ijk}u_j B_k$$

Stress energy tensor

$$T_{ab}^{(EM)} = \frac{1}{4\pi}(b^2 u_a u_b + \frac{b^2}{2}g_{ab} - b_a b_b),\ b_a = \frac{1}{\omega}[B_a + u_a(B^k u_k)]$$

Maxwell eq.

$$\partial_k(\sqrt{\gamma}B^k) = 0$$

$$\partial_t(\sqrt{\gamma}B^k) = \partial_k\{\sqrt{\gamma}(v^i B^k - v^k B^i)\}$$

Extension to relativistic magnetohydrodynamics

Relativistic MHD-Euler eq. & Energy eq.

$$\partial_t S_i + \partial_k [S_i v^k + \alpha\sqrt{\gamma}(P + \frac{b^2}{8\pi})\delta^k{}_i - \frac{\alpha\sqrt{\gamma}}{4\pi w^2} B^k (B_i + u_i B^j u_j)]$$

$$= -S_0 \partial_i \alpha + S_{ki}\beta^k - \frac{\alpha\sqrt{\gamma}}{2} S_{jk}\partial_i \gamma^{jk}$$

$$\partial_t S_0 +_k [S_0 v^k + \sqrt{\gamma}(P + \frac{b^2}{8\pi})(v^k + \beta^k) - \frac{\alpha\sqrt{\gamma}}{4\pi w} B^k (u_j B^j)]$$

$$= \alpha\sqrt{\gamma} S_{ij} K^{ij} - S_k D^k \alpha$$

where

$$S_i = \rho\sqrt{\gamma} w h u_i + \frac{\sqrt{\gamma}}{4\pi w}[B^2 u_i - (B^j u_j) B_i]$$

$$S_0 = \rho\sqrt{\gamma} w h - P\sqrt{\gamma} + \frac{\gamma}{4\pi}[B^2 - \frac{1}{2\omega^2}(B^2 + (B^k u_k)^2])$$

Numerics

▶ For Einstein solver, finite difference scheme is straightforward.

Tayler expansion tells you the 4th order finite difference should be

$$\partial_x \phi|_{x=x_j} = \frac{-\phi(x_{j+2}) + \phi(x_{j-2}) + 8\phi(x_{j+1}) - 8\phi(x_{j-1})}{12\Delta x} + O(\Delta x^4)$$

Evaluation 1st and 2nd derivative terms in Einstein's equation with 4th-order finite difference scheme.

Time updating is done with the 4th-order Runge-Kutta method.

Numerics

▶ Convergence study is important. Otherwise, you cannot draw a scientific conclusion.

Order of convergence

$$\partial_{tt}\phi + c^2\partial_{xx}\phi = 0$$

Apply the 2nd order scheme;

$$\frac{\phi_j^{n+1} - 2\phi_j^n + \phi_j^{n-1}}{\Delta t^2} = \partial_{tt}\phi|_j^n + \frac{2}{4!}\Delta t^2\partial_{tttt}\phi|_j^n + O(\Delta t^4)$$

$$\frac{\phi_{j+1}^{n} - 2\phi_j^n + \phi_{j-1}^{n}}{\Delta x^2} = \partial_{xx}\phi|_j^n + \frac{2}{4!}\Delta x^2\partial_{xxxx}\phi|_j^n + O(\Delta x^4)$$

Original equation is transformed into

$$\partial_{tt}\phi + c^2\partial_{xx}\phi = -\frac{2}{4!}(\Delta t^2 - c^4\Delta x^2)\partial_{xxxx}\phi|_j^n + O(\Delta x^4)$$

Numerics

▶ In hydrodynamics simulations, shock wave may appear.
Shock = Discontinuous physical quantities

Therefore, Tayler expansion is no longer valid at shock.

⇒ Shock Capturing Scheme is necessary

Numerics

▶ For relativistic hydrodynamics solver, the high-resolution shock capturing scheme is employed.

$$\partial_t Q + \partial_i F^i = 0$$

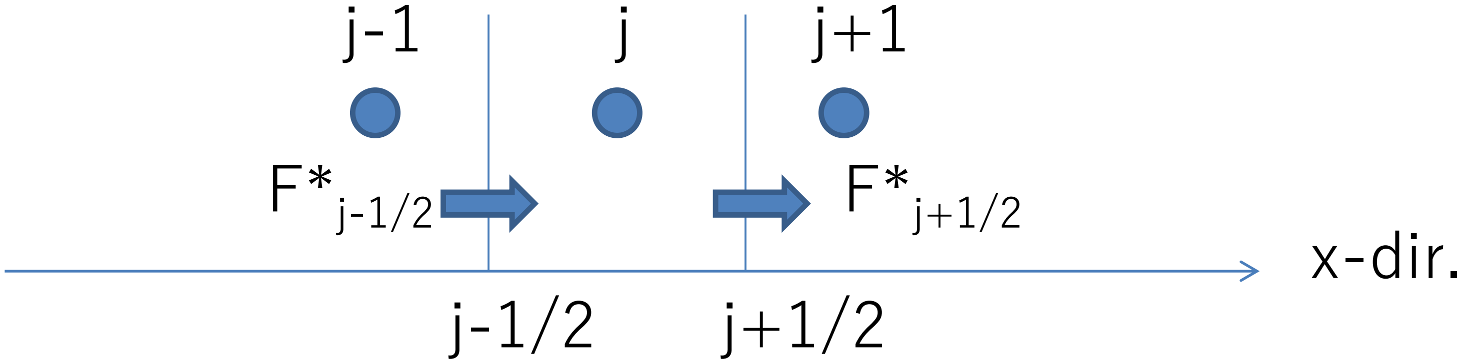

▶ Evaluation of the numerical flux F* at the interface

▶ Update the conservative variables Q with the numerical flux F*

▶ Many options to estimate the numerical flux F*, our choice is Harten-Lax-Lee flux solver

Numerics

▶ Mesh refinement technique is employed

Adaptive mesh refinement

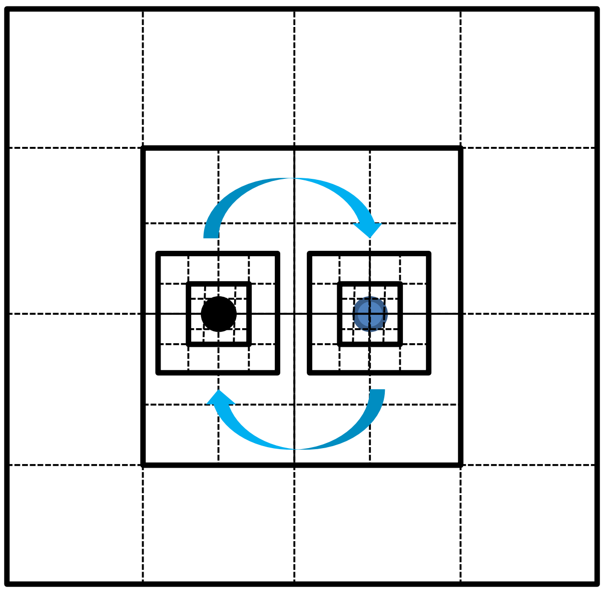

Fixed mesh refinement

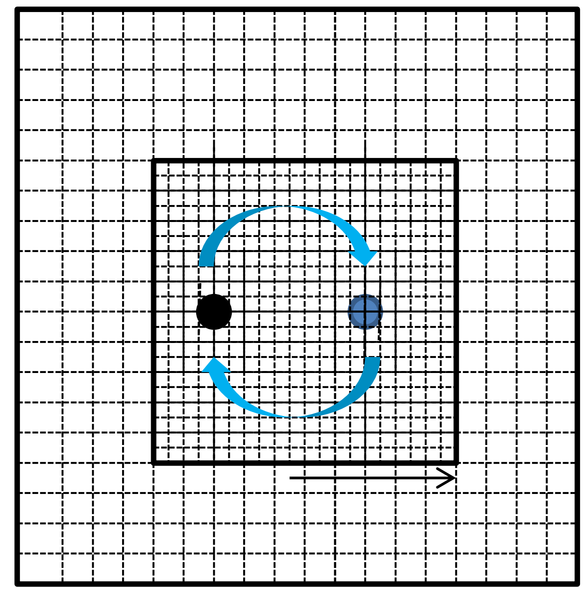

▶ Normally, grid resolution of the coarser level is twice of the finer level.
It is possible to resolve NS/BH(O(10km)) and GW wavelength (O(100km)) simultaneously.

Competition in the world

A Role of simulations in GW physics

<u>Figuring out a realistic picture of BH-BH, NS-NS, BH-NS mergers</u>

Numerical relativity simulations on super-computer with a code implementing all the fundamental interactions

▶ Einstein eq.
▶ Magneto Hydro Dynamics
▶ Neutrino radiation transfer
▶ Nuclear Equation of State

▶The NR simulations of the BH-BH merger played an essential role for the first detection

Frontiers in Numerical Relativity

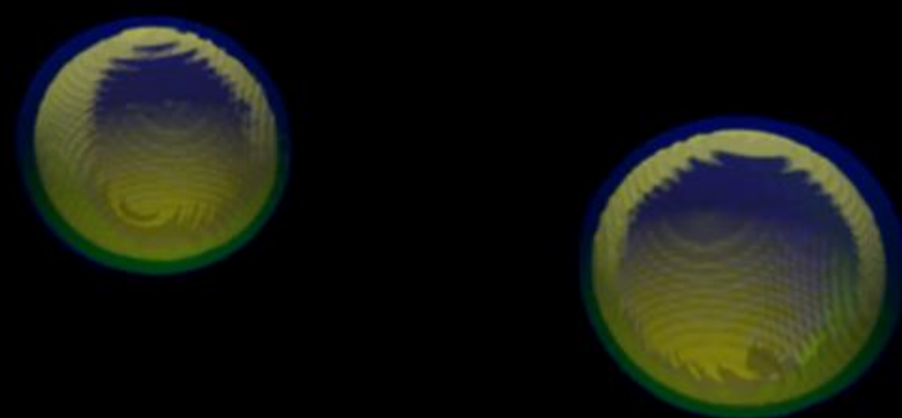

Kenta Kiuchi (AEI/YITP)

Max-Planck-Institut
für Gravitationsphysik
Albert-Einstein-Institut

YITP
YUKAWA INSTITUTE FOR
THEORETICAL PHYSICS

Numerical relativity simulation of binary neutron star mergers

Overview of binary neutron star merger (Bartos et al. 13)

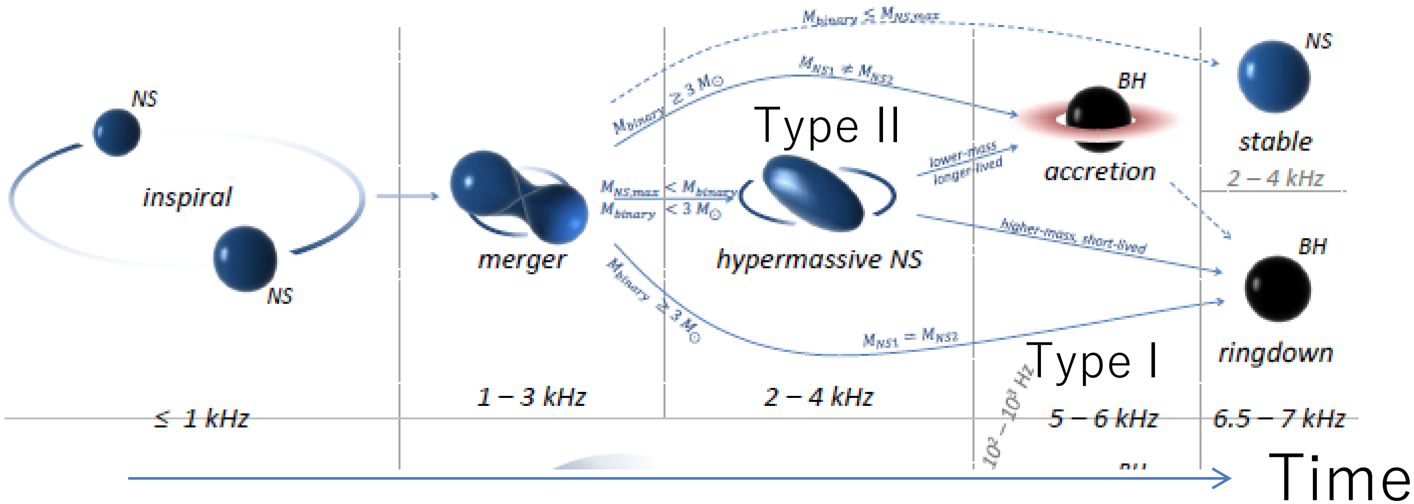

Type I or Type II is determined by M and M_{max}

M: total mass, M_{max} : Maximum mass of spherical and cold NS (EOS dependent)

- $M > k\ M_{max}$ ⇨ Type I (Direct BH formation)
- $M < k\ M_{max}$ ⇨ Type II

$1.4 \lesssim k \lesssim 1.7$ (Hotokezaka+ 11)

What's the origin of k greater than 1 ? ⇨ Rotation and thermal pressure (Shibata-Taniguchi 06, Sekiguchi et al. 11, Keplan et al. 14)

Observational evidence

M-R relation

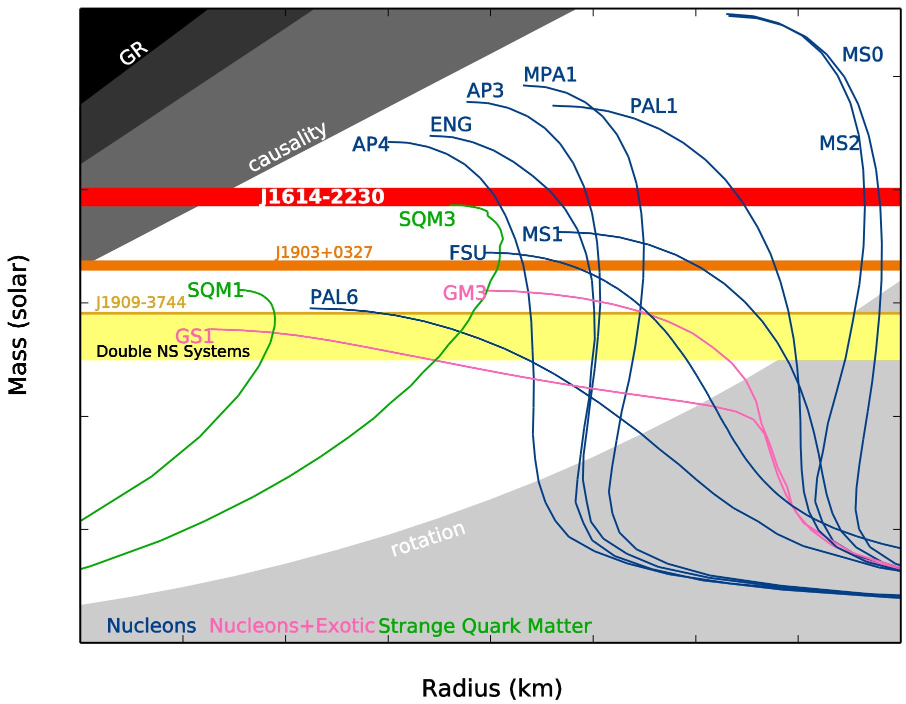

Mass of observed NSs (Lattimer & Paraks 06)

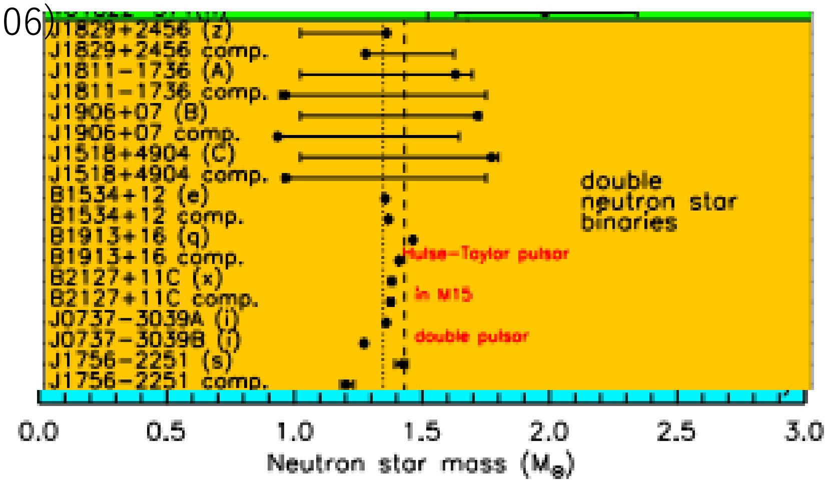

- Lower bound of maximum mass of NS is 2.01 ±0.04 $M_\odot$

(Demorest et al. 10, Antoniadis et al.13)

- Canonical total mass = 2.6-2.8 $M_\odot$

The type II is likely to be realistic ($2.74^{+0.04}_{-0.01} M_\odot$ GW170817)

Binary Neutron Star

Type Ⅰ GW waveforms (Different EOS or mass ratio)

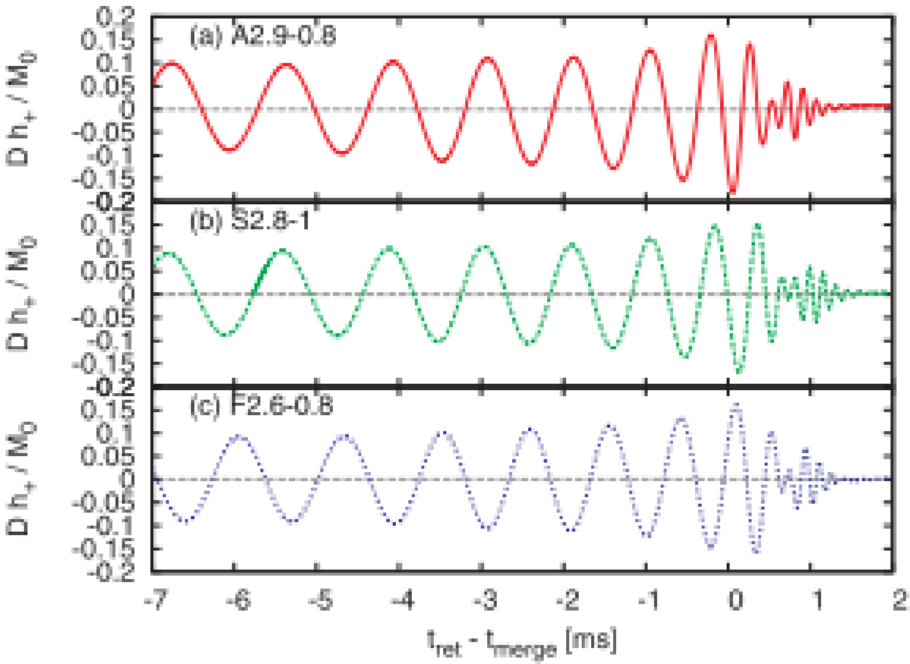

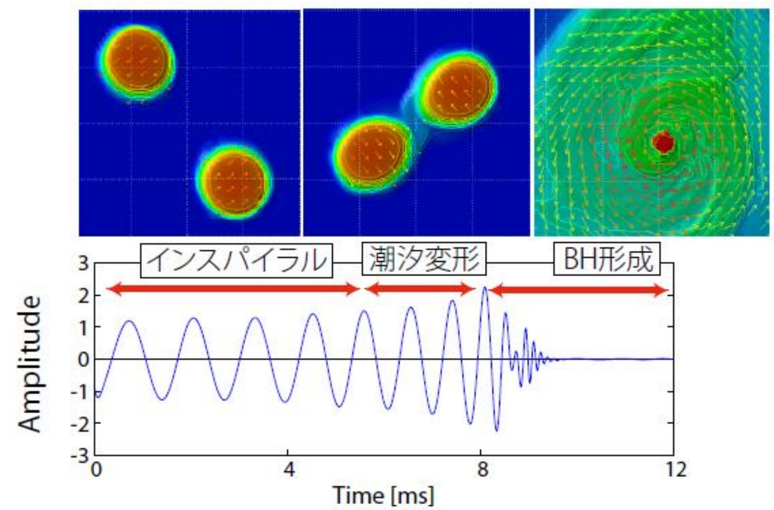

Do we solve the inverse problem ? (GW ⇨ EOS)

Binary Neutron Star

Type I　GW spectrum

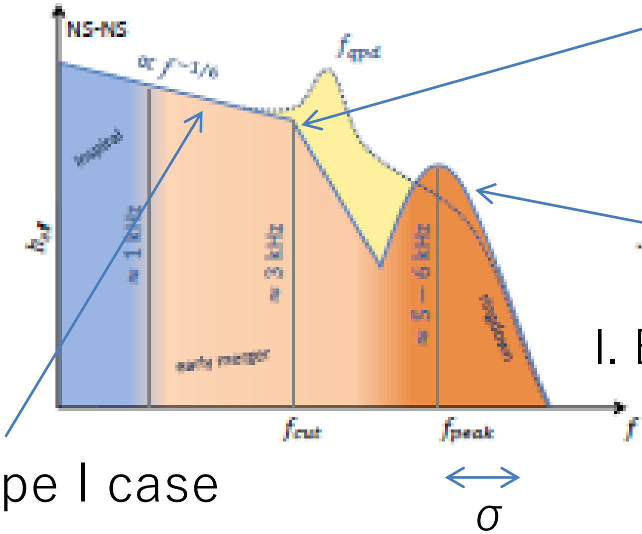

Type I case

I. Bartos et al. 13

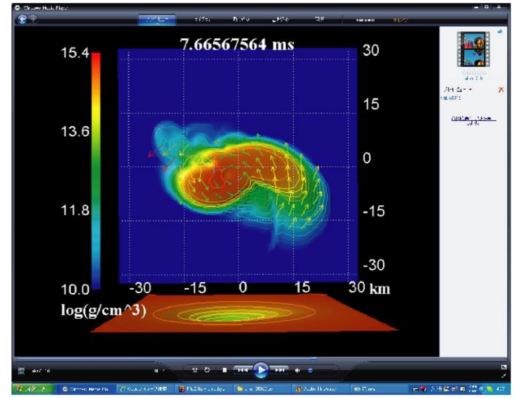

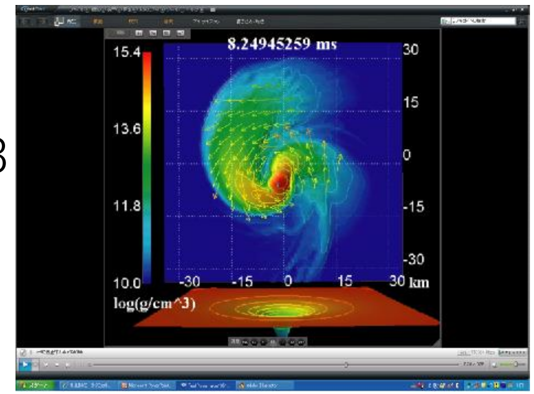

Cut off frequency f_{cut} reflects a point where binary configuration is lost.
→ f_{cut} imprints a radius of NS (KK et al.10)

Extract f_{cut} by fitting simulation GW spectra for various models.

Binary Neutron Star

Type I

<u>f_{cut} – Compactness relation</u>

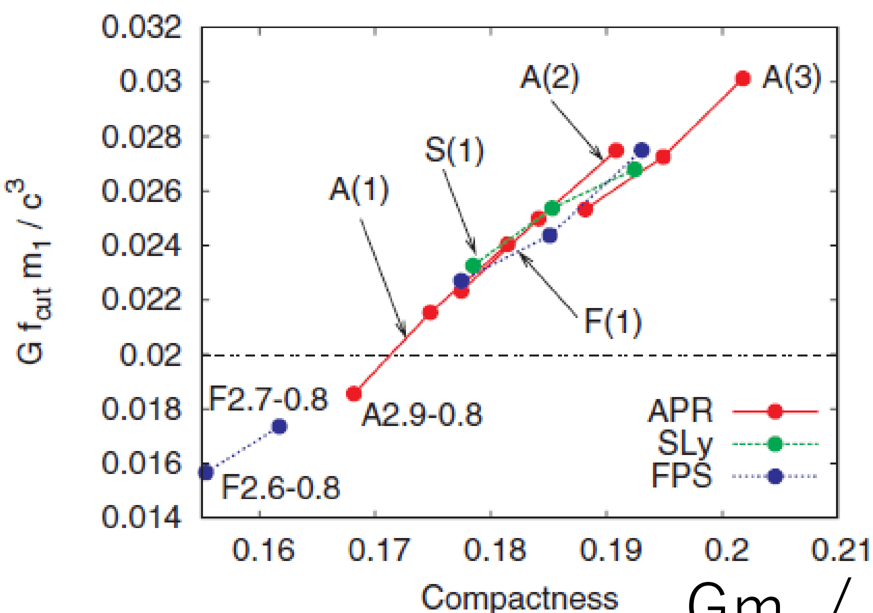

Gm_1 / Rc^2

m_1 : mass of light companion

<u>Clear correlation of f_{cut} – Compactness</u>

‣ Mass and mass ratio are determined from inspiral waveforms
(PN waveforms)

‣ f_{cut} from merger waveform
⇒ Reconstruction of M-R relation

Binary Neutron Star

Type I

Merger hypothesis of SGRB

f_{cut} – Compactness relation

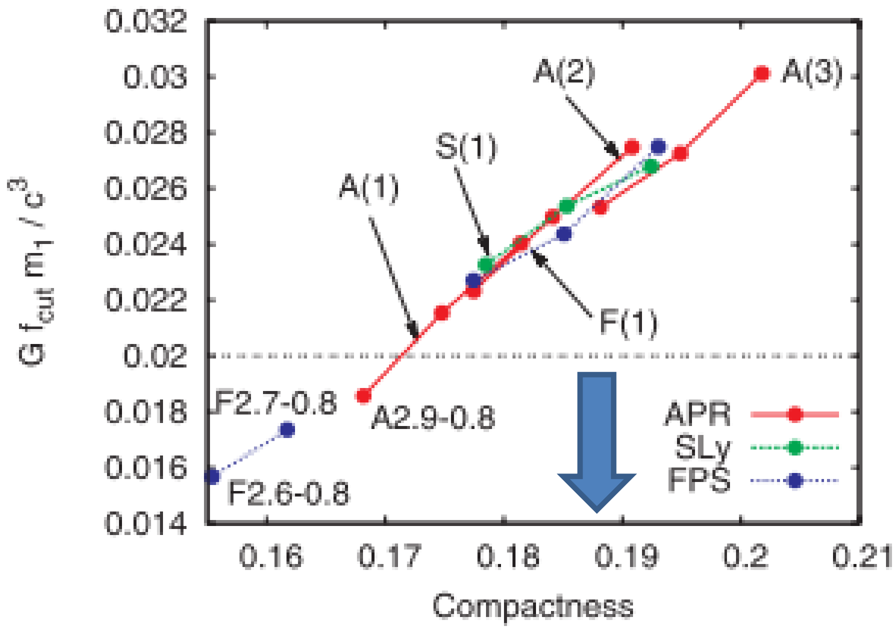

Disk mass – σ / f_{peak} relation

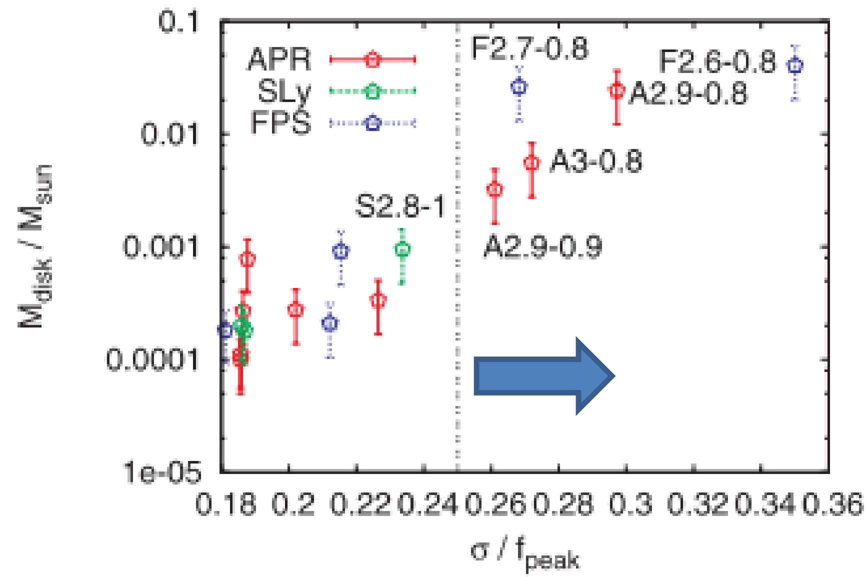

$Gf_{\rm cut}m_1/c^3 \lesssim 0.02$

$\sigma/f_{\rm peak} \gtrsim 0.25$

$\Rightarrow$

$M_{\rm disk} \gtrsim 0.01 M_\odot$

Candidate of central engine of SGRB

Simultaneous observation of GW and SGRB would verify the merger hypothesis.

Type II merger (Hotokezaka et al. 13)

Density contour on the orbital plane (EOS = H4, 1.4-1.4$M_\odot$)

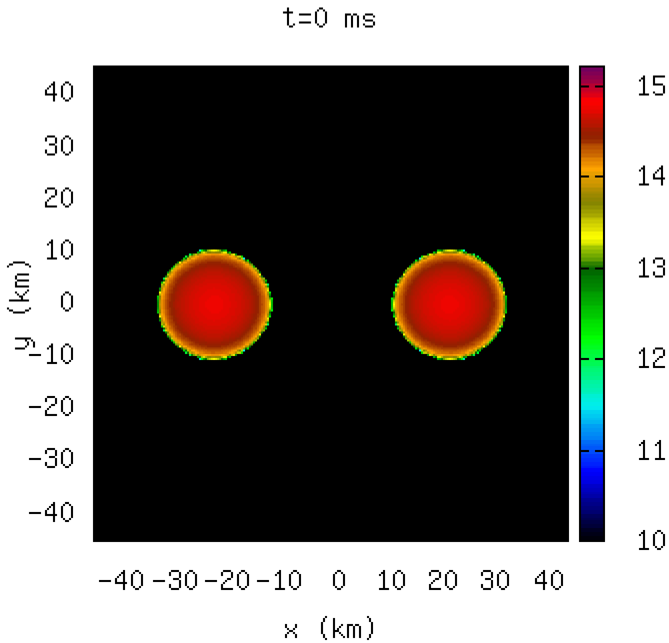

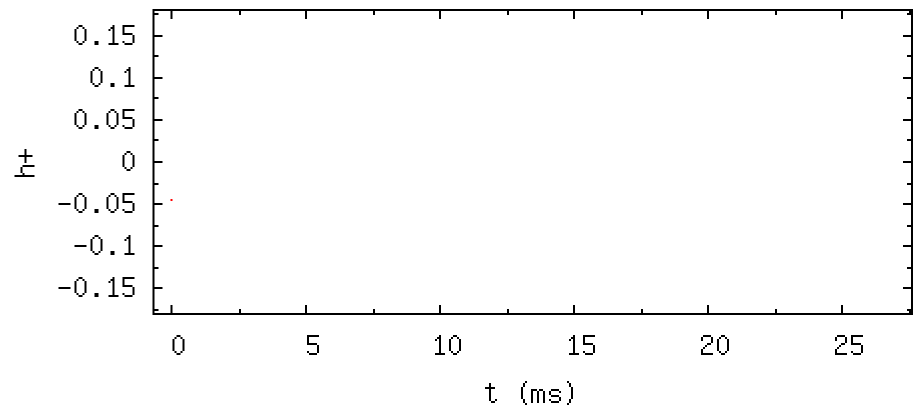

Animation by Hotokezaka

Hypermassive neutron star oscillations ⇨ sinusoidal GWs after the merger.

Type II merger (Hotokezaka et al. 13)

GW spectrum

Type II

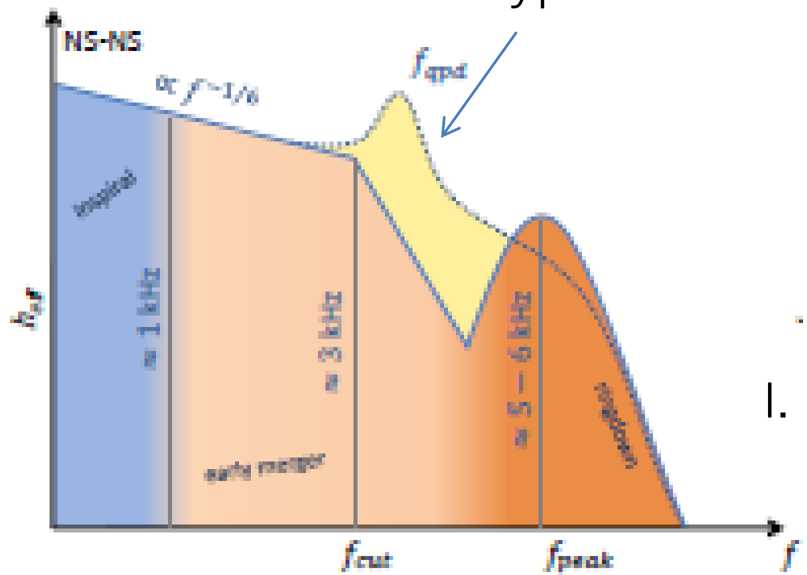

I. Bartos+ 13

Peak frequency of massive neutron star reflects a structure of NS

⇒ Measurement of f_{peak} constrains the EOS.

Type II merger (Hotokezaka et al. 13)

f_{peak} - R relation ($M_{tot} = 2.7M_{\odot}$)

Bauswein & Janka (2012)

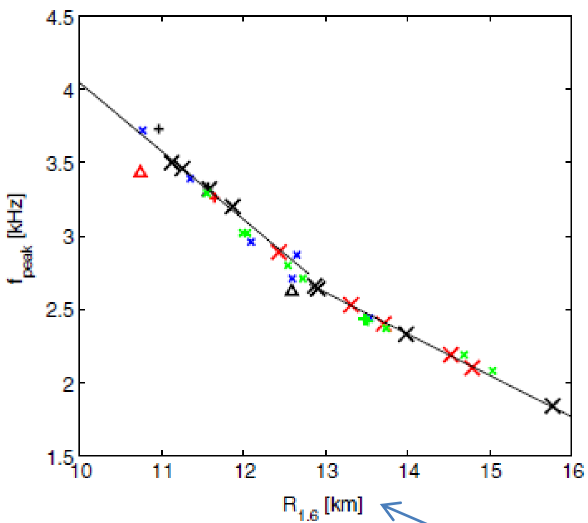

Hotokezaka et al.13

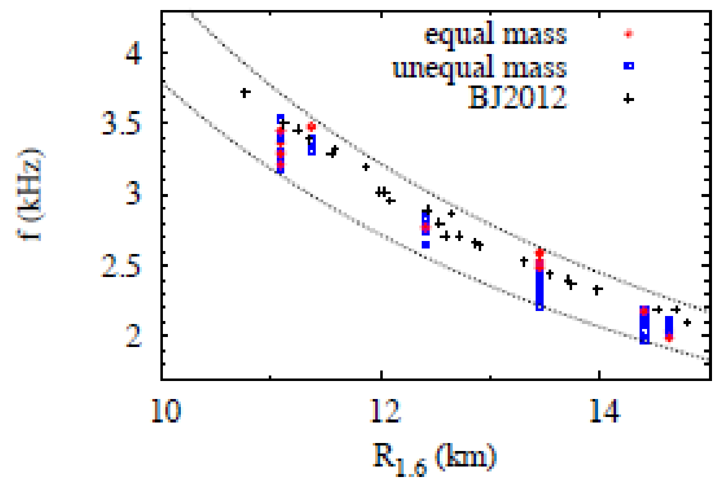

Spherical NS radius of 1.6 $M_{\odot}$

NS radius of 1.6 $M_{\odot}$

- Strong correlation of f_{peak} and NS radius (small dispersion)

If you could determine f_{peak}, you can infer $R_{1.6}$.

With an accuracy of $\Delta f = 40$ Hz, the error bar would be $\Delta R = 144 – 200$m where the event rate for Adv. LIGO is 0.015-1.2/yr. (see also Clark et al. 14)

Exploring a realistic picture of NS-NS mergers

(Bartos et al. 13)

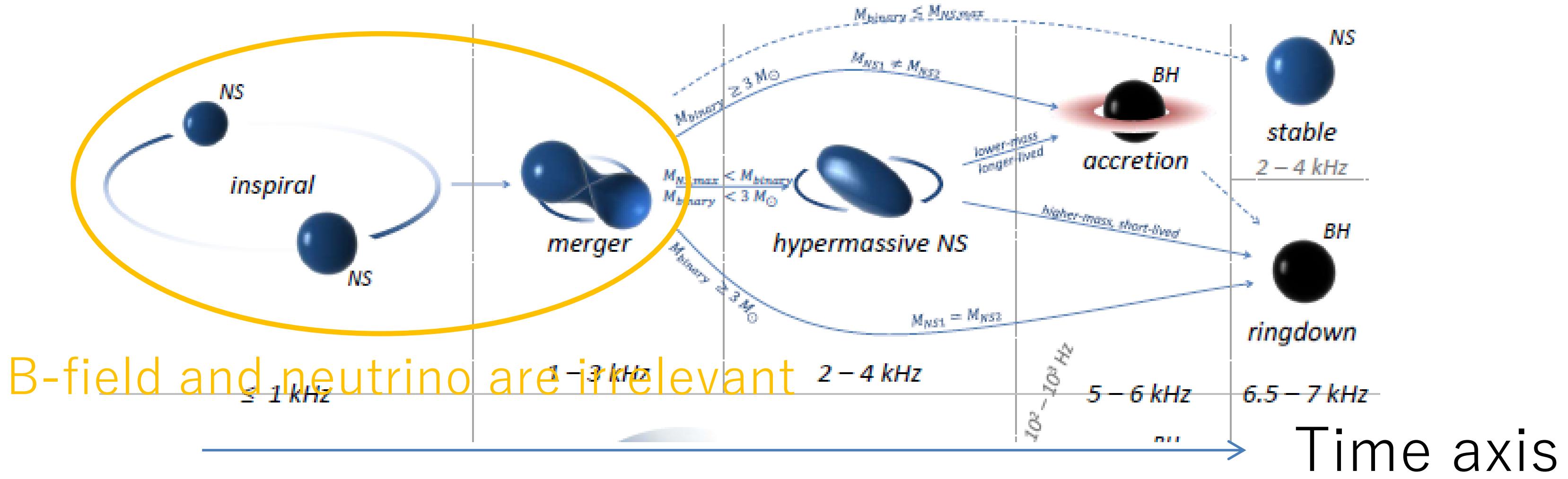

Science target : Measuring a tidal deformability of NS

From inspiral to late inspiral phase

Earth tide

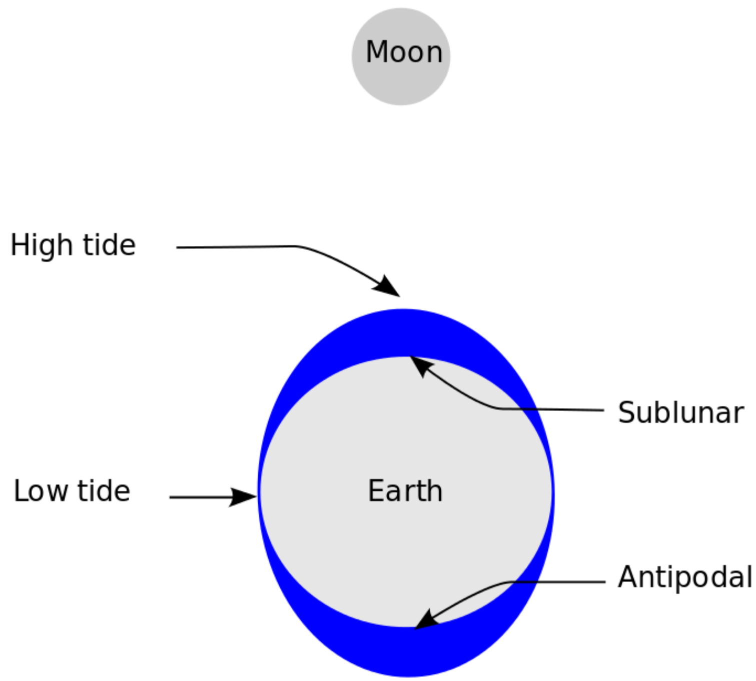

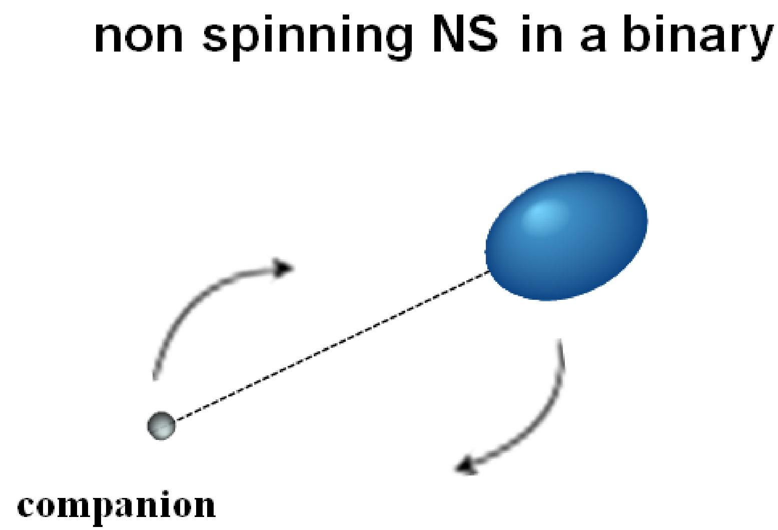

NS just before the merger could be deformed by a tidal force of its companion.

$$Q_{ij} = -\lambda \mathcal{E}_{ij},$$

$$\Lambda = \frac{2}{3} k_2 \left(\frac{GM}{Rc^2} \right)^{-5}, k_2 = \frac{3}{2} \lambda R^{-5}$$

From inspiral to late inspiral phase

Tidal deformability depends on NS EOSs.

EOS ⇒ Pressure(P) as a function of the density(ρ)

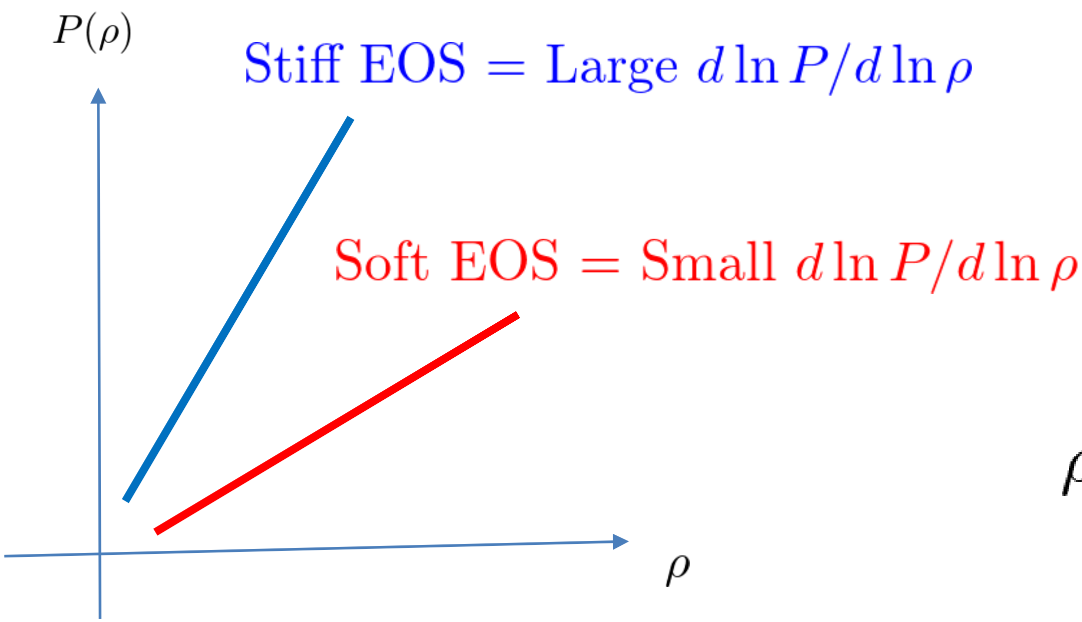

$$\nabla P = -\rho\nabla\phi_{\rm g}$$

$\phi_{\rm g}$ is a gravitaional potential

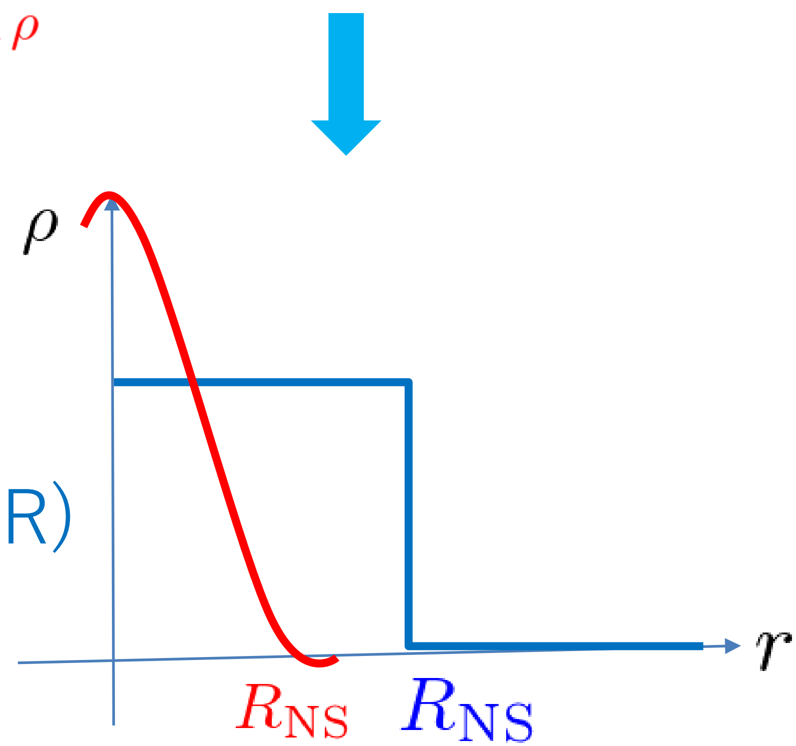

Stiff EOS ⇒ Uniform ρ (large R)

Soft EOS ⇒ Centrally concentrated ρ (small R)

From inspiral to late inspiral phase

Tidal deformation

Stiff EOS (large R) | Soft EOS (small R)

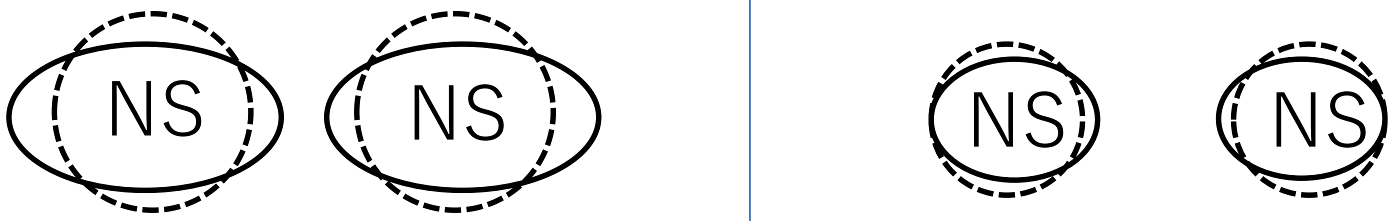

Easily tidally deformed

Hard to be tidally deformed

Tidal deformability depends on NS EOSs

Tidal deformability imprinted in GWs

$$h = \underbrace{A(t)}_{\text{Amplitude}} e^{i\underbrace{\Phi(t)}_{\text{Phase}}}$$

Tidal force is attractive force ⇒
Tidal deformation accelerates the phase evolution

Theoretical template of GWs

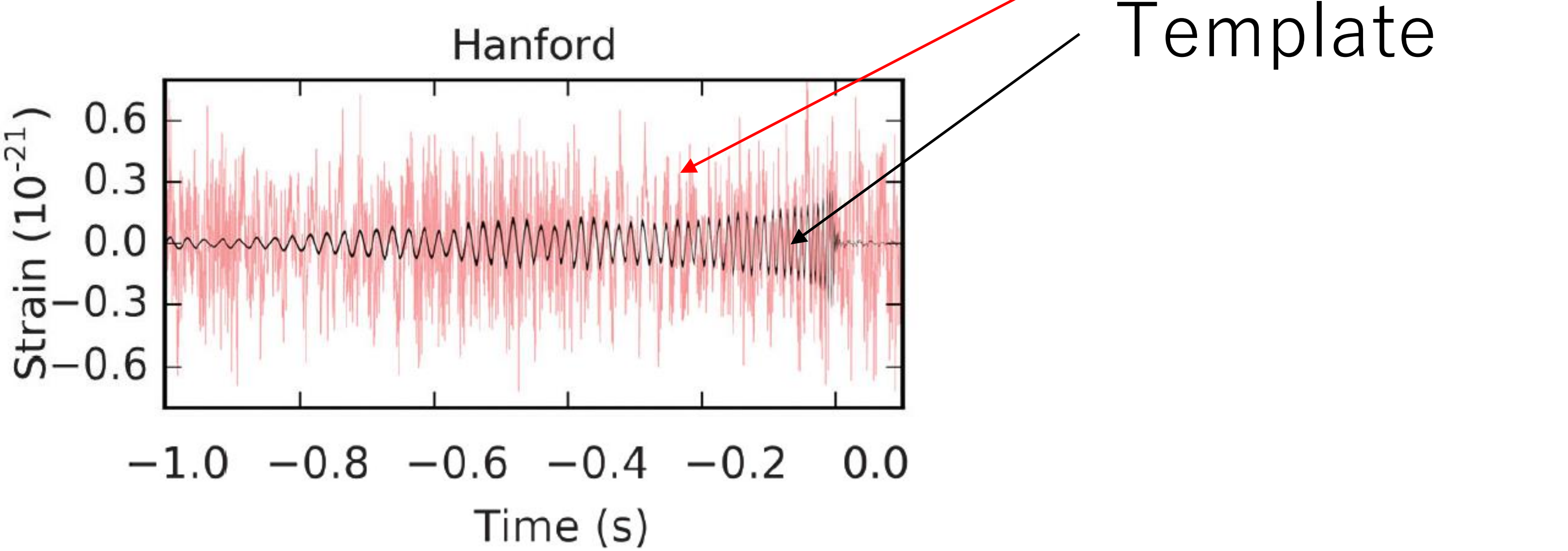

Toward a theoretical template bank

Large tidal deformability ⇒ Rapid phase evolution

Numerical diffusion ⇒ Rapid phase evolution

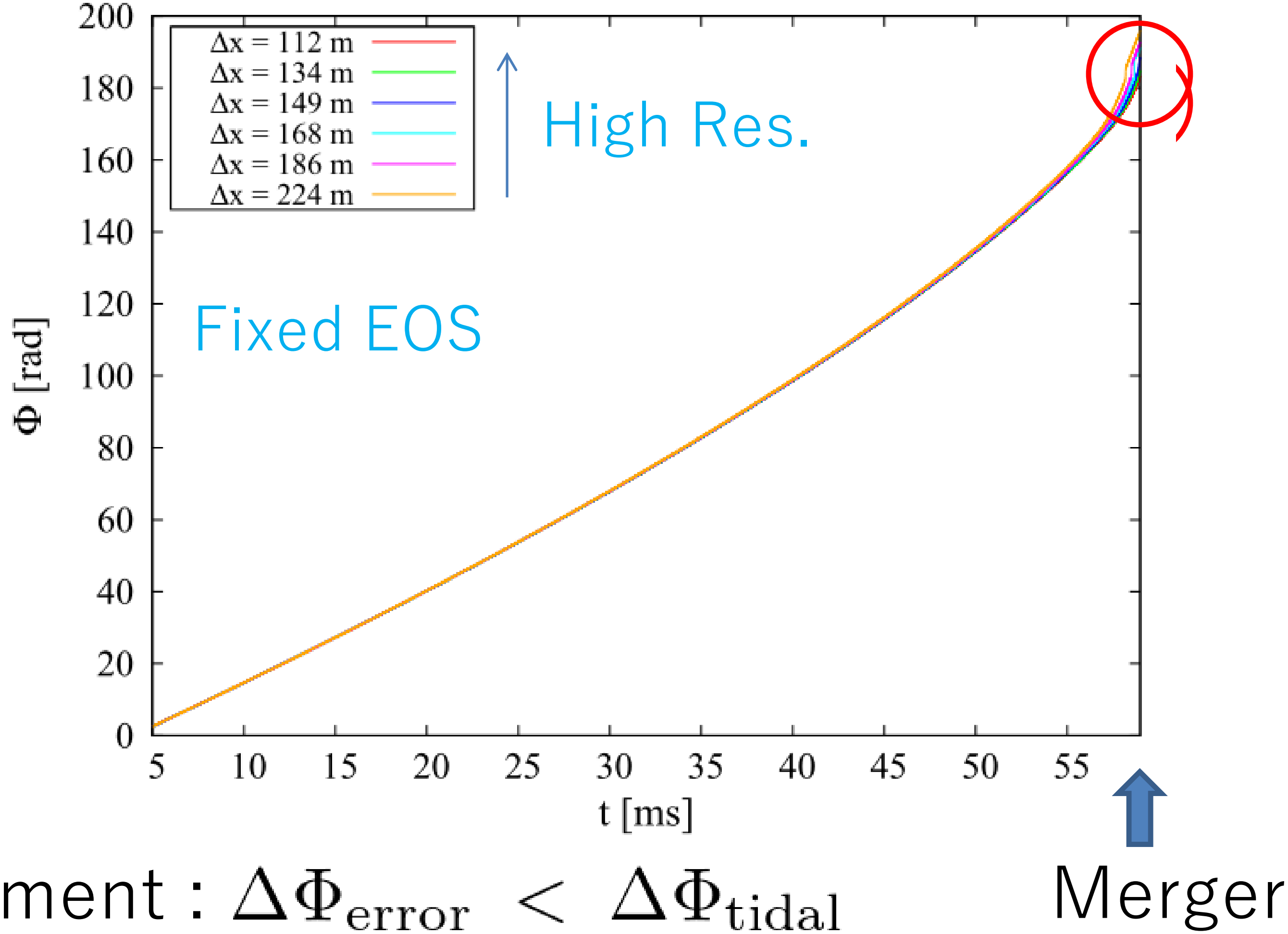

Requirement : $\Delta\Phi_{\mathrm{error}} < \Delta\Phi_{\mathrm{tidal}}$

Convergence study ⇒ Continuum limit

Toward a theoretical template bank

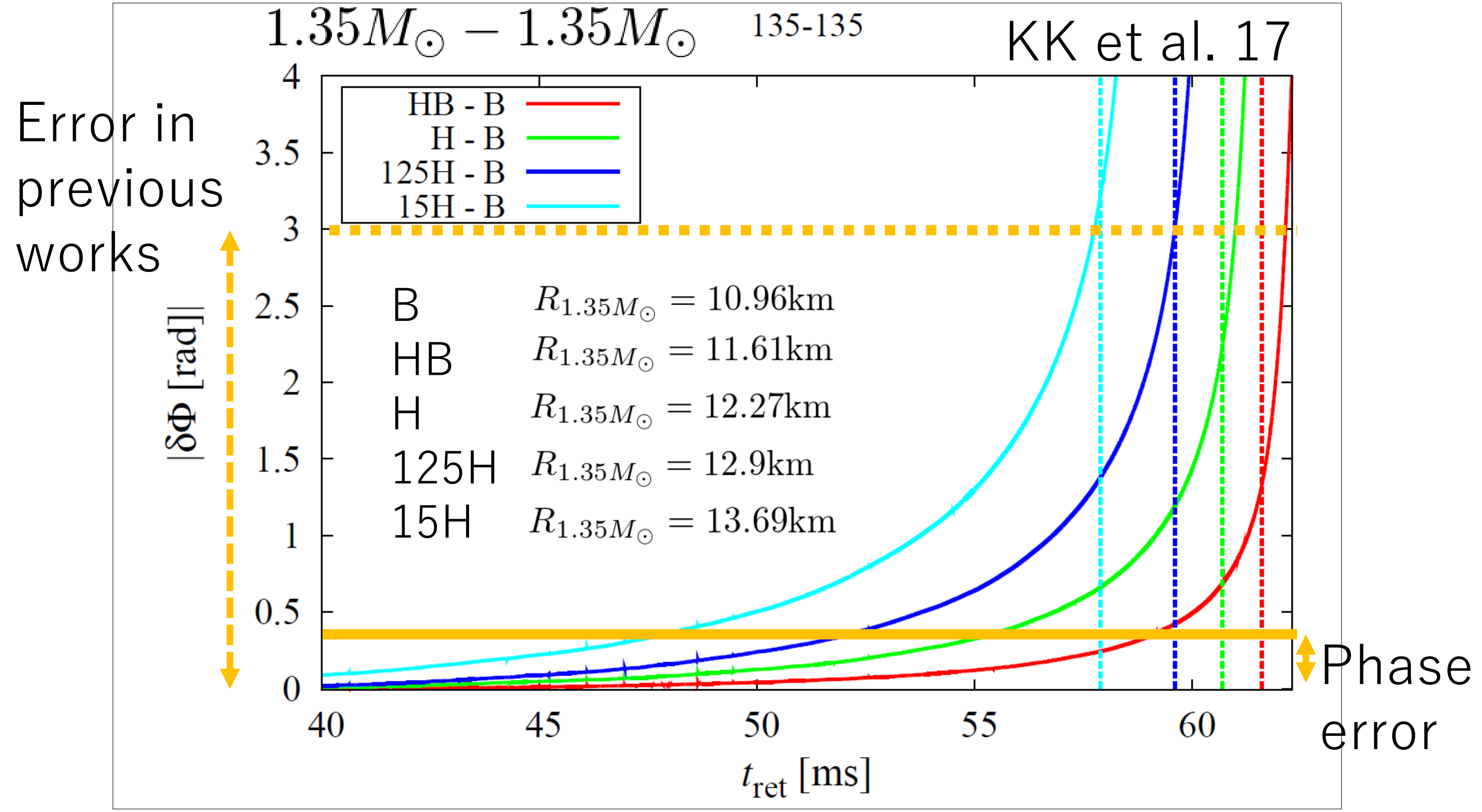

▶ Phase error is significantly suppressed.
c.f. 3-4 radian (Hotokezaka et al. 13) , 0.5-1.5 rad. (Dietrich et al. 17)

A step towards accurate late inspiral waveform

Super computers accelerate NR waveform production.

Systematic study is possible !

Key ingredients

▶ Resolution study (4-5 res.)

▶ Low eccentricity initial data ($e \sim 10^{-3}$)

▶ Long term evolution (15-16 orbits before the merger)

AEI-Kyoto BNS waveform data bank

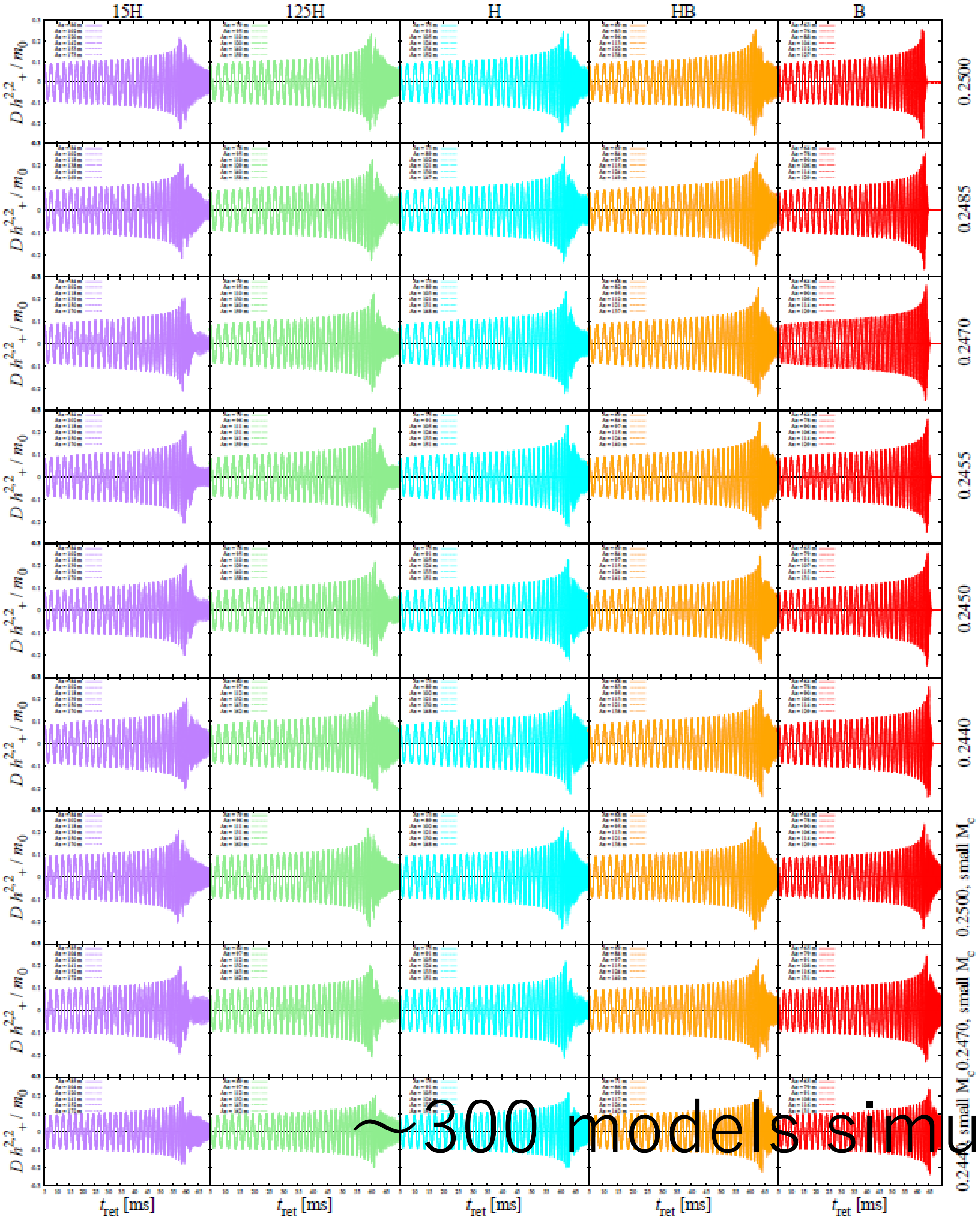

~300 models simulated so far

Phase shift of GWs $1.35M_\odot - 1.35M_\odot$

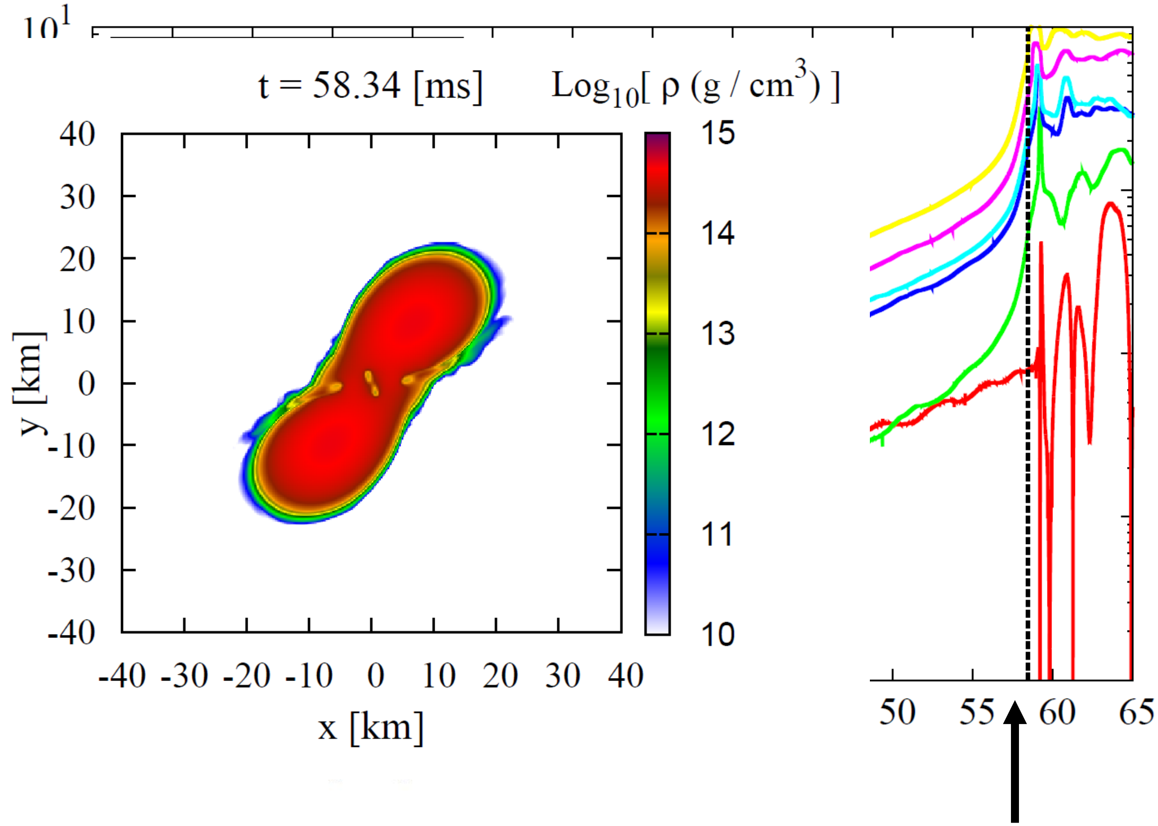

Peak time (58.42ms)

- ▶ Peak time = Time at maximum amplitude of GWs
- ▶ Phase shift is < 0.1 radian over 200 radian
- ▶ Merger before ∼0.5 ms is no longer two body problem

Toward a theoretical template bank

Error in previous works

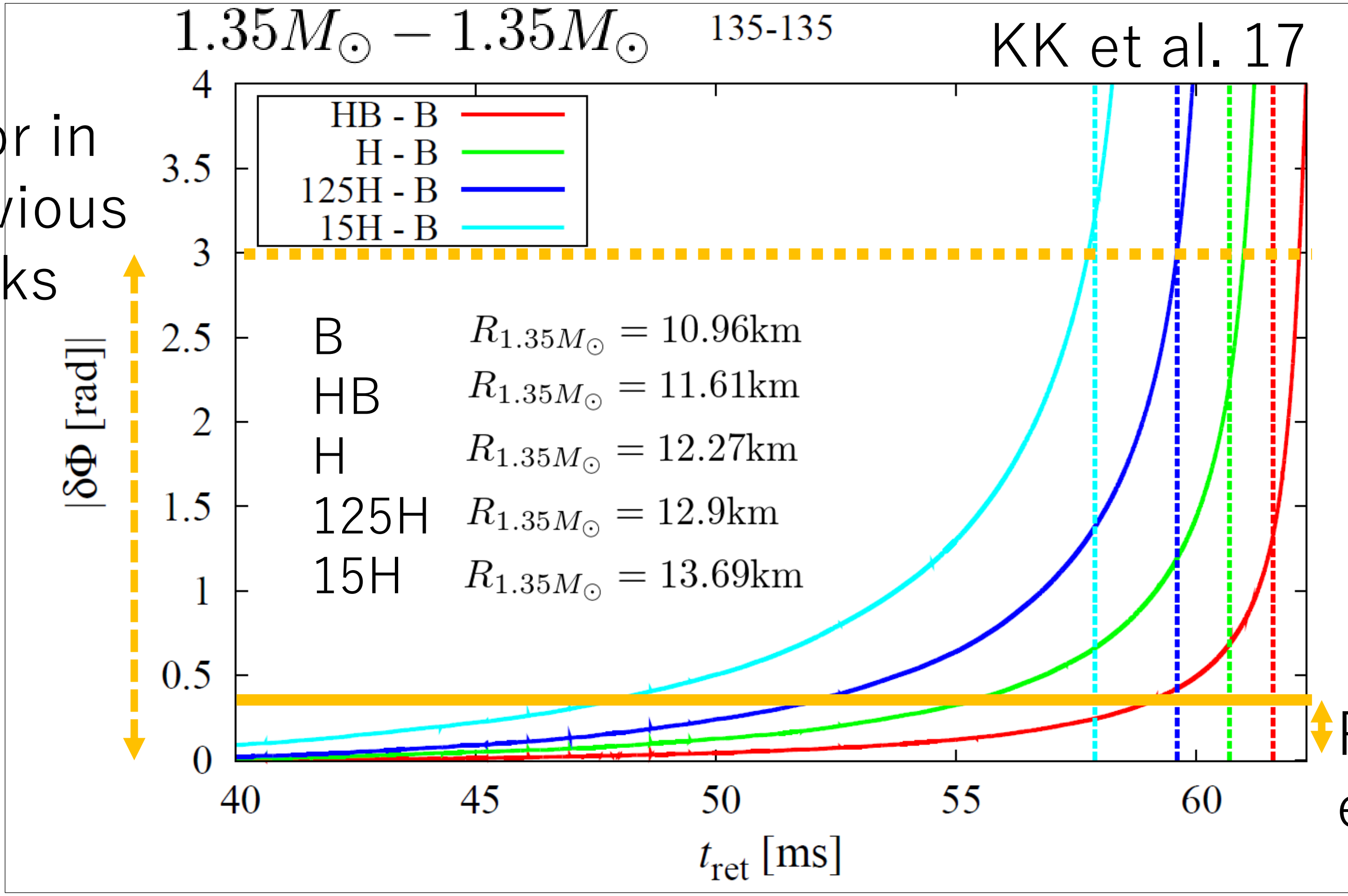

Phase error

▶ Phase error is significantly suppressed.

c.f. 3-4 radian (Hotokezaka et al. 13) , 0.5-1.5 rad. (Dietrich et al. 17)

Kyoto template (Kawatuchi, KK et al 18)

GW phase

$$\Phi_{\rm GW} = \underline{\Phi_{\rm point\ particle}} + \Phi_{\rm tidal}$$

Modeling in binary black hole systems (Nagar et al. 16)

Tidal part (Damour et al 12)

$$\Phi_{\rm tidal}^{2.5PN} = \frac{3}{32}\left(-\frac{39}{2}\Lambda\left(1 + a\Lambda^{2/3}x^{p}\right)\right)x^{5/2}$$

$$\times\left(1 + \frac{3115}{1248}x - \pi x^{3/2} + \frac{28024205}{3302208}x^{2} - \frac{4283}{1092}\pi x^{5/2}\right)$$

Λ : Tidal deformability

$x = (\pi m_0 f)^{3/2}$: Post-Newtonian parameter

Kyoto template (Kawaguchi, KK et al 18)

$$\Phi^{2.5PN}_{\mathrm{tidal}} = \frac{3}{32}\left(-\frac{39}{2}\Lambda(1 + a\Lambda^{2/3}x^{p})x^{5/2} \times \cdots\right)$$

Fitting by a NR simulation $a = 12.55, p = 4.24$

$\mathcal{M}_c = 1.175M_\odot,\ 1.088M_\odot,\ \eta = 0.25$

$\mathcal{M}_c = 1.175M_\odot,\ \eta = 0.25,\ 0.247,\ 0.244$

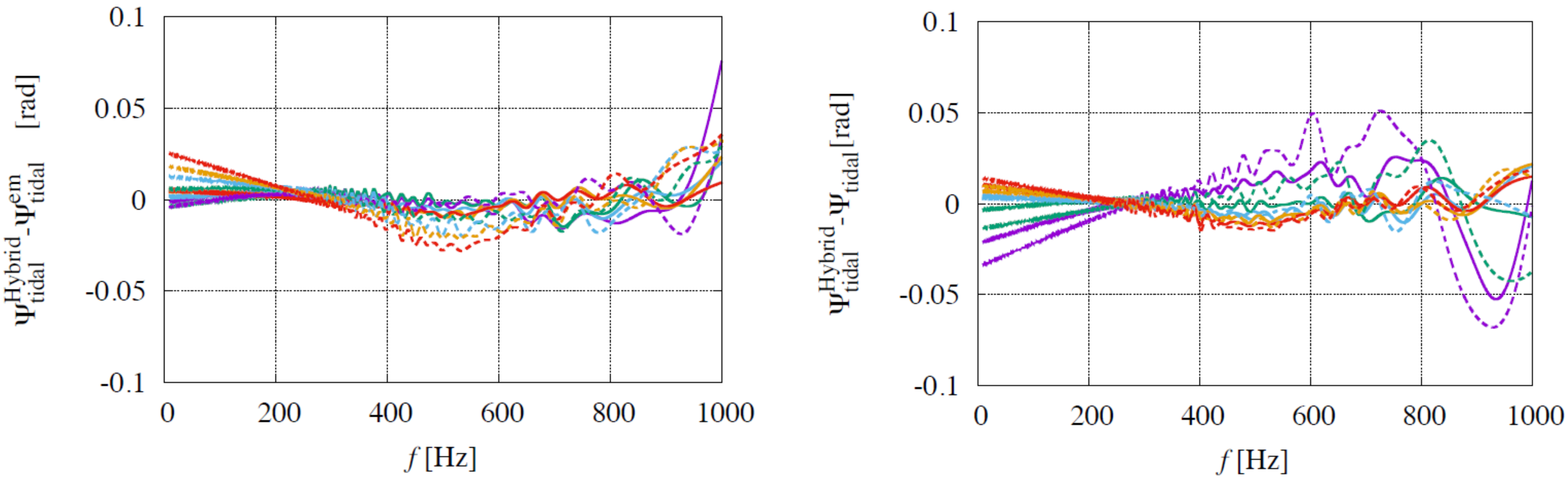

Statistical error in the measurement

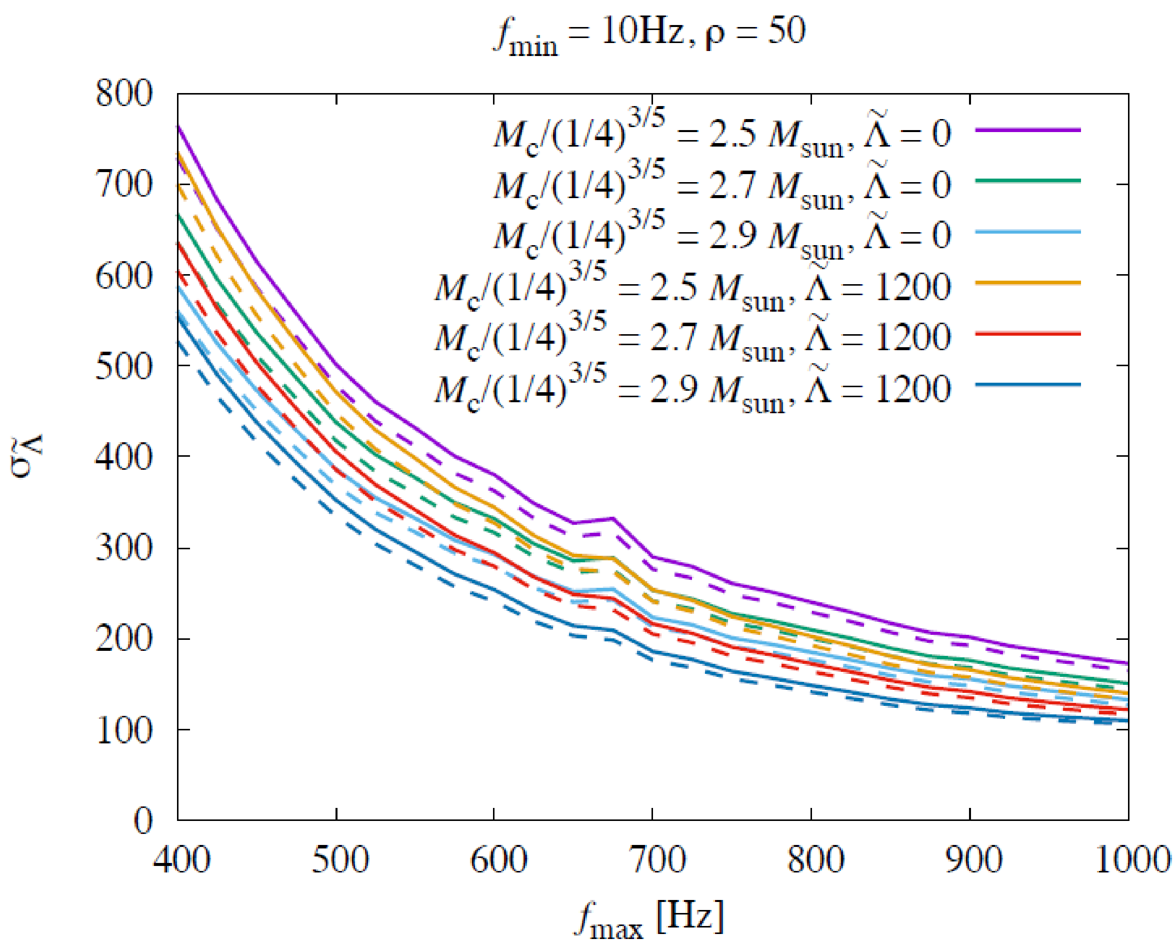

▶ Statistical error is improved as increasing f_{max}

Calibration of Kyoto template (KK et al. 19 in prep)

$$(\mathcal{M}_c, \eta) = (1.17524 M_\odot, 0.245)\ /\ (1.08819 M_\odot, 0.244)$$

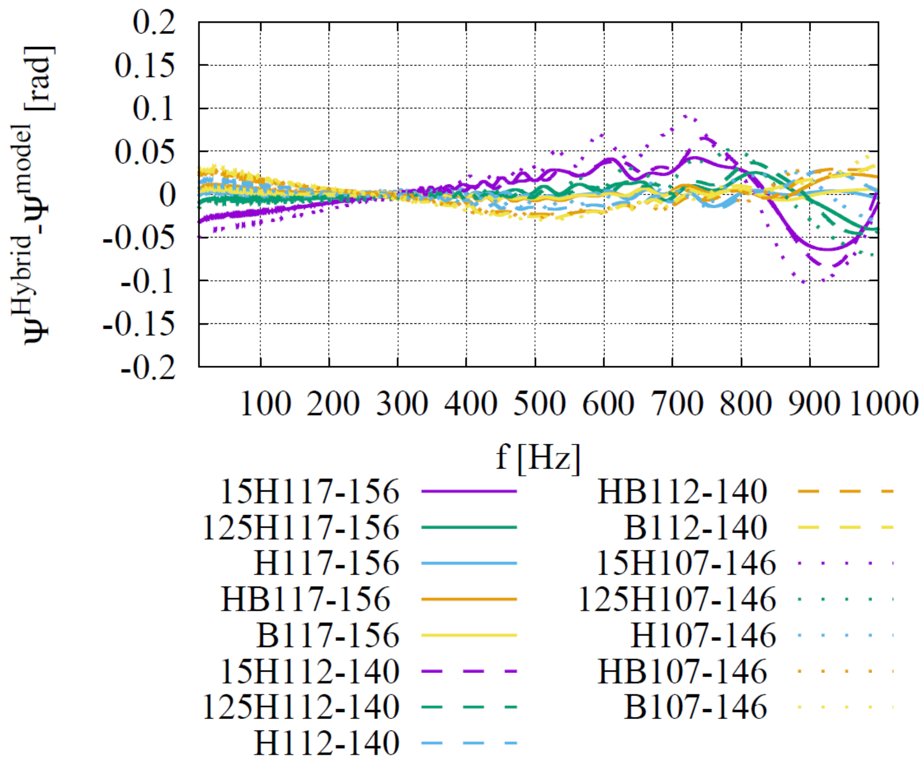

▶ Systematic error is less than 0.1 rad.

▶ Independent analysis of Adv. LIGO data of GW170817

Unlikely prompt collapse in GW170817 (KK et al. 19 in prep.)

▶EM observation suggests $M_{eje} \sim 0.05 M_\odot$ (e.g., Drout et al. 2017)

▶More sophisticated modeling of the ejecta could reduce to $M_{eje} \sim 0.03 M_\odot$ (e.g., Kawaguchi et al. 2018)

$$M_{eje} = M_{dyn} + M_{wind}$$

$M_{dyn} = 10^{-4} - 10^{-2}\ M_\odot$ (Hotokezaka, KK et al. 2013, Sekiguchi, KK et al. 2015)

$M_{wind} = O(10\%) \times M_{disk}$ (Fernandez & Metzger 2013)

Unlikely prompt collapse in GW170817 (KK et al. 19 in prep.)

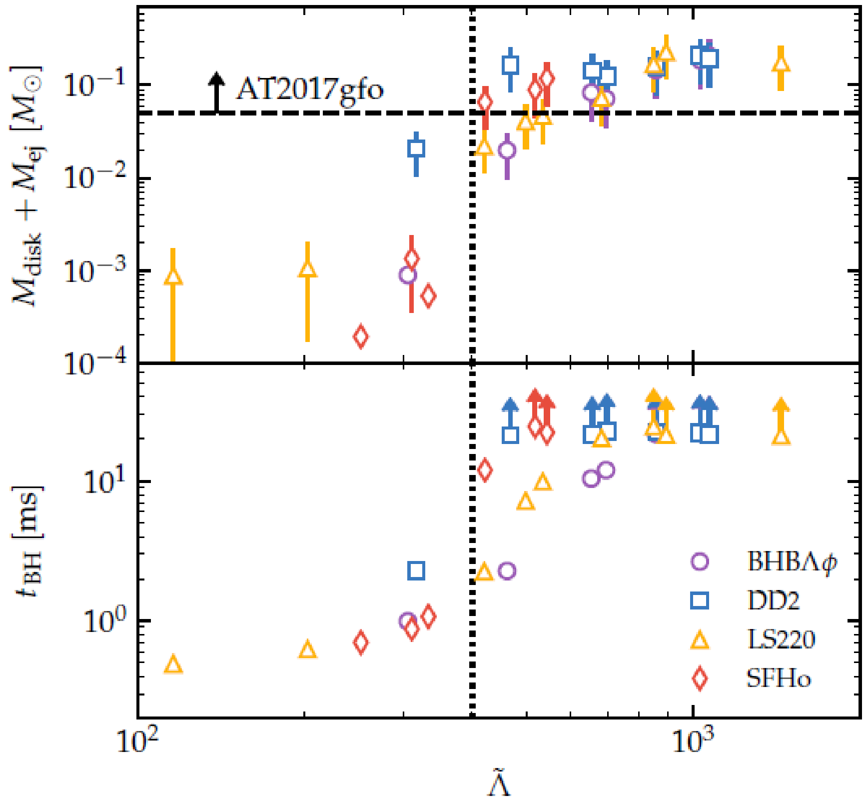

▶ Radice concluded the EM observation suggests $\Lambda \gtrsim 400$. (Radice et al. 2018)

▶ Caution : Employed EOSs have a correlation between M_{max} and Λ

Unlikely prompt collapse in GW170817 (KK et al. 19 in prep.)

Piece-Wise Polytropic EOS (Read et al. 2009)

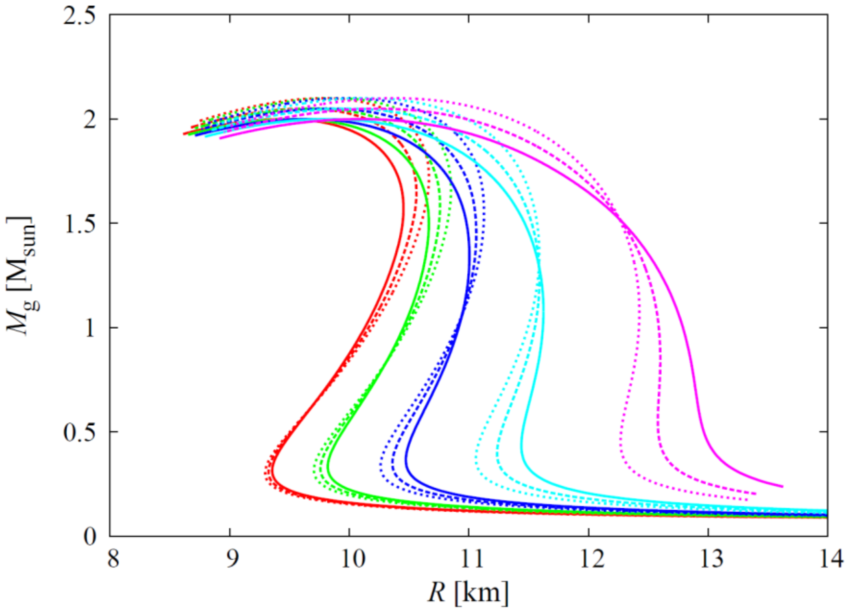

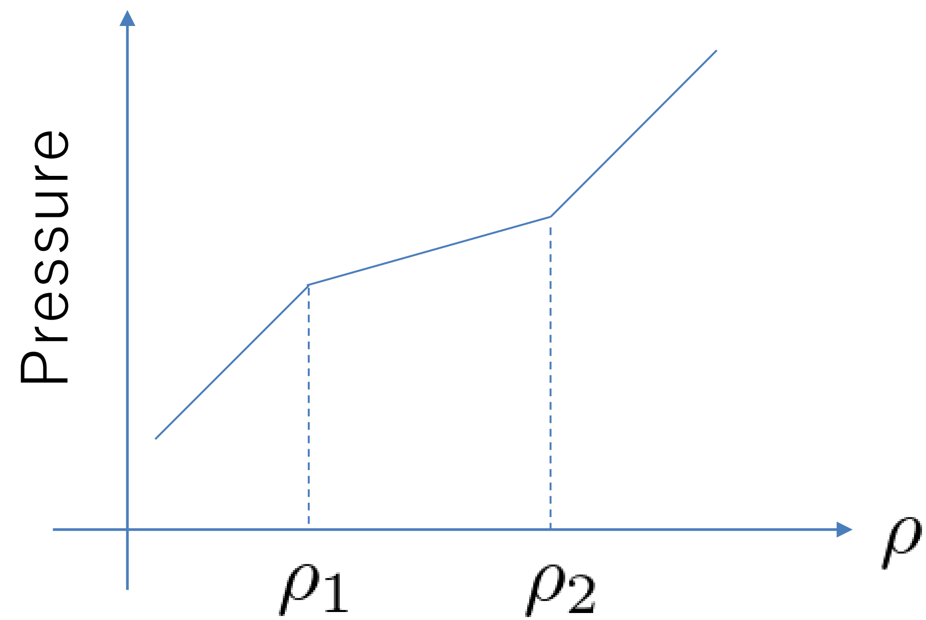

- $M_{max} = 2.00\text{-}2.10\ M_\odot$
- $\tilde{\Lambda}_{2.75 M_\odot} \approx 200 - 600$

- $1.375\text{-}1.375 M_\odot$ (equal mass). $1.2\text{-}1.55 M_\odot$ (unequal mass) (cf. $2.74^{+0.04}{}_{-0.01} M_\odot$ for GW170817)

Unlikely prompt collapse in GW170817 (KK et al. 19 in prep.)

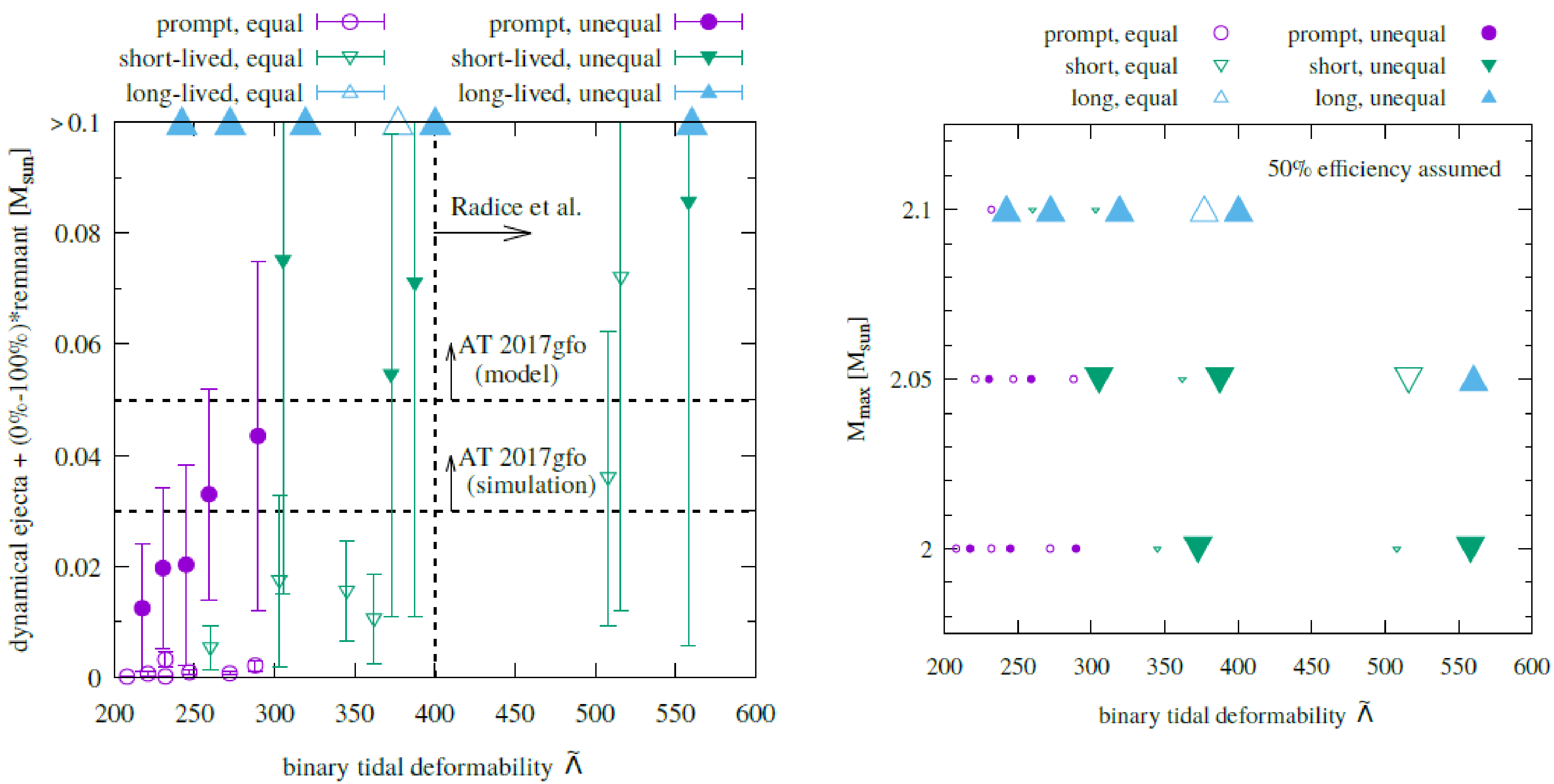

50% efficiency assumed
big (small) symbol : successful (failed) model to explain AT2017gfo

Post merger evolution of BNSs

(Bartos et al. 13)

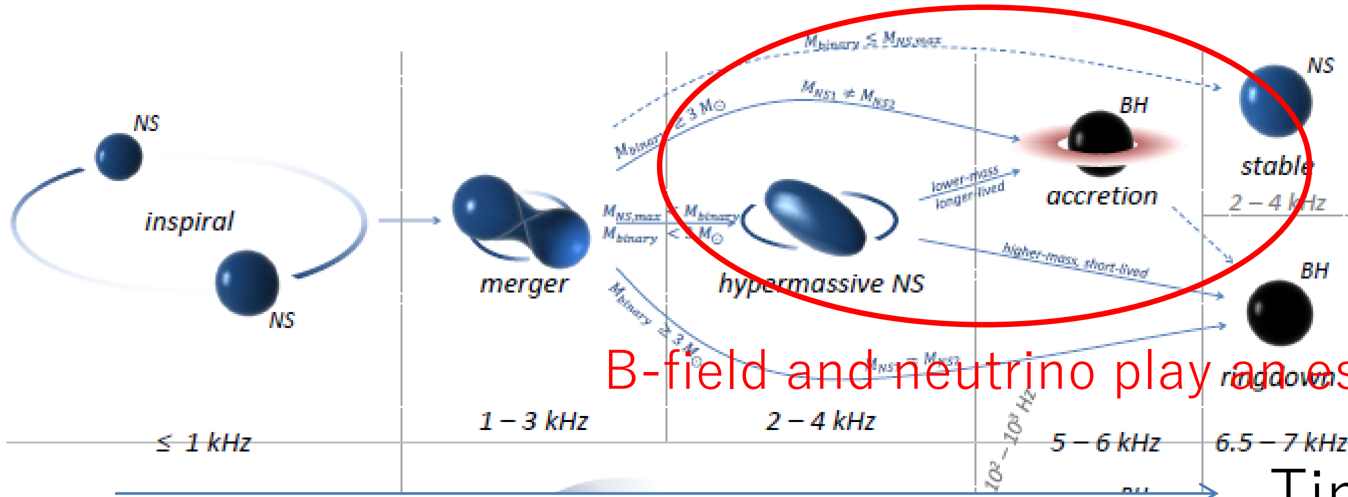

B-field and neutrino play an essential role

Time axis

Key ingredients

▶ Effective turbulent viscosity: MHD instability

▶ Electron fraction ≡ (# of electron)/(# of baryon) : Neutrino reaction

Importance of MHD turbulence

EOM : $\partial_t(\rho j) + \partial_R(\rho j v^R - \nu \rho R^2 \partial_R (j/R^2)) = 0$

ρ =density, j=specific angular momentum, ν = viscosity

▶ Angular momentum transfer by the viscous term.

▶ Energy dissipation due to the viscosity

Q. What is the "viscosity" ?

A. MHD turbulence :

$q = q_{ave} + \delta q$ s.t. $\langle q \rangle = q_{ave}$ and $\langle \delta q \rangle = 0$ where $\langle \cdot \rangle$ denotes time ensemble.

EOM : $\partial_t \langle \rho j \rangle + \partial_R(\langle \rho j v^R \rangle + R W_{R\varphi}) = 0$

Reynolds+Maxwell stress : $W_{R\varphi} = \langle \delta v^R \delta v^\varphi - \frac{B^R B^\varphi}{4\pi\rho} \rangle$

To B or not to B in binary NS merger

$\boxed{P - \dot{P} \text{ Diagram}}$

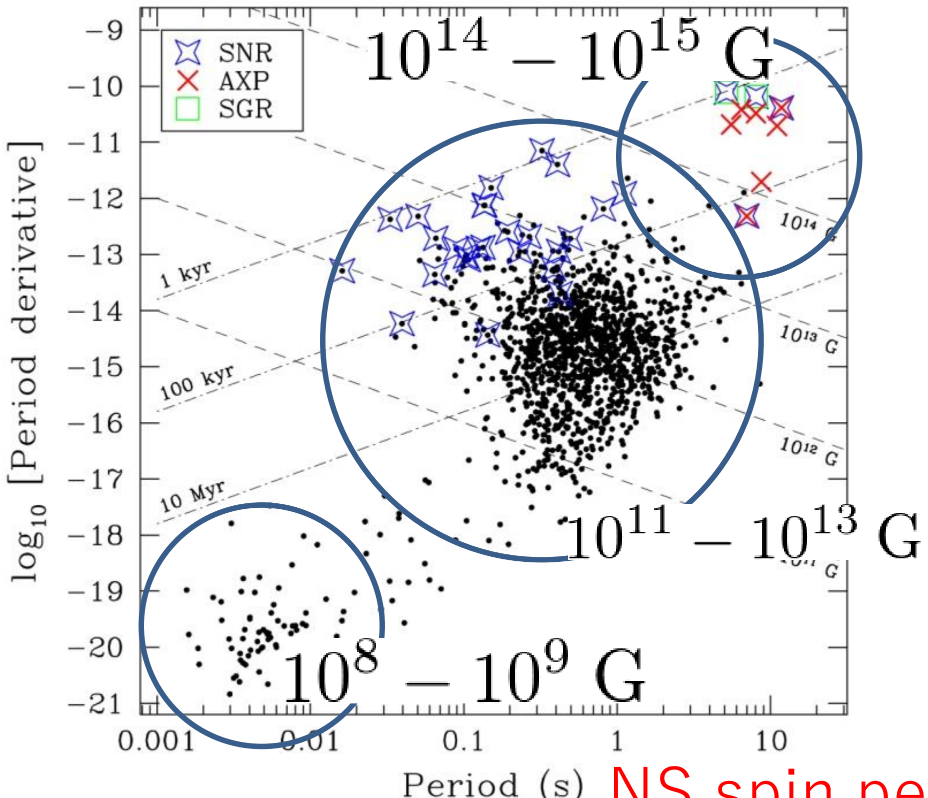

NS spin period

Image of the binary pulsar

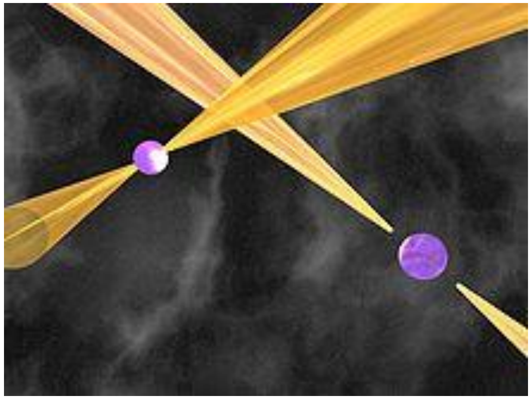

▶ Assumption : Rotational energy is dissipated by the magnetic dipole radiation $\Rightarrow B \propto (P\dot{P})^{1/2}$

To B or not to B in binary NS merger

▶ B-field in observed binary NSs : $10^{9.7} - 10^{12.2}$ G

Kinetic energy at the merger $\sim 10^{53}$ g cm^2 s^{-2} $\times (M/2.7M_{sun})(v/0.3c)^2$

B-field energy $\sim 10^{41}$ g cm^2 s^{-2} $(B/10^{12}G)^2(R/10^5cm)^3$

B-field is irrelevant in BNS mergers ?

No ⇒ Several amplification mechanisms (Magneto Hydro Dynamical instabilities) could amplify the B-filed

B-field amplification @ the merger

Kelvin Helmholtz instability (Rasio and Shapiro 99, Price & Rosswog 05)

Mini

k_{min}

⇒ If

m^3)]

-5 0 5

x [km]

-12 -8 -4 0 4 8 12

x [km]

GRMHD by AEI(Giacomazzo et al. 11)

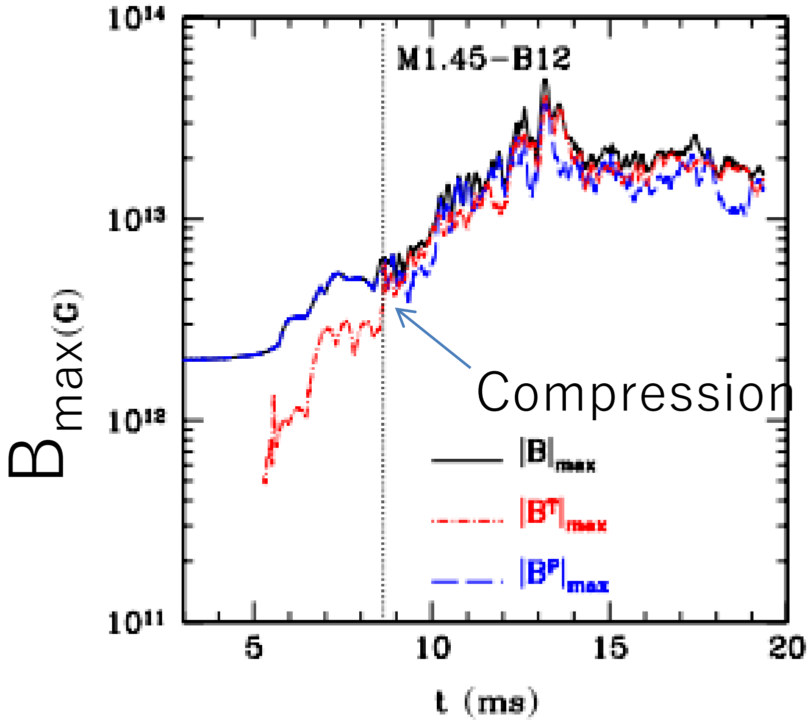

Local box simulation (Zrake and MacFadyen 13, Obergaulinger et al. 10)

Time evolution of <B>

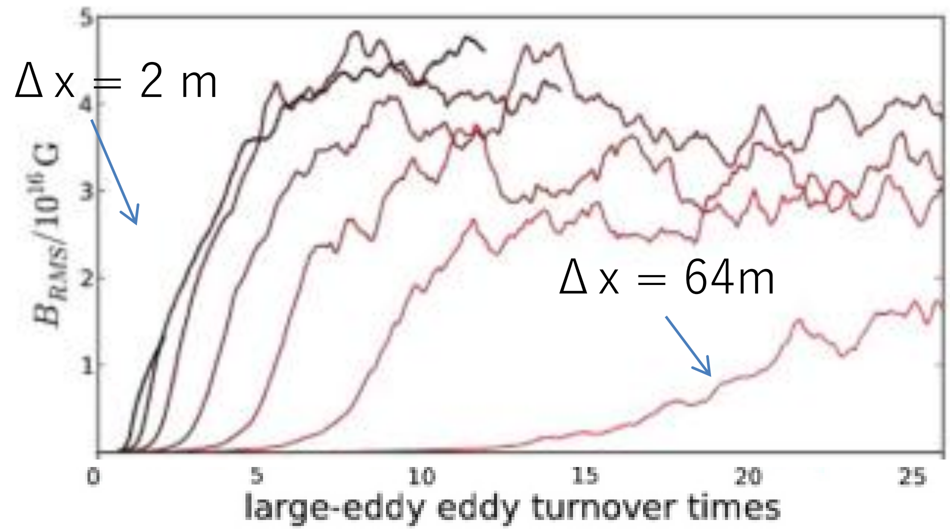

1=0.1ms

Can really the KH vortices amplify the B-fields ?

Explore the B-field amplification on K

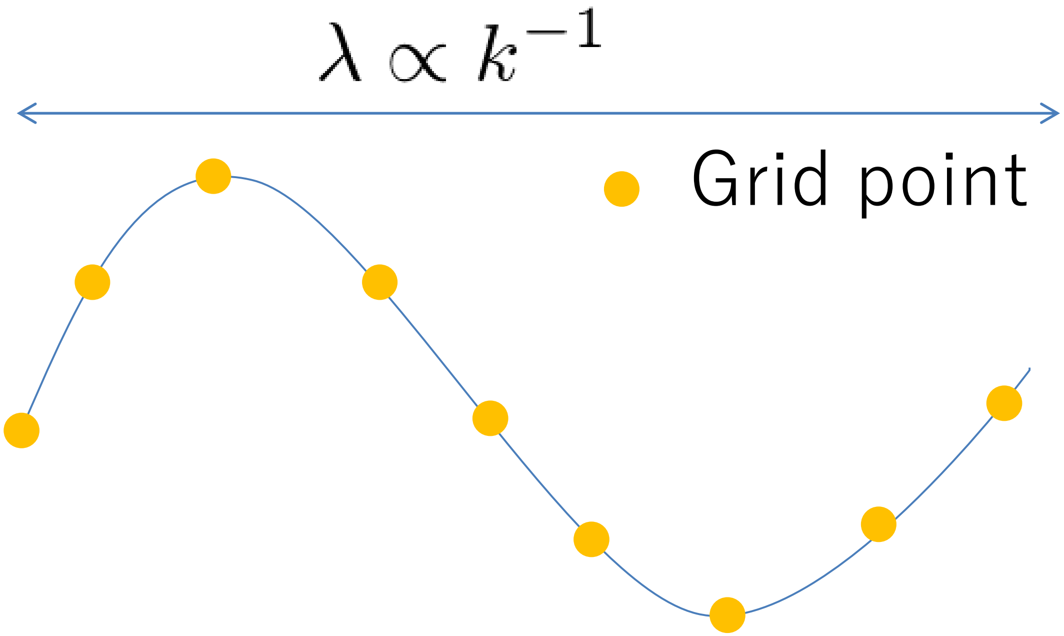

Note : growth rate ∝ wave number in the KH instability ⇒ Large scale simulation is necessary

Magnetic field amplification

B-field energy evolution

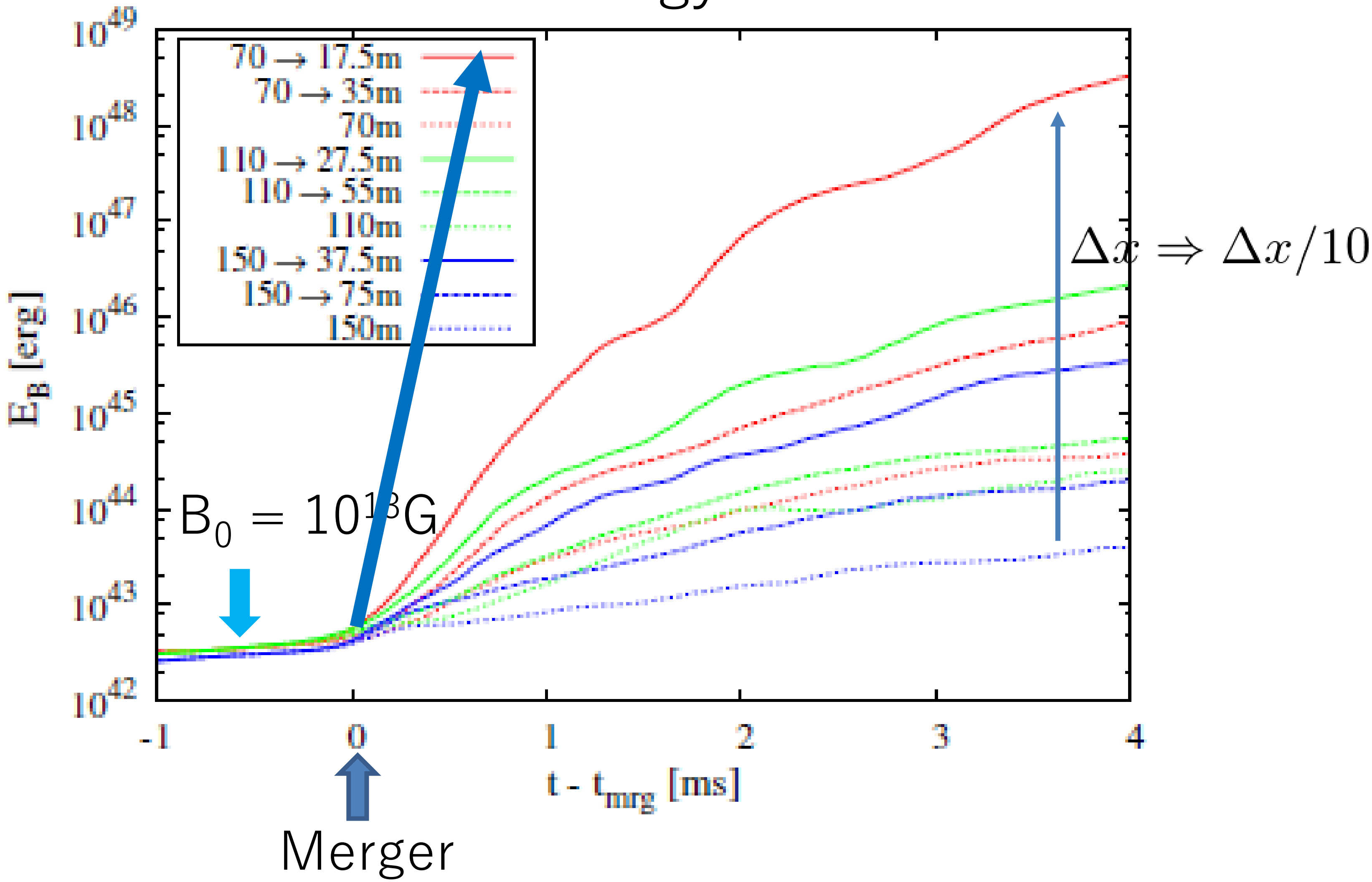

▶ The growth rate shows the divergence. c.f. $\sigma \propto$ wave-number for KH instability.

Long term evolution of remnant massive NS

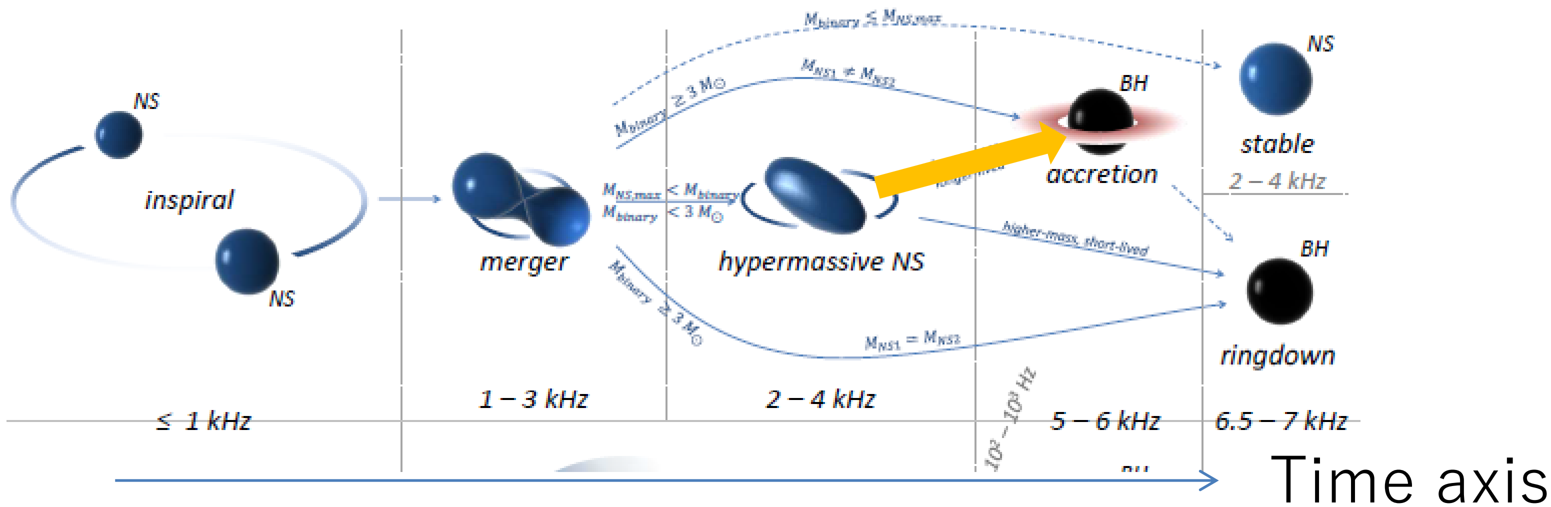

Our strategy

▶High res. GRMHD simulation ⇒ Evaluation of effective viscosity

▶Relativistic viscous simulation ⇒ Given a viscosity parameter, systematic study is doable.

Magneto Rotational Instability (MRI)

▶ (Balbus & Hawley 91)

Differential rotation $\nabla\Omega < 0 \Rightarrow B(t) \propto \exp(\sigma t),\ \sigma \approx \Omega$

Intuitive explanation of MRI

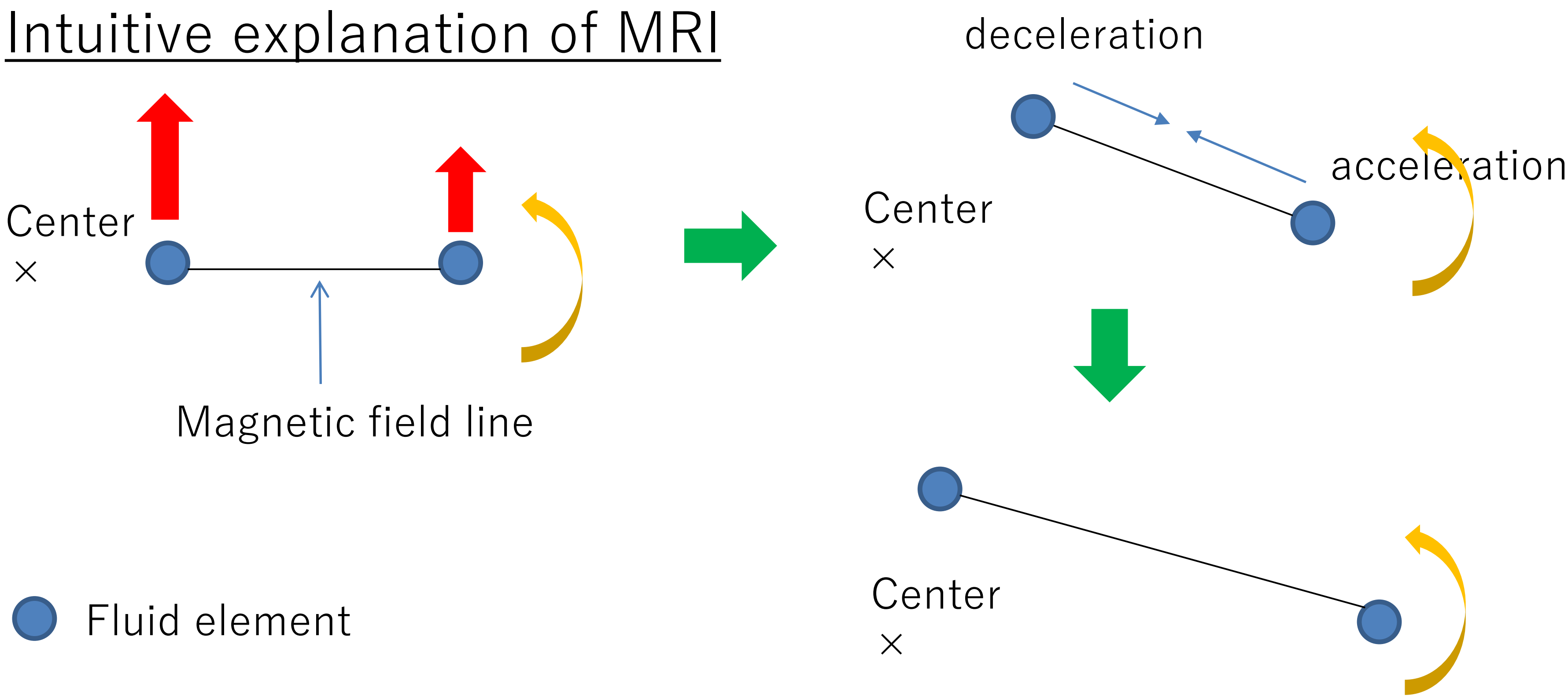

MRI produces turbulence as well.

High res. GRMHD simulation of remnant NS

(KK et al. 2018)

To do list: Read α-viscosity parameter from MHD simulation data

$$\alpha = \left\langle \frac{W_{R\varphi}}{P} \right\rangle$$

$W_{R\phi}$: Reynolds + Maxwell stress

Caveat: Resolution study is essential again because numerical diffusion kills the "turbulence",

i.e., underestimate the viscous parameter

Result

Simulation setup

▶1.25 $M_\odot$ -1.25 $M_\odot$ BNS with H4 EOS (Glendenning and Moszkowski 91), M_{max}=2.03 $M_\odot$

▶ “Long” term simulation of 30ms with Δx=12.5m, 70, 110

▶ Assume a relatively high-B field of 10^{15}G justified by the Kelvin-Helmholtz vortex amplification (Kiuchi et al. 15)

Power spectrum of the B field

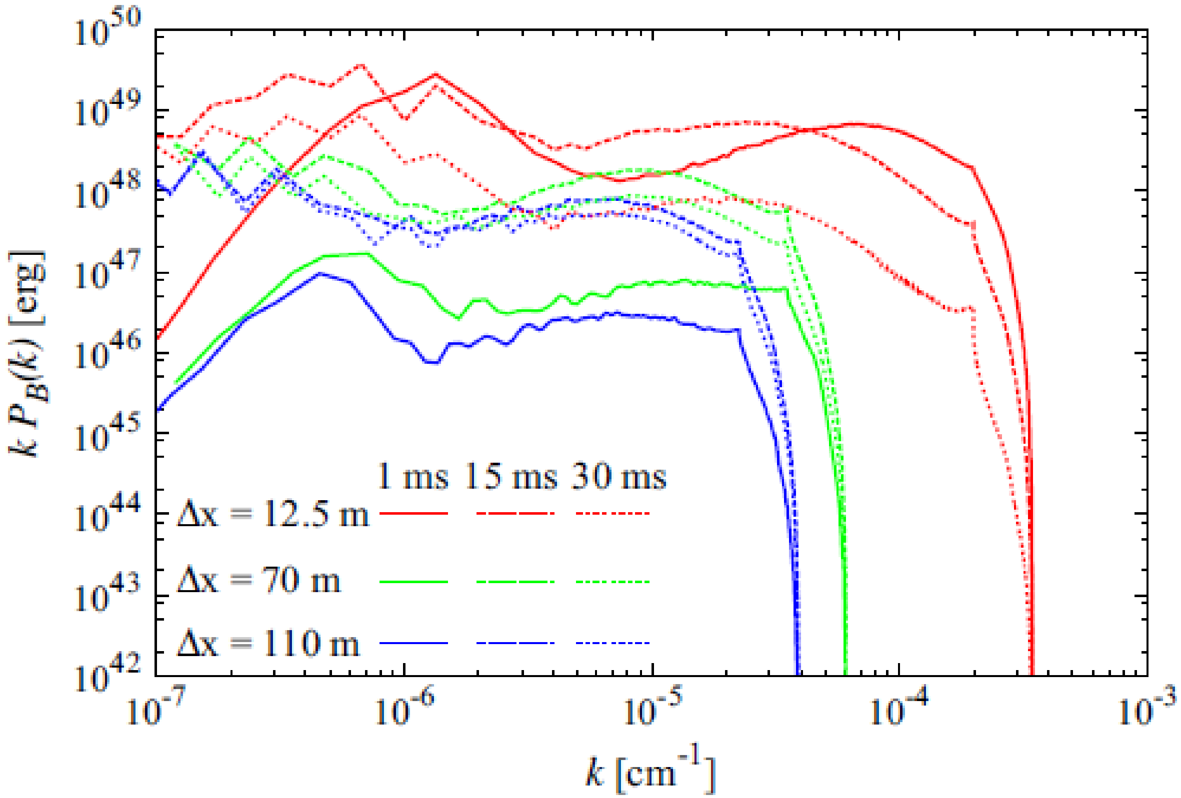

▶ KH instability amplifies the small scale magnetic field efficiently

▶ Magneto Rotational Instability sustains the turbulence

α -viscosity parameter

$$13 \leq \log_{10}[\rho\,(\mathrm{g\,cm^{-3}})] < 14$$

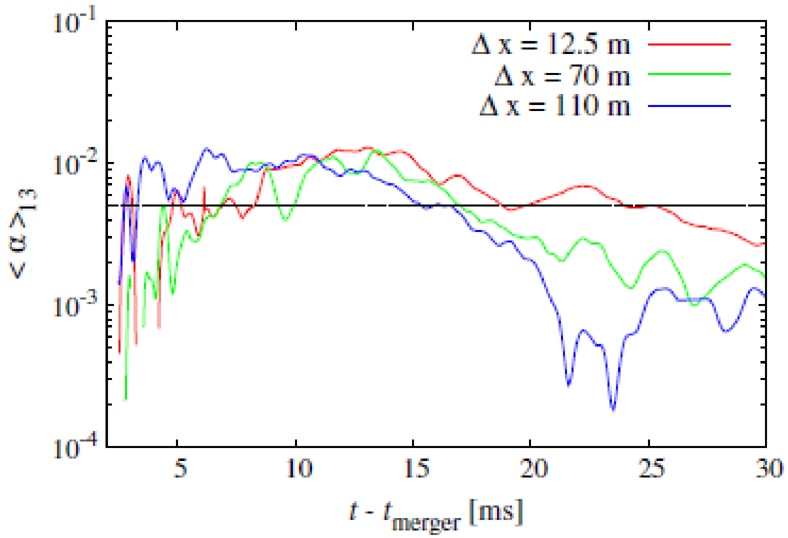

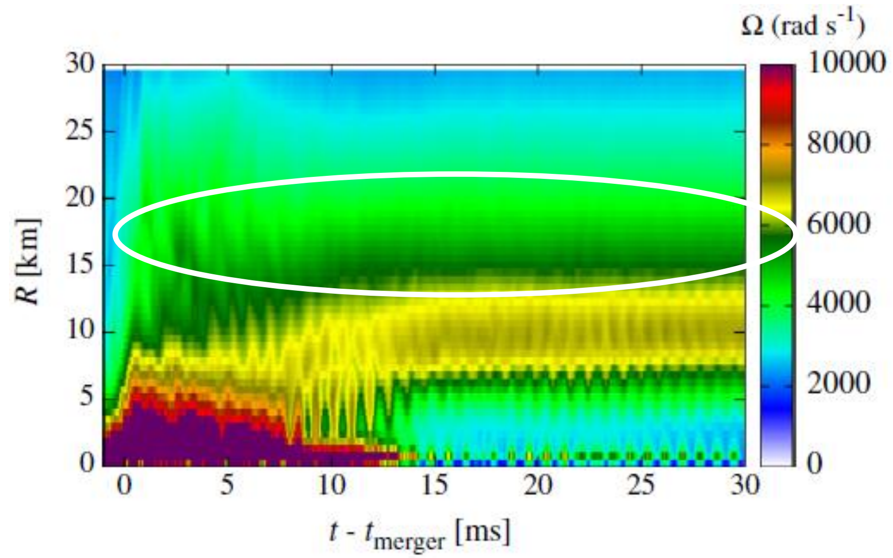

▶ $<<\alpha>> \gtrsim 4\times10^{-3}$ for the core

▶ $t_{vis} \lesssim 120$ ms $(<<\alpha>>/\,4\times10^{-3})^{-1}$
$\times(<j>/1.7\times10^{16}\mathrm{cm^2s^{-1}})(<c_s>/0.2c)^{-2}$

α -viscosity parameter

$$12 \leq \log_{10}[\rho\ (\mathrm{g\ cm^{-3}})] < 13$$

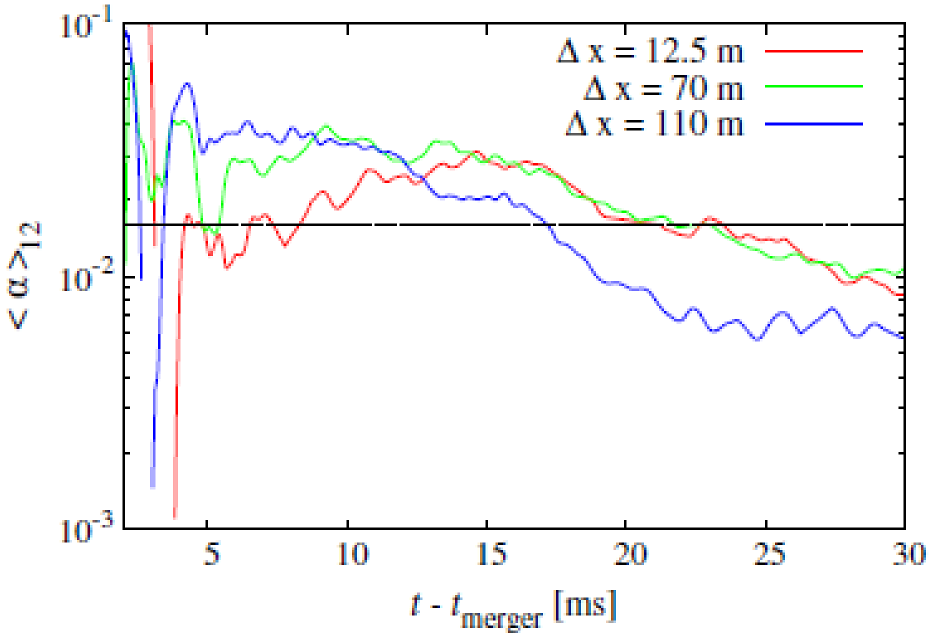

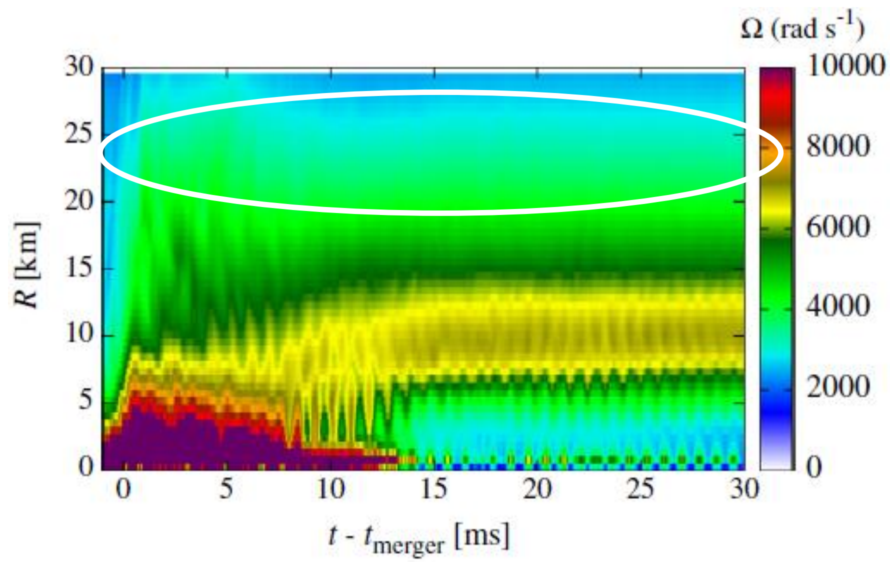

▶ $<<\alpha>> \approx 1 \times 10^{-2}$ for the envelope

Short summary of the fate of remnant NSs

▶ MHD simulation ⇒ α viscosity evaluation ⇒ Angular momentum transport

MHD simulation is too expensive.

▶ Viscous simulation is a second best approach to explore the angular momentum transfer problem in remnant massive NS.

Effects of the viscosity on GWs from merger remnant (Shibata & KK 17a, b. Radice 17)

▶ α is likely to be $O(10^{-2})$ in merger remnants
⇒ Angular momentum transport may affect post merger GW signals.
▶ Implementation of the Israel-Stewart formulation of a viscous fluid (Causality preserving formulation)

<u>Set up.</u>
Hydro simulation of BNS merger without viscosity up to ~5ms after the merger.
⇒ Switch on the viscosity $\nu = \alpha \frac{c_s^2}{\Omega}$
⇒ Perform a simulation for a viscous timescale

Effects of the viscosity on GWs from merger remnant (Shibata & KK 17a, b)

$\alpha = 0$ $\qquad\qquad$ $\alpha = 0.02$

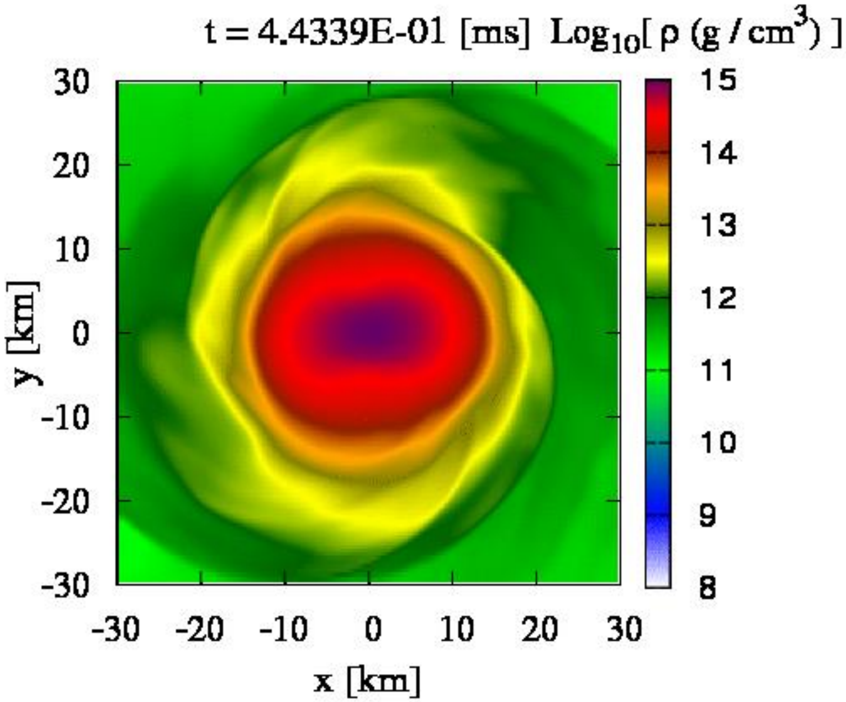

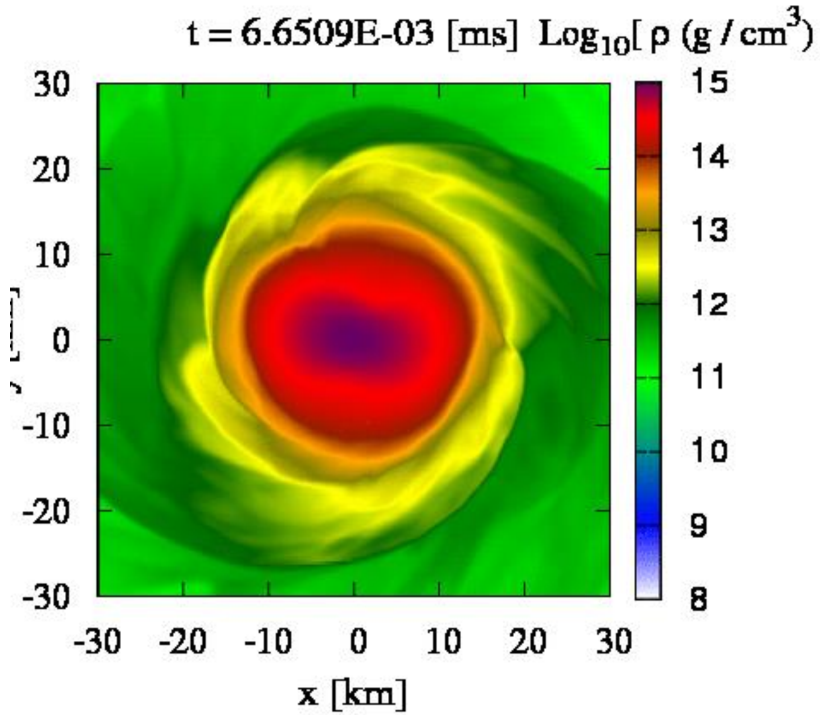

▶ Non-axisymmetric structure of the HMNS remains for the inviscid case (many references).

▶ Nearly axi-symmetric structure for the viscid case

Angular velocity evolution

$\alpha = 0.00$

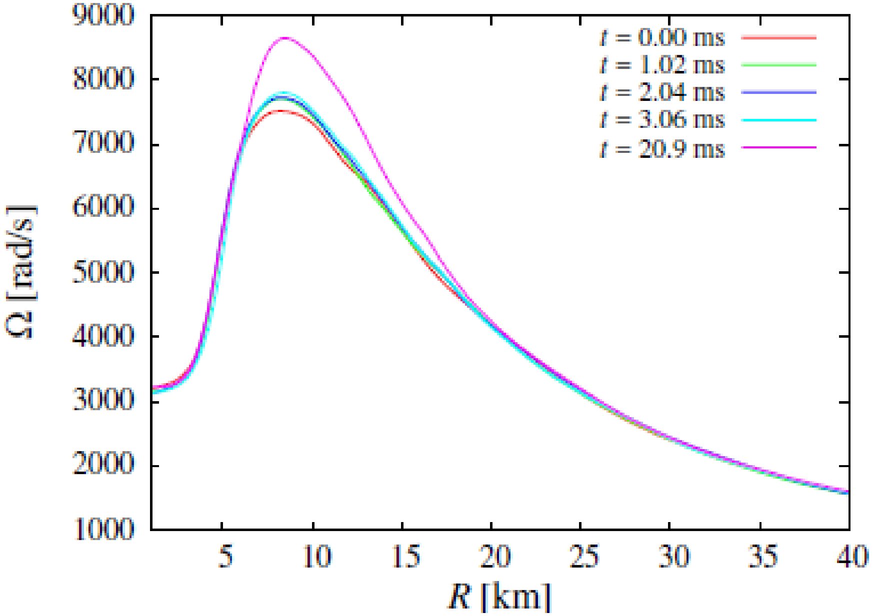

$\alpha = 0.02$

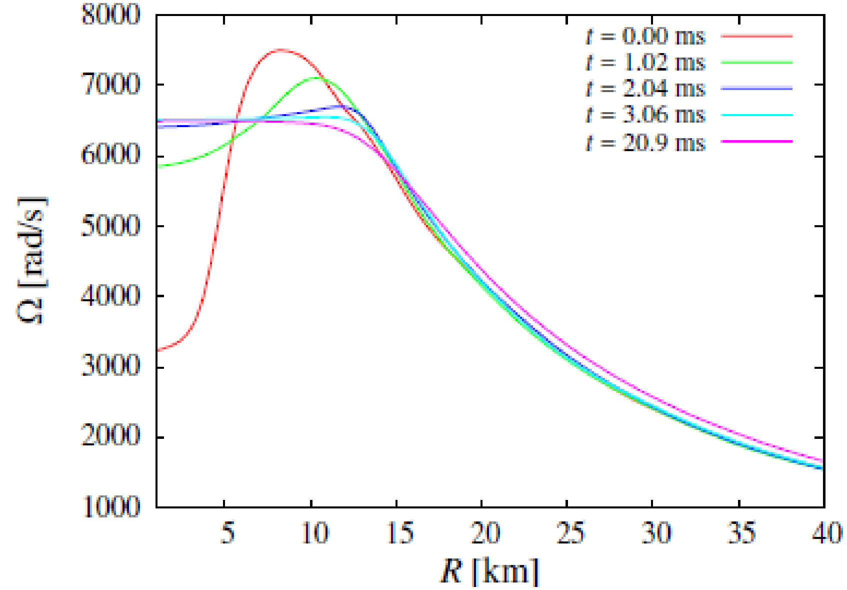

▶ Inner part quickly relaxes into an uniform rotation

cf. $t_{\mathrm{vis}} \approx 4.4\,\mathrm{ms}(\alpha/0.01)^{-1}(c_s/0.5\,c)^{-2}(R/10\,\mathrm{km})^2(\Omega/10^4\,\mathrm{rad/s})$

▶ The density structure relaxes into an axi-symmetric structure.

Effects of the viscosity in GWs from merger remnant (Shibata & KK 17a, b)

Waveforms

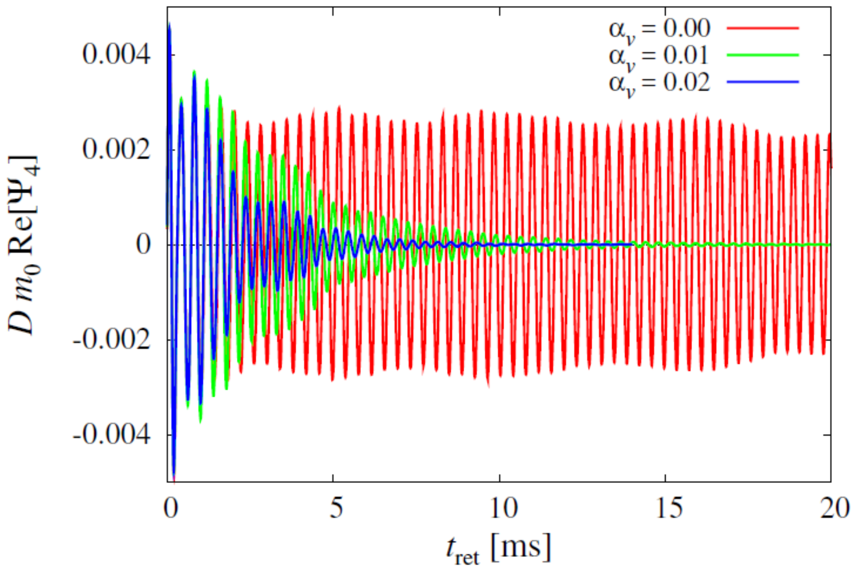

Spectrum

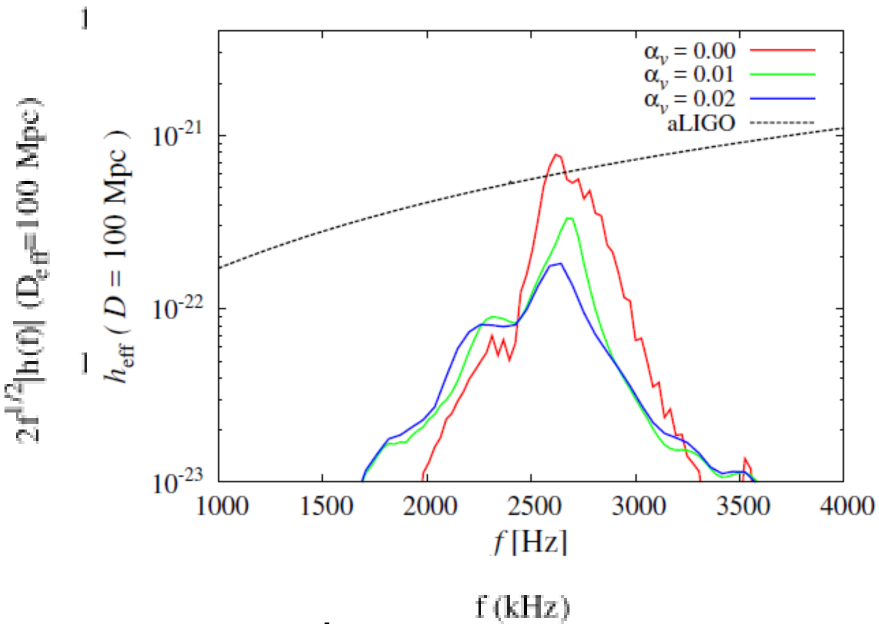

- ▶ Quasi periodic GWs for the inviscid case.
- ▶ Peak frequency around 2-4 kHz imprints information of the EOS. Shibata 05, Shibata & Tanguchi 09, Hotokezaka et al. 13, Bawswein et al. 12, 13, 15, Takami et al. 14, 15, 16
- ▶ No post merger signal from GW170817 (LSC collaboration 17)

Optical-Infrared emission from BNS mergers
(Metzger et al. 10)

Role of the r-process elements

▶ Heating source via radio-active decay

$$\dot{\epsilon} \approx 10^{10}\,\mathrm{erg\,s^{-1}\,g^{-1}} \left(\frac{t}{\mathrm{day}}\right)^{-1.3}$$

▶ Opacity source (Lanthanide elements) (Barnes & Kasen 13, Tanaka & Hotokezaka 13)

$$\kappa \approx 10\,\mathrm{cm^2\,g^{-1}}$$

Properties of electromagnetic emission (Optical-IR)

▶ Peak time (diffusion time = dynamical time)

$$t_{\mathrm{peak}} \approx 5.7\,\mathrm{day} \left(\frac{\kappa}{10\,\mathrm{cm^{-2}\,g^{-1}}}\right)^{1/2} \left(\frac{M_{\mathrm{eje}}}{0.03M_{\odot}}\right)^{1/2} \left(\frac{v_{\mathrm{ej}}}{0.2c}\right)^{-1/2}$$

▶ Peak Luminosity

$$L \approx \dot{\epsilon} M_{\mathrm{ej}} \approx 6 \times 10^{41}\,\mathrm{erg\,s^{-1}} \left(\frac{M_{\mathrm{eje}}}{0.03M_{\odot}}\right) \left(\frac{t}{\mathrm{day}}\right)^{-1.3}$$

R-process nucleosynthesis and its opacity

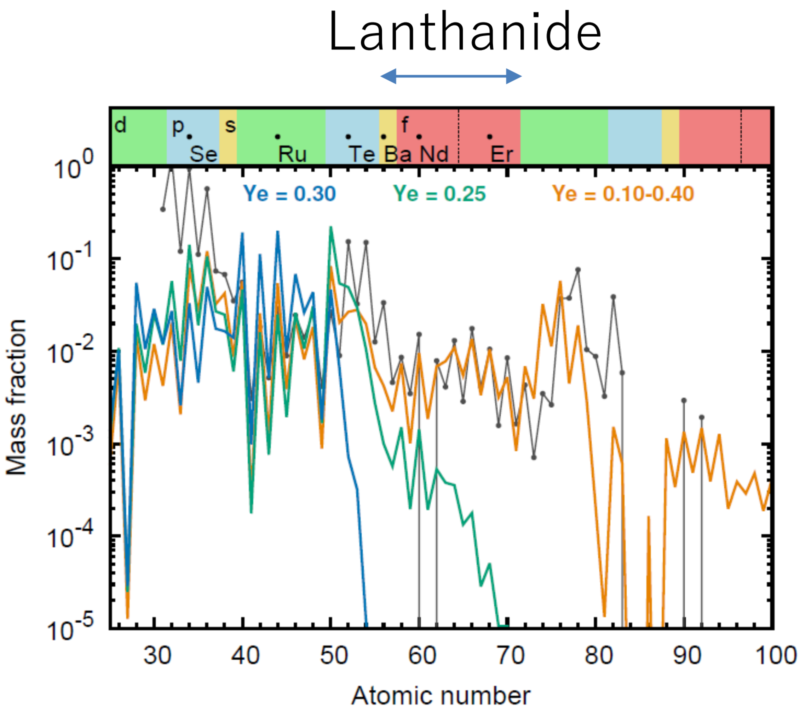

Tanaka et al. 17

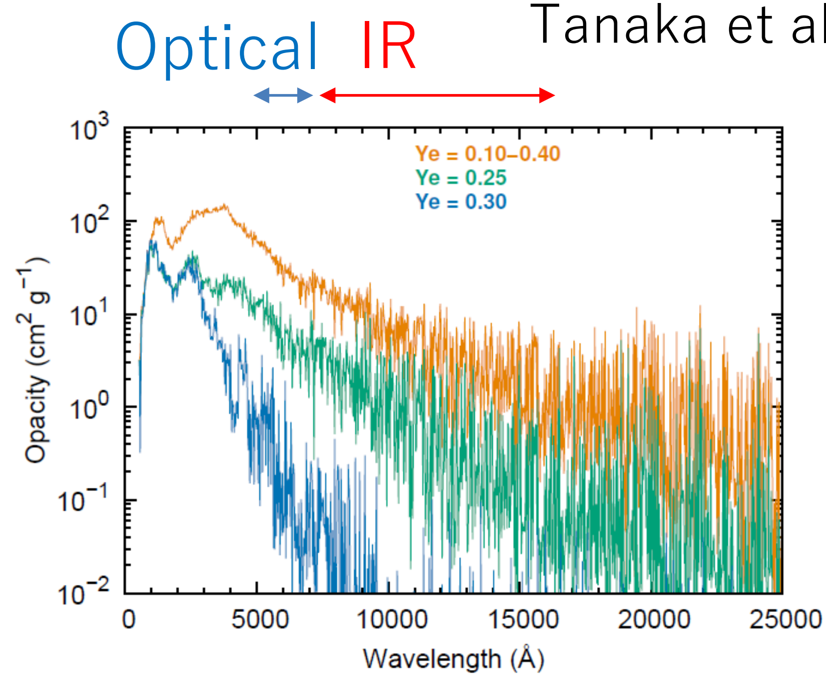

- ▶ Electron fraction Y_e is a key quantity
- ▶ $Y_e \gtrsim 0.25$ produces negligible / small amount of lanthanide ⇒ low opacity in optical
- ▶ $Y_e \lesssim 0.25$ produces lanthanide ⇒ high opacity in IR
- ▶ Neutrino reaction determine Y_e of the ejecta

Detected UV-Optical-Infrared emission

- Long-duration IR component (Red)

$$t_{\rm peak} \approx \ 7.1 \ {\rm day} \left(\frac{\kappa}{10 \ {\rm cm^2 g^{-1}}}\right)^{1/2} \left(\frac{M}{0.035 M_\odot}\right)^{1/2} \left(\frac{v_{\rm eje}}{0.25c}\right)^{-1/2}$$

- Short-duration UV-IR component (Blue)

$$t_{\rm peak} \approx \ 1.5 \ {\rm day} \left(\frac{\kappa}{1 \ {\rm cm^2 g^{-1}}}\right)^{1/2} \left(\frac{M}{0.025 M_\odot}\right)^{1/2} \left(\frac{v_{\rm eje}}{0.25c}\right)^{-1/2}$$

Short-duration blue component suggests the low-opacity (Lanthanide-free elements) ejecta.

We build a model of GW170817 based on the NR simulations : neutrino radiation transfer & effective turbulent viscosity

Numerical modeling of GW170817 (Shibata et al. 18, Fujibayashi, KK et al. 17)

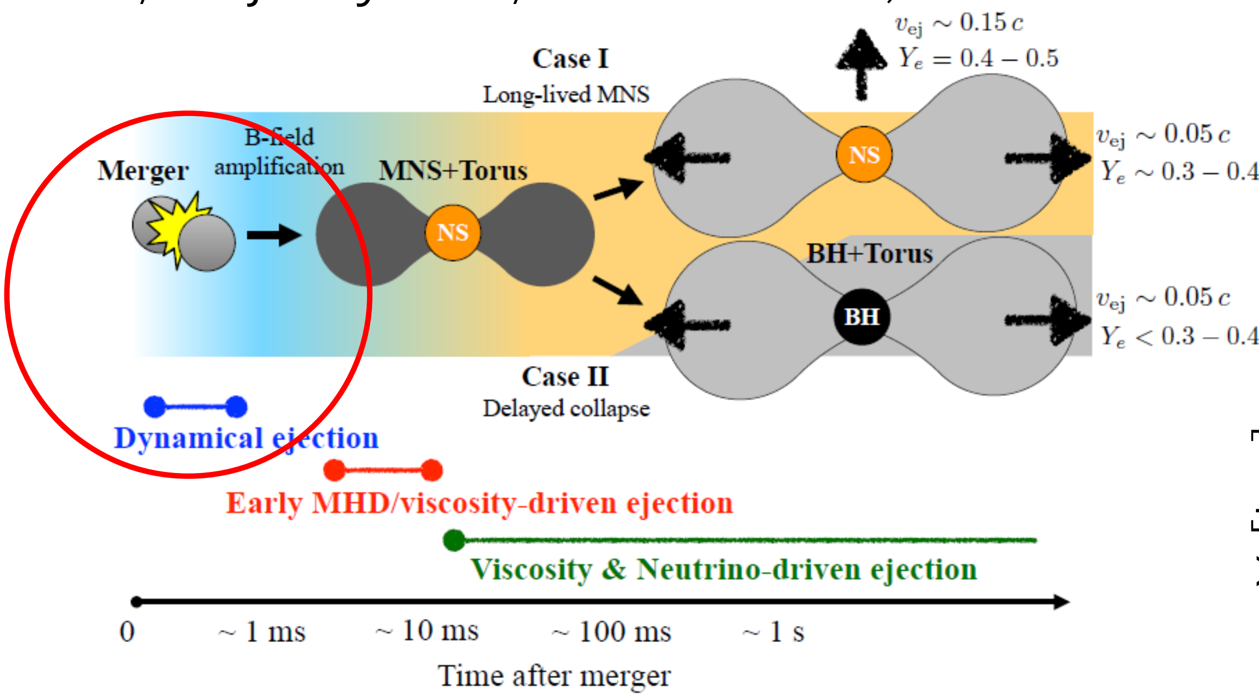

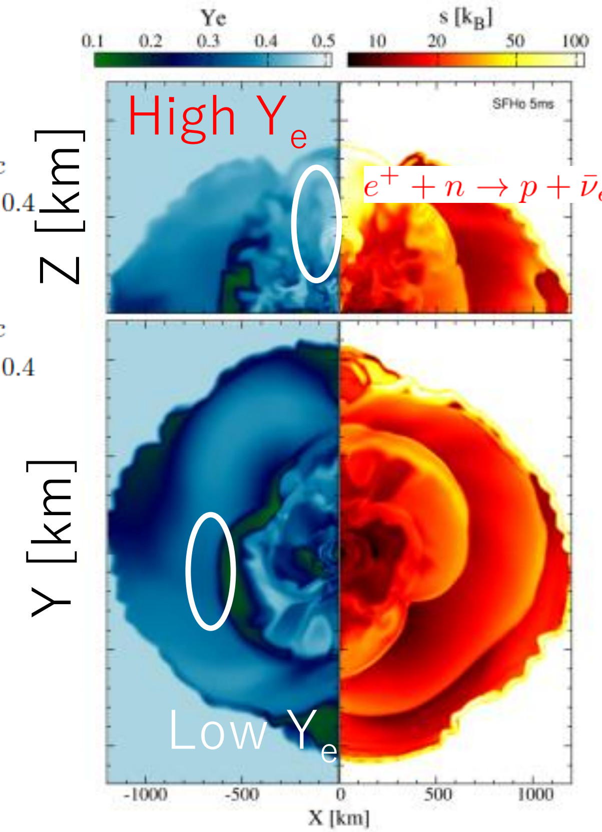

▶ $Y_e \lesssim 0.1$ before the merger

▶ The positron capture ($n+e^+ \Rightarrow p+\nu_e$) and neutrino absorption ($n+\nu_e \Rightarrow p+e^-$) increases Y_e.

▶ Dynamical ejection is primarily driven by tidal torque (orbital direction) ⇒ $M_{eje} \sim O(10^{-3}) M_\odot$, $Y_e \approx 0.05\text{-}0.5$, $\theta \gtrsim 45°$ ⇒ High opacity (red component)

Neutrino radiation transport simulation of BNS mergers (Sekiguchi, KK et al. 15, 16, Wanajo et al. 14)

EOS : SFHo (Steiner et al. 2013), NS mass : 1.35-1.35$M_\odot$

Ye Entropy

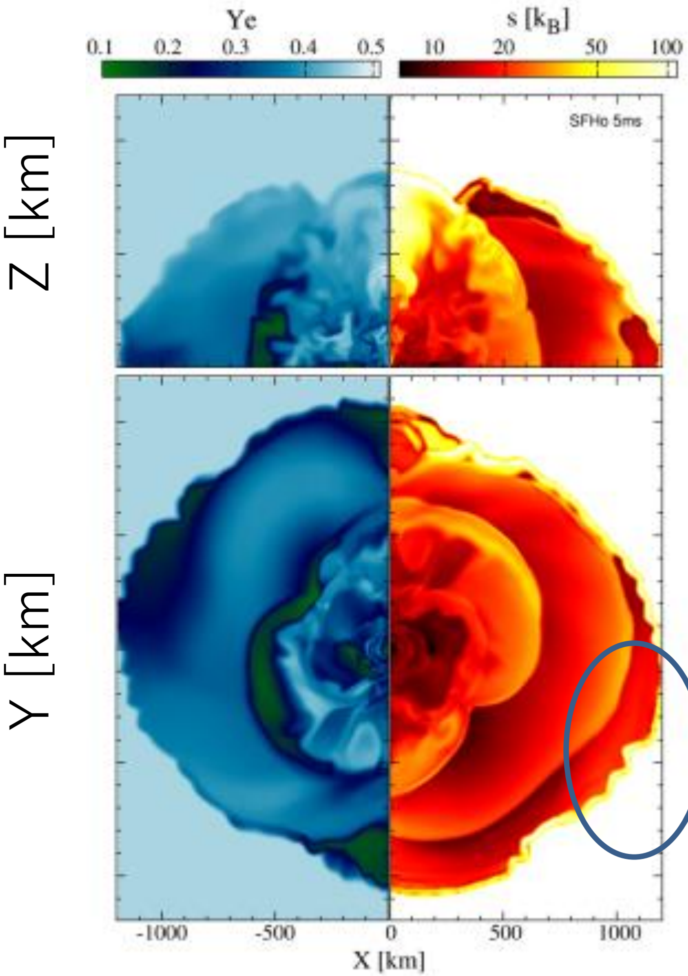

Mass histogram of Ye

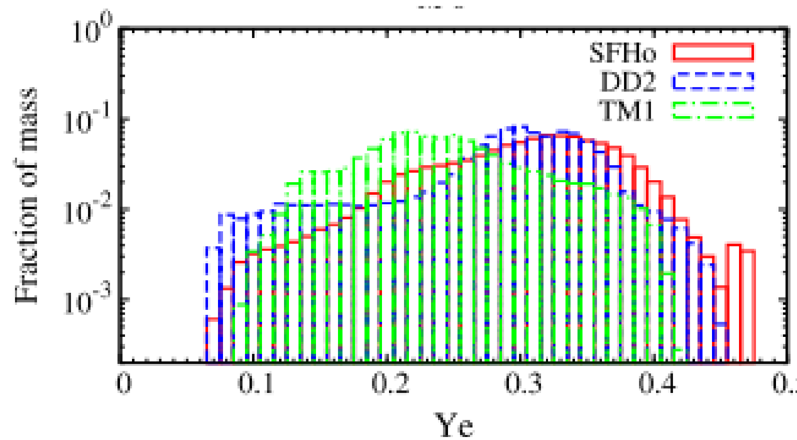

R-process

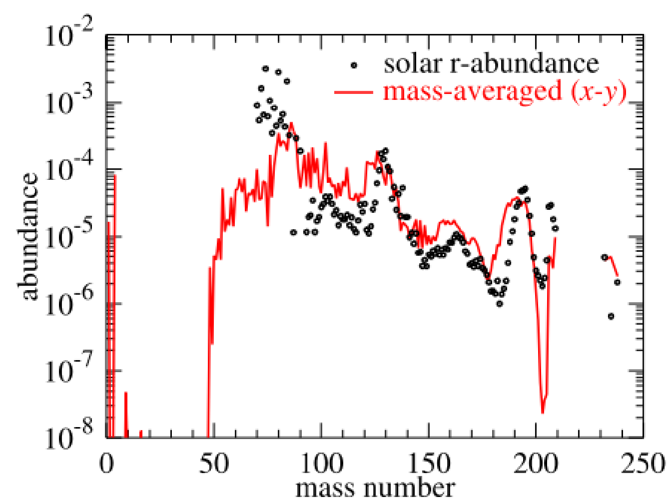

<u>Neutrino radiation transport simulation of BNS mergers</u> (Sekiguchi, KK et al. 15, 16, Wanajo et al. 14)

Previous works in which the neutrino effect is neglected (Korobkin et al. 12)

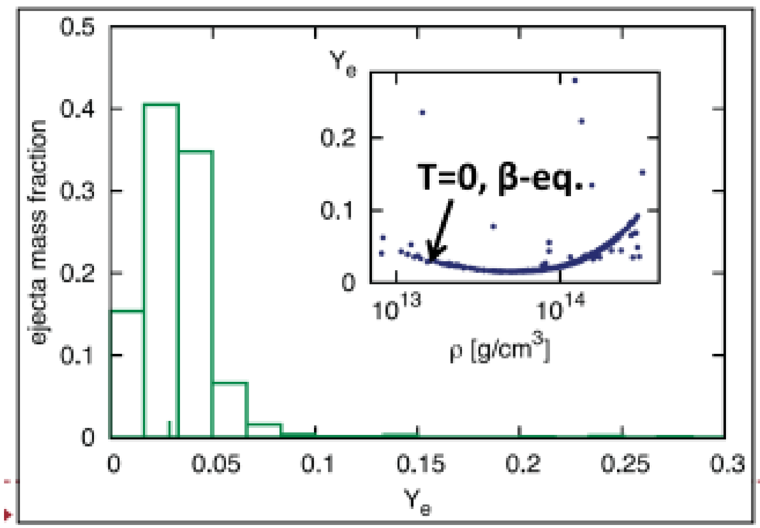

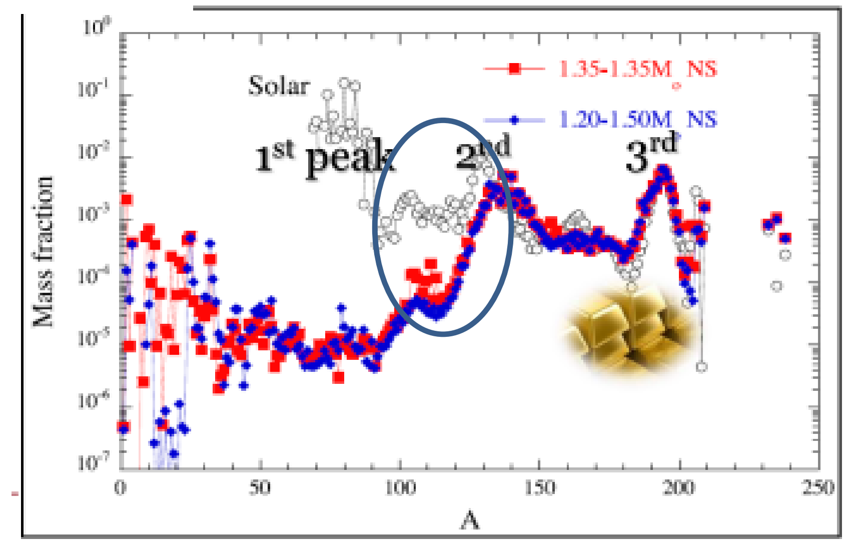

Similar result is obtained in Newtonian neutrino radiation transport simulation.

Caveat : Neutrino radiation transport (and GR) is essential to reproduce the solar abundance of the r-process elements.

Numerical modeling of GW170817 (Shibata et al. 18, Fujibayashi, KK et al. 17)

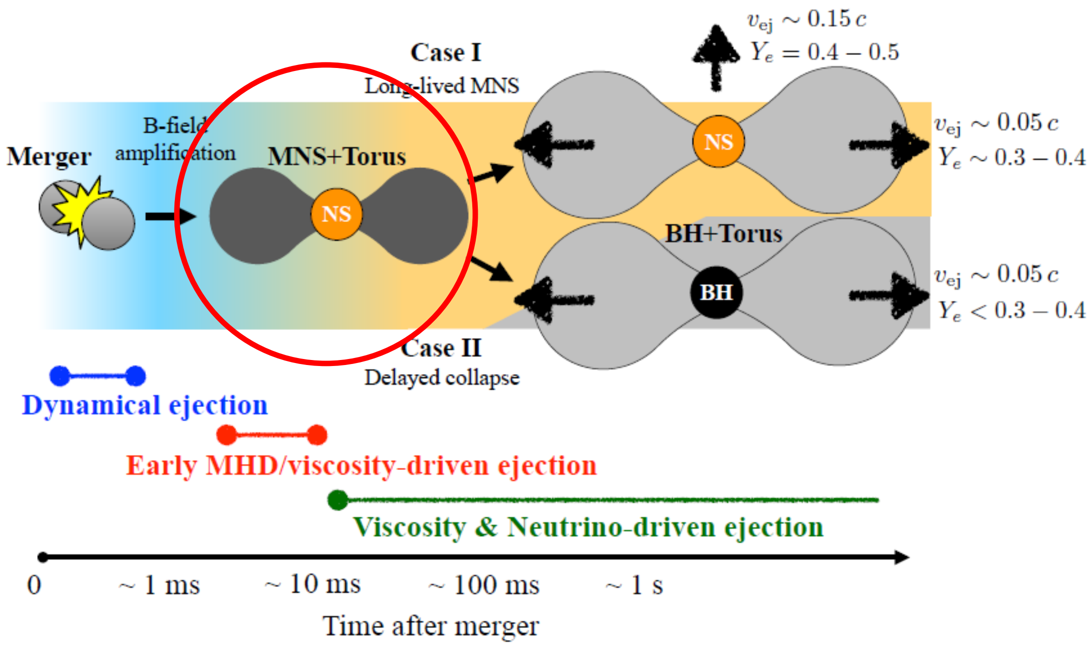

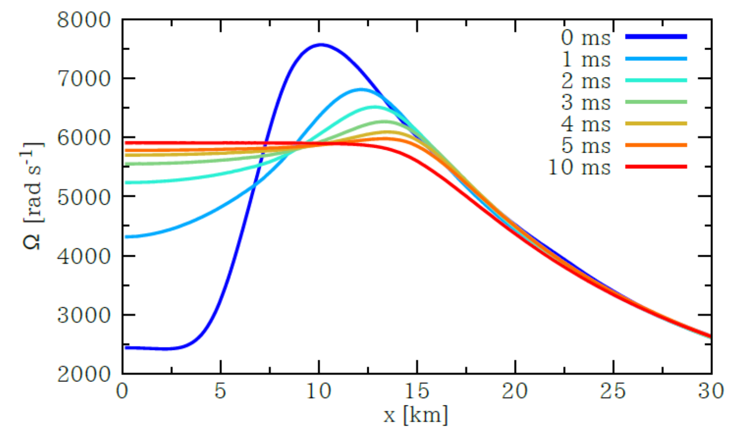

- Magneto-turbulent viscosity drives a quick angular momentum transport ⇒ Revelation of the differential rotational energy ⇒ Sound wave generation

$M_{eje} \sim 10^{-2} M_{\odot} (\alpha/0.02)$, $Y_e \approx 0.2$-0.5, $\theta \gtrsim 30°$, $v \sim 0.15$-$0.2c$ ⇒ Low opacity (blue component)

Numerical modeling of GW170817 (Shibata et al. 18, Fujibayashi, KK et al. 17)

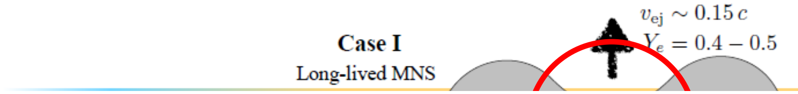

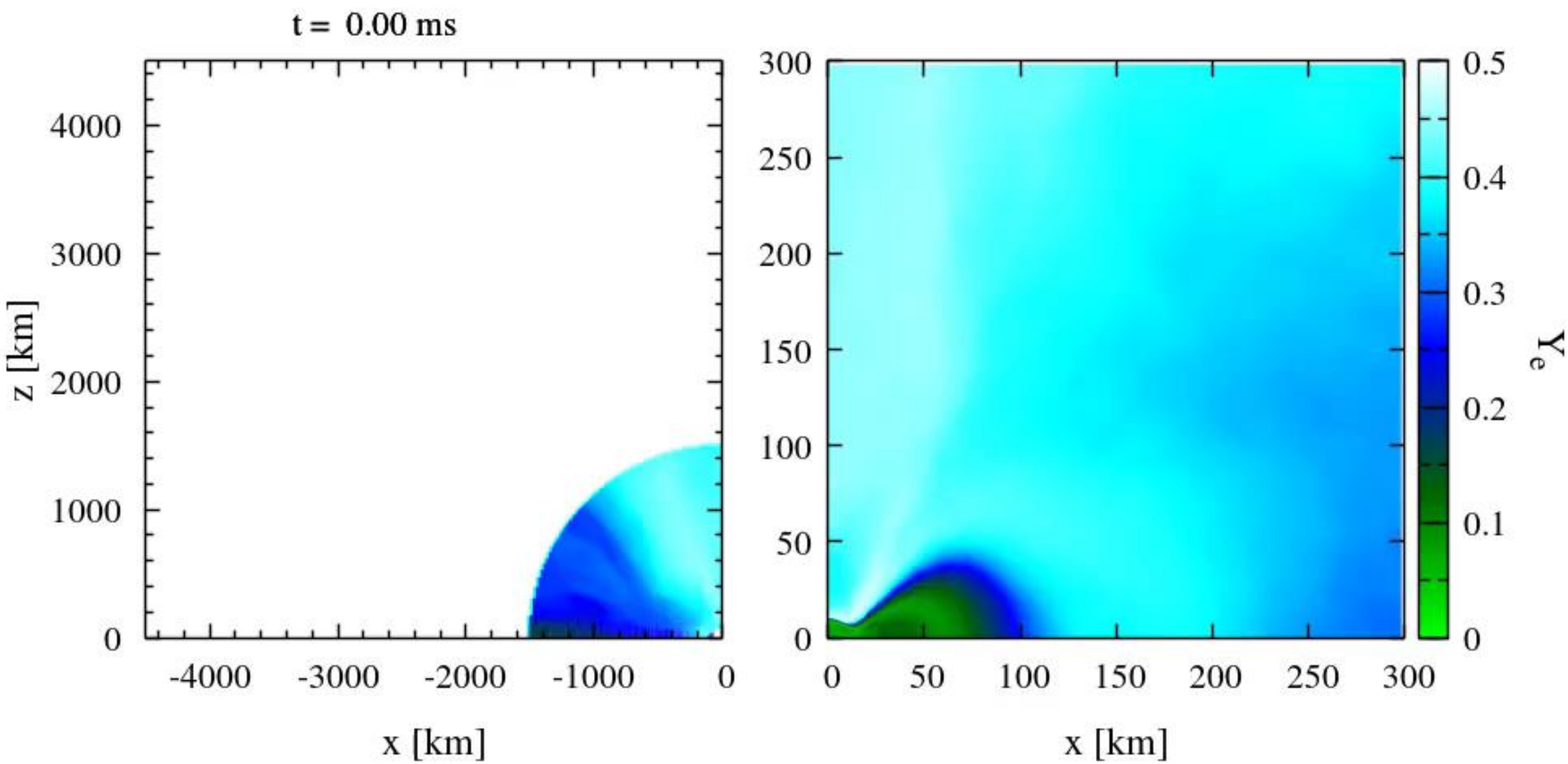

of the torus) ⇒ $\gtrsim 10^{-2}\ M_\odot$, $Y_e \approx 0.3$-0.4, $\theta \gtrsim 30°$ ⇒

Low opacity (blue component)

Numerical modeling of GW170817 (Shibata et al. 18, Fujibayashi, KK et al. 17)

<u>Schematic picture</u>

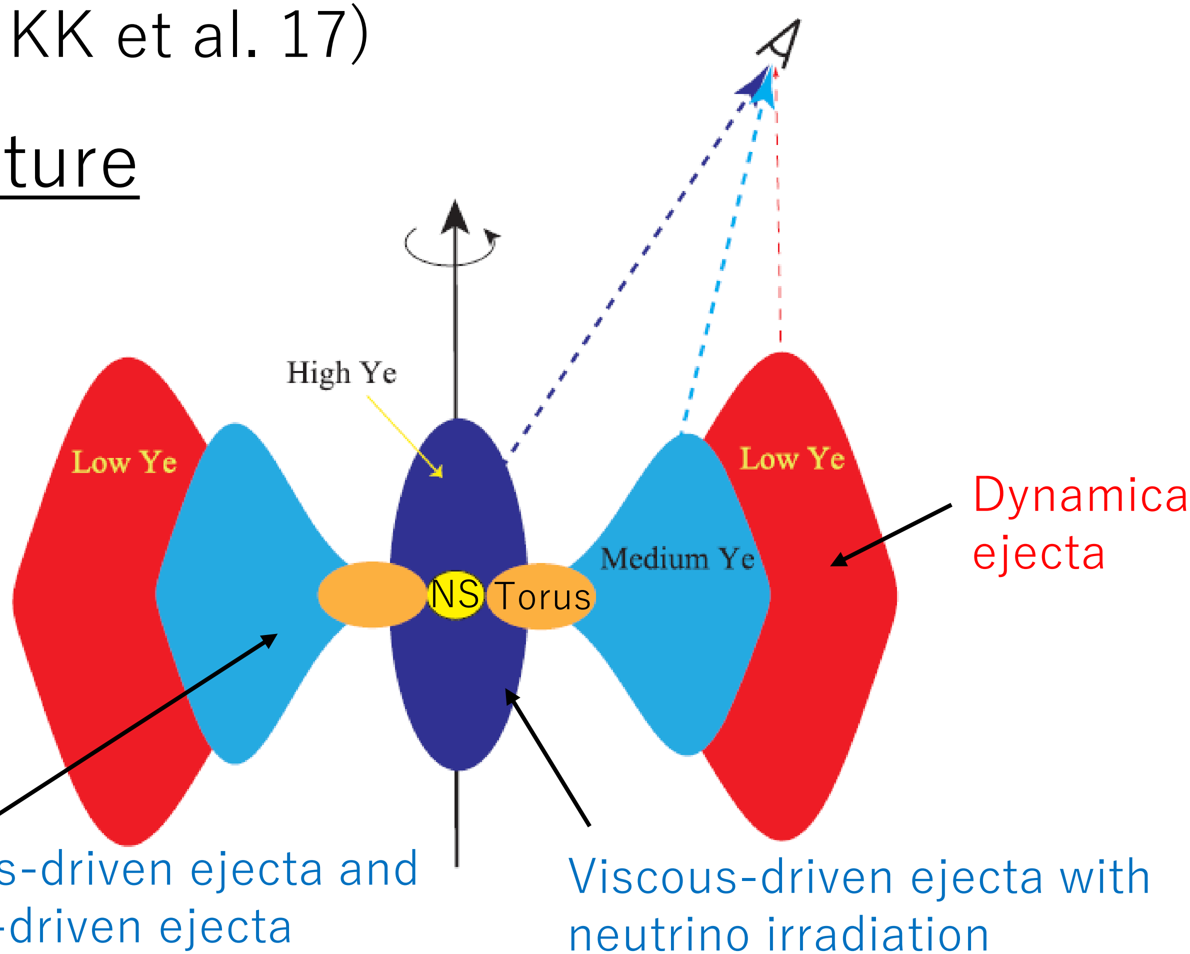

▶ Ejecta has several components and red/blue depends on the viewing direction.

⇒GW and EM observations suggest the viewing angle is $\leq 28°$

Optical-Infrared emission from GW170817
(Tanaka et al. 17)

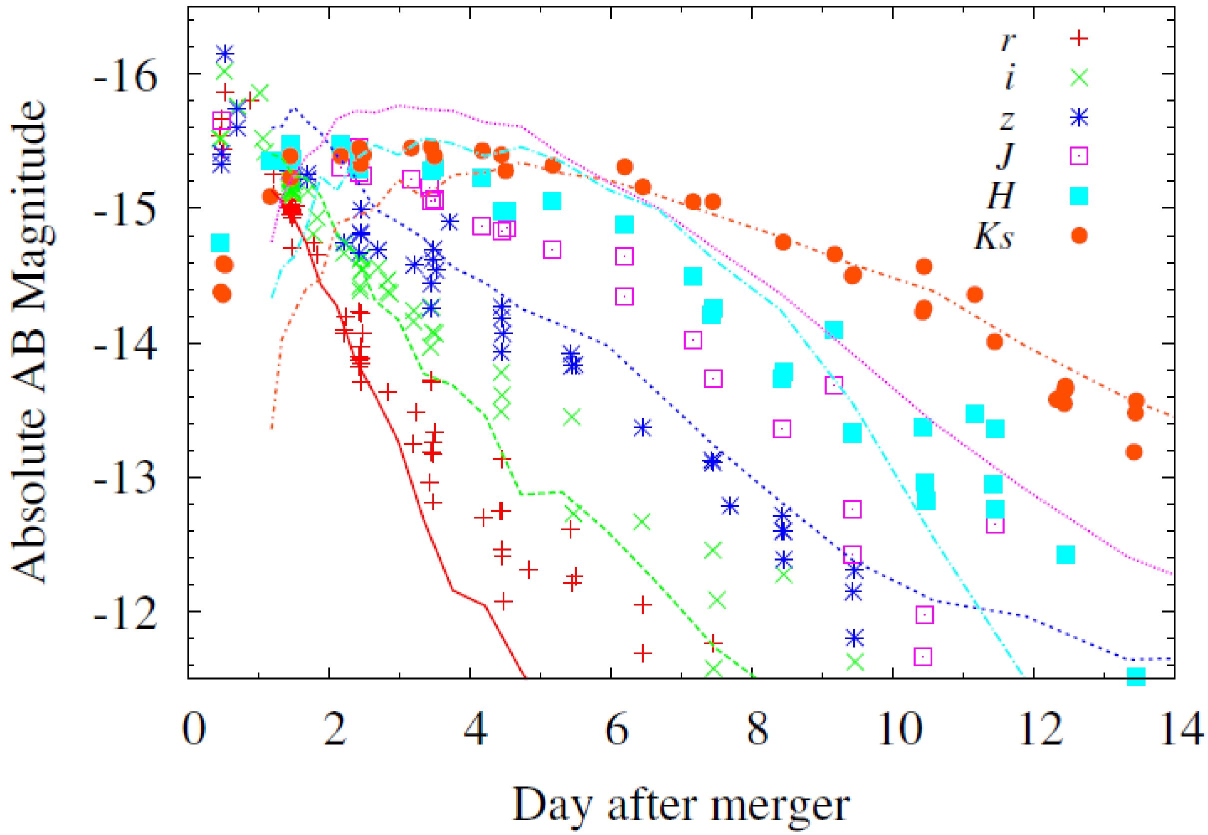

▶ Light curve (HSC) fitting by a photon radiation hydro. simulation with Ye of ～0.25
⇒ Agree with our numerical modeling

Numerical modeling of GW170817 (Shibata et al. 18, Fujibayashi, KK et al. 17)

▶ If a merger remnant is a very/permanently long-lived NS, the rotational energy of 10^{53} erg may be released by a magnetic dipole radiation.
⇒ Energy injection to ejecta
⇒ Optical counterpart of GW170817 did not show such an feature ($E_{kin} \approx 10^{50}$ erg)
⇒ Inferred merger remnant is a BH

▶Binary mass of GW170817 ≈ 2.73-2.78$M_{\odot}$
▶Mass (energy) radiated from a remnant via GW, neutrino, and ejecta ≈ 0.15∓0.03 $M_{\odot}$
⇒ Estimated remnant mass ≈ 2.60∓0.05 $M_{\odot}$
⇒ $M_{max,sph} = M_{max,rigid}/1.2 = 2.15\text{-}2.25\ M_{\odot}$

Numerical modeling of GW170817 (Shibata et al. 18, Fujibayashi, KK et al. 17)

▶ Estimated merger rate from GW170817

⇒ $R \approx 0.8^{+1.6}_{-0.6} \times 10^{-4}\ \mathrm{yr}^{-1}/\mathrm{gal}$

▶ Assuming all the r-process elements are synthesized in BNS mergers,

$$R_{\text{r-process}} \approx 10^{-4}\ \mathrm{yr}^{-1}/\mathrm{gal}\ (M_{A\geq 90}/5\times 10^{-3} M_{\odot})$$

Consistent in order of magnitude estimation

Three possibilities to explain X-ray and radio observations

Structured Jet

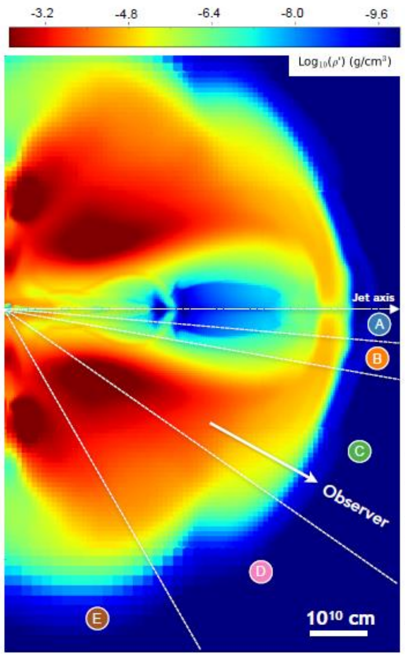

Lazzati et al. 18

Cocoon emission

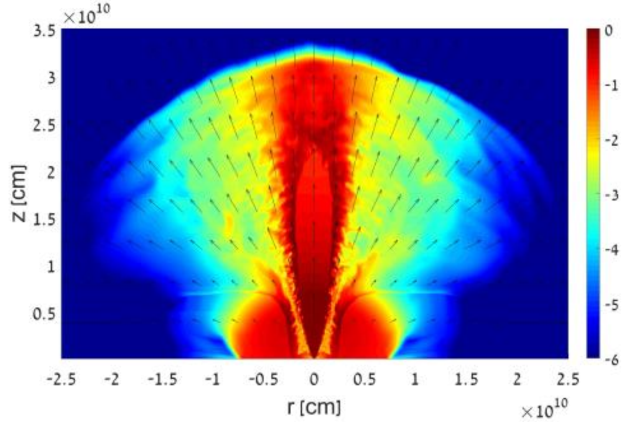

Gottieb, Nakar, Piran 18

Fast tail of dynamical ejecta

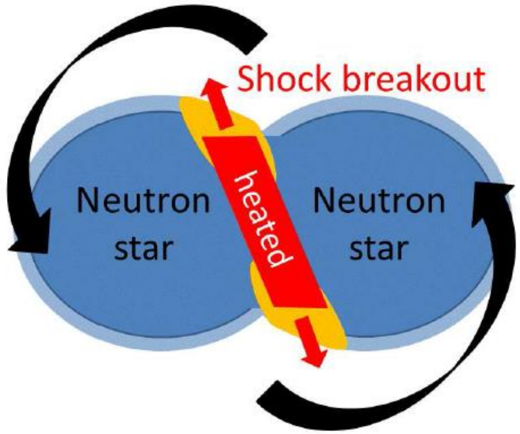

Kyutoku, Ioka, Shiata 13

We explore the third possibility based on NR simulations.

Basics of synchrotron emission (Sari et al. 98)

Characteristic frequency

$$\nu(\gamma_e) = \Gamma \gamma_e^2 \frac{q_e B}{2\pi m_e c}, \ \gamma_e \ : \text{ electron Lotentz factor}$$

Electron power law distribution

$$N(\gamma_e) d\gamma_e \propto \gamma_e^{-p} d\gamma_e,$$

$$\gamma_e \ \geq \ \gamma_m = \epsilon_e \frac{p-2}{p-1} \frac{m_p}{m_e} (\Gamma - 1)$$

Critical Lorentz factor

$$\gamma_c = \frac{3 m_e}{16 \epsilon_B \sigma_T m_p c} (t \Gamma^3 n)^{-1}$$

Electron with $\gamma_e \geq \gamma_c$ loses the energy within the time t.

Basics of synchrotron emission (Sari et al. 98)

$$\nu_m = \nu(\gamma_m),\ \nu_c = \nu(\gamma_c),\ \nu_a\ :\ \text{self-absorption}$$

Slow cooling ($\nu_c > \nu_m$)

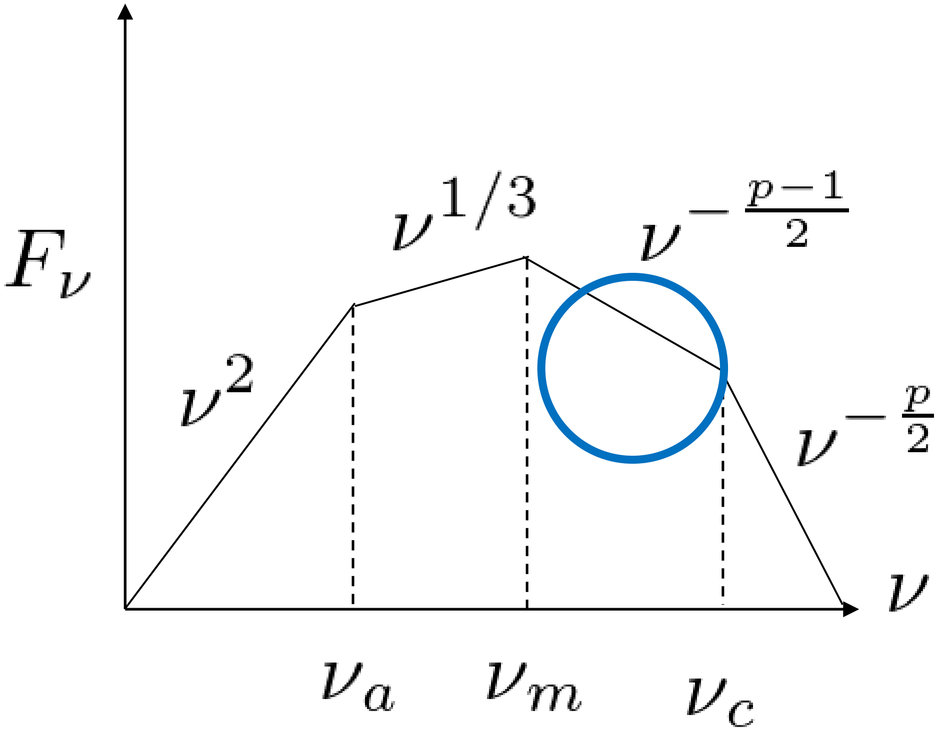

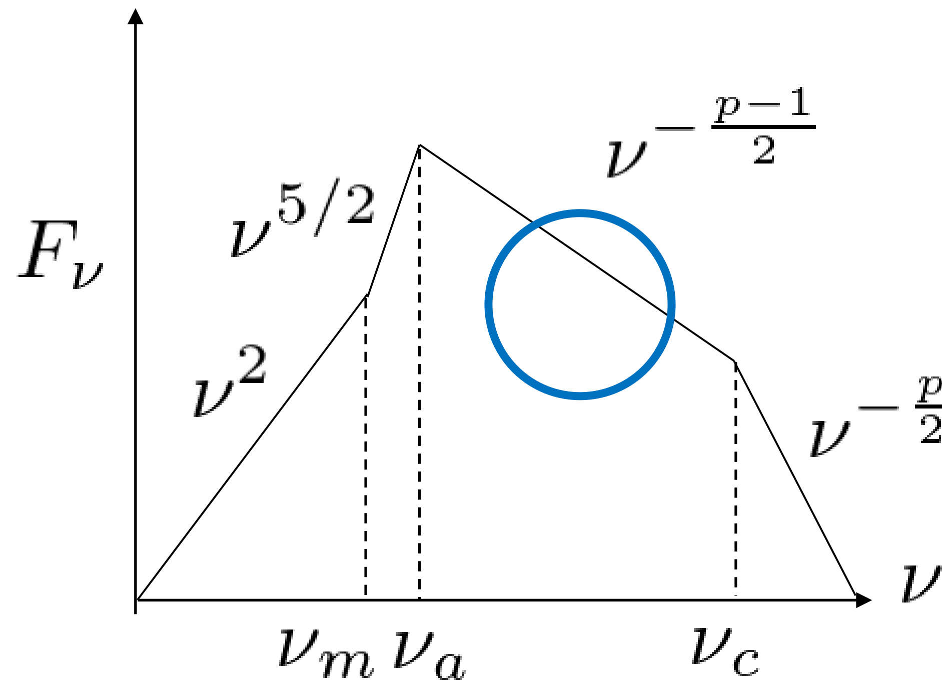

$$\nu_c \approx 0.5\ \text{keV} \left(\frac{n}{0.01\text{cm}^{-3}}\right)^{-3/2} \left(\frac{\epsilon_B}{0.05}\right)^{-3/2} \left(\frac{t}{100\ \text{day}}\right)^{-2} \left(\frac{\beta}{0.6}\right)^{-3}$$

$$\nu_m \approx 60\ \text{MHz} \left(\frac{\epsilon_B}{0.05}\right)^{1/2} \left(\frac{\epsilon_e}{0.1}\right)^{2} \left(\frac{n}{0.01\text{cm}^{-3}}\right)^{1/2} \Gamma^4$$

$$\nu_a \approx 30\ \text{MHz} \left(\frac{E_{\text{iso}}}{10^{49}\text{erg}}\right)^{\frac{2}{3(p+4)}} \left(\frac{n}{0.01\ \text{cm}^{-3}}\right)^{\frac{3p+4}{6(p+4)}} \left(\frac{\epsilon_B}{0.05}\right)^{\frac{2+p}{2(p+4)}} \left(\frac{\epsilon_e}{0.1}\right)^{\frac{2(p-1)}{p+4}} \left(\frac{\beta}{0.6}\right)^{\frac{15p-10}{3(p+4)}}$$

Basics of synchrotron emission (Sari et al. 98)

Given $E(>\Gamma\beta)$,

$$\frac{4}{3}\pi n m_p R^3 (c\Gamma\beta)^2 = E(>\Gamma\beta),$$

$$\frac{dR}{dt} = \frac{c\Gamma\beta}{\sqrt{1+(\Gamma\beta)^2}}$$

NR simulation found a fast component ($\Gamma\ \beta$ >1)

(Kiuchi et al. 17, See also Hotokezaka et al. 13, Bauswein et al. 13)

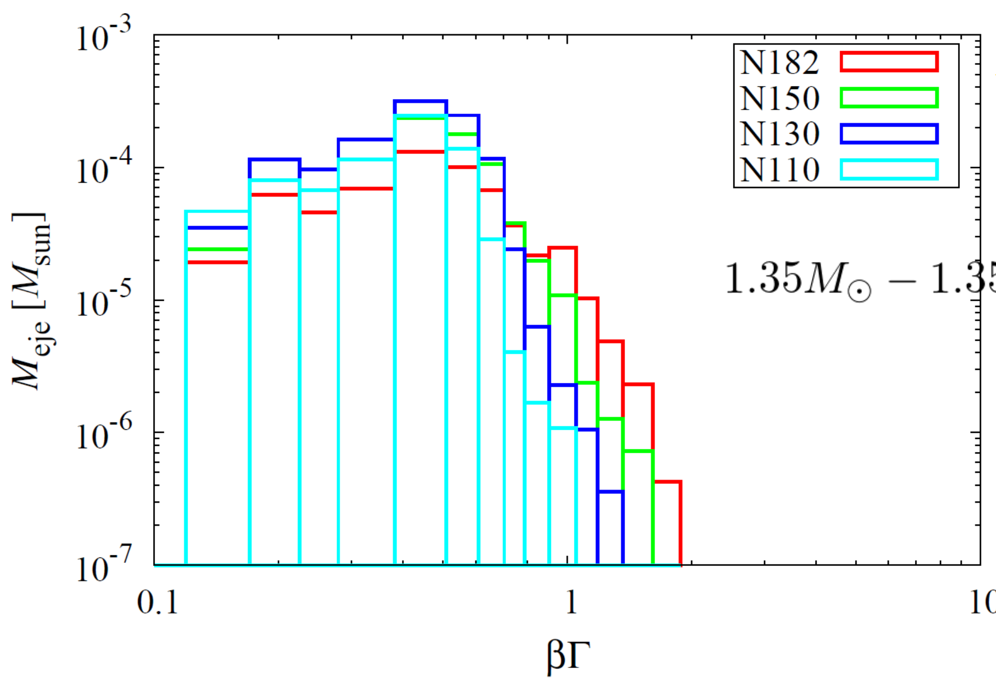

Increasing the resolution

$1.35M_\odot - 1.35M_\odot,\ R_{1.35\mathrm{M}_\odot} \approx 11\ \mathrm{km}$

Long-term radio, X-ray observations
(Hotokezaka, KK et al. 18)

Mildly relativistic dynamical ejecta

kinetic energy above $\gamma\,\beta$

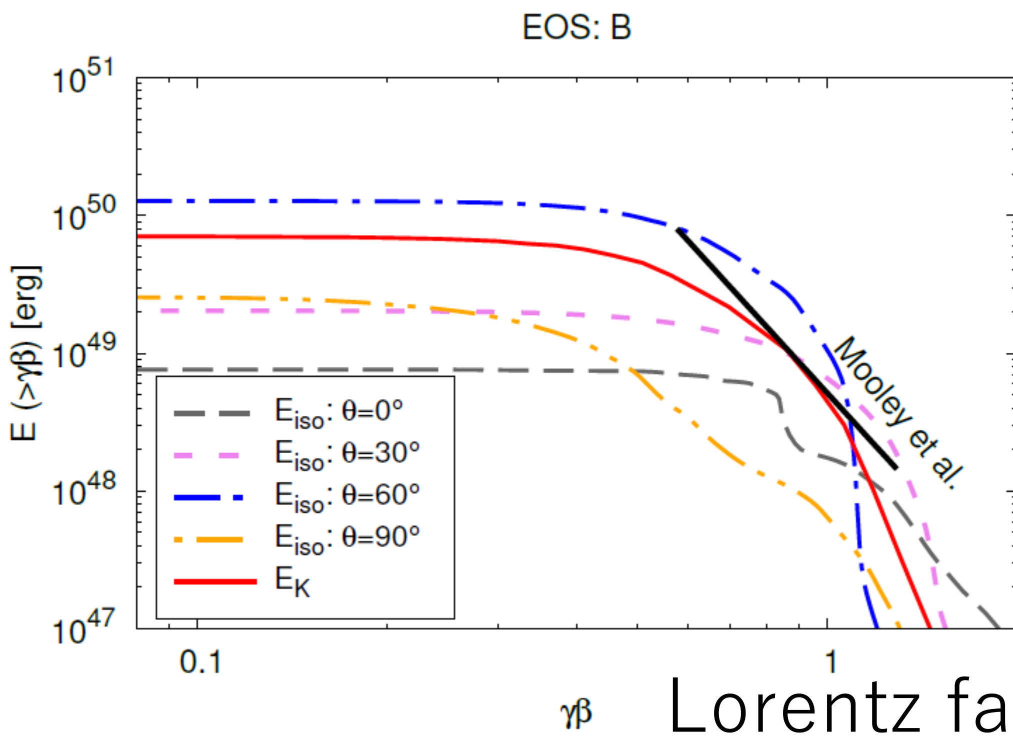

Lorentz factor × v/c

▶ Fast component coming from a contact interface
⇒ Mildly relativistic component $\beta = v/c \sim 0.6$

Long-term radio, X-ray observations
(Hotokezaka, KK et al. 18)

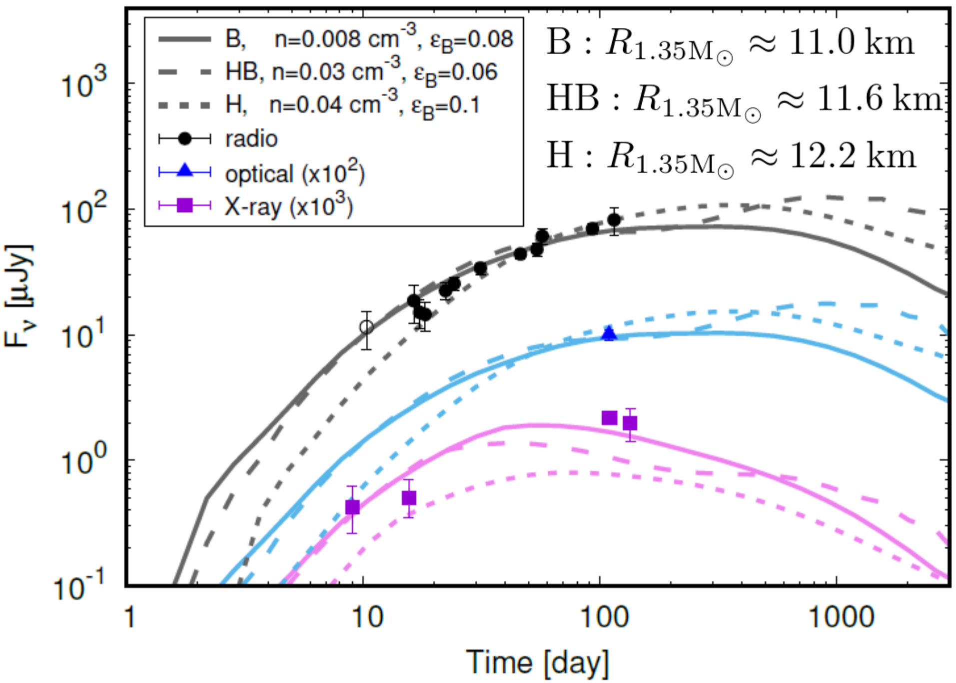

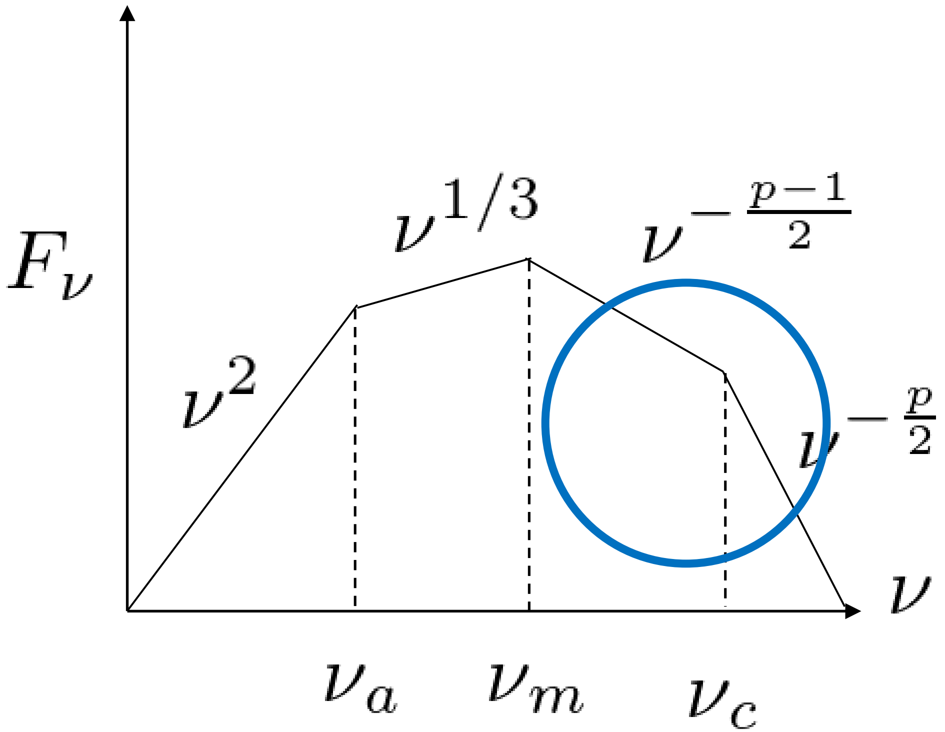

- ▶ Radio and X-ray emission favors a small NS radius.
- ▶ Prediction : Cooling frequency enters the X-ray band around t ~ O(100)days

Long-term radio, X-ray observations
(Hotokezaka, KK et al. 18)

Mooley et al. 2018

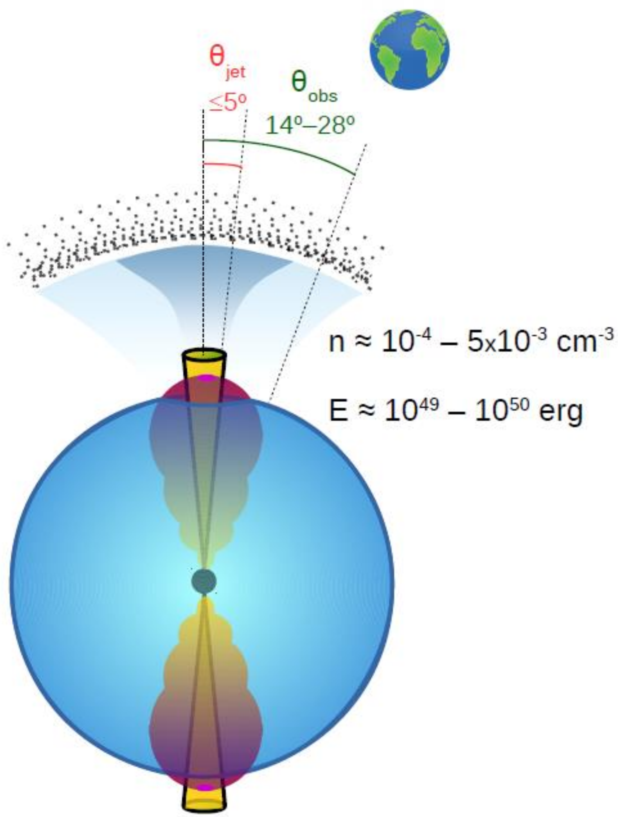

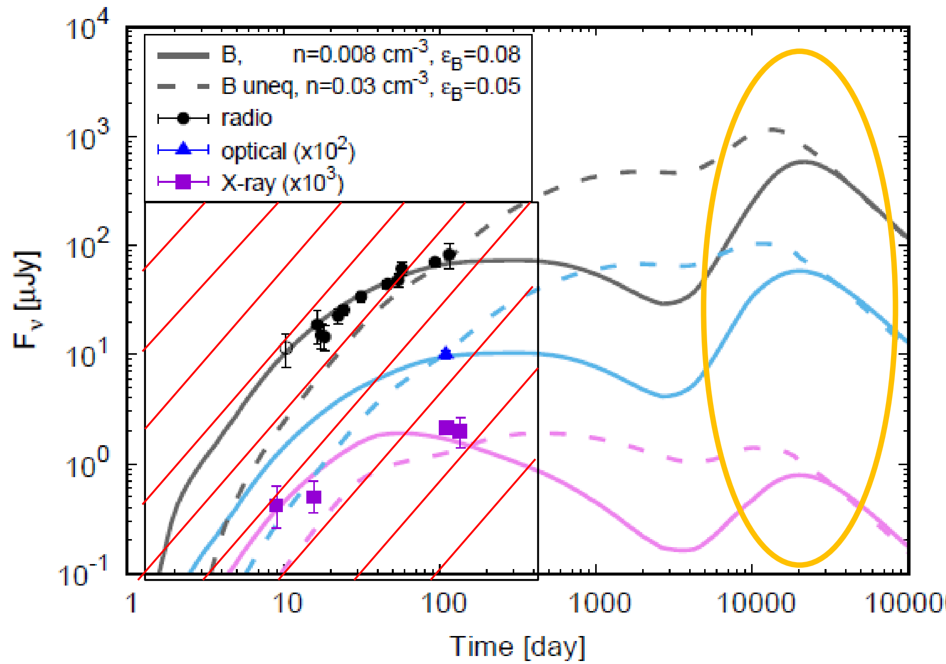

▶ Fast tail could be masked by structured jet/cocoon emission. But the slower component could be observed in the future

Summary

▶ Opening of the real multi messenger astronomy of compact binary merger (rich information!)

▶ Equation of state of neutron star matter (tidal deformability) is constrained for the first time.
⇒ We build a template band based on NR simulations and data analysis is on going.

▶ R-process nucleosynthesis is very likely to occur in GW170817. ⇒ Blue and Red component

▶ Our numerical modeling explains the observational features of the optical-IR observations.

Numerical relativity simulation of the black hole-neutron star binary mergers

Overview of Black Hole – Neutron Star

Q: Tidal disruption or not ? Bartos et al. 13

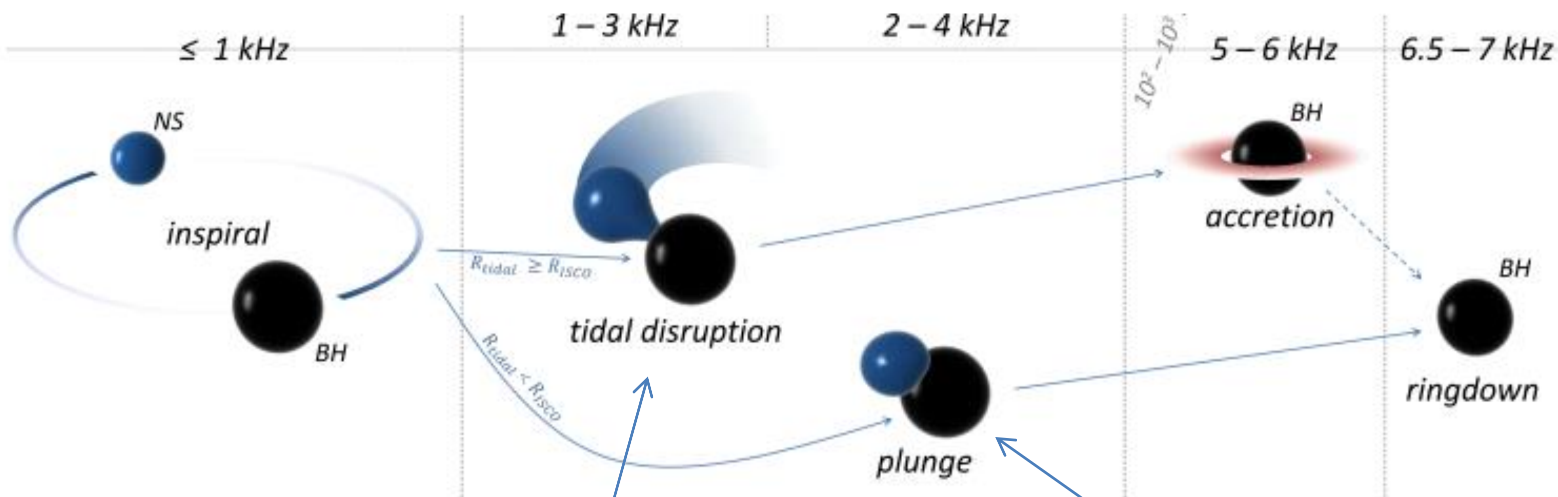

Time

GW forms (Kyutoku et al. 11) *More detailed classification

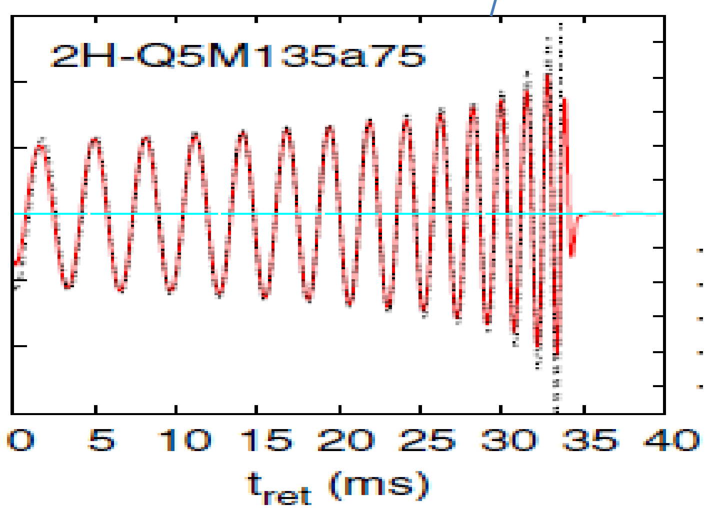

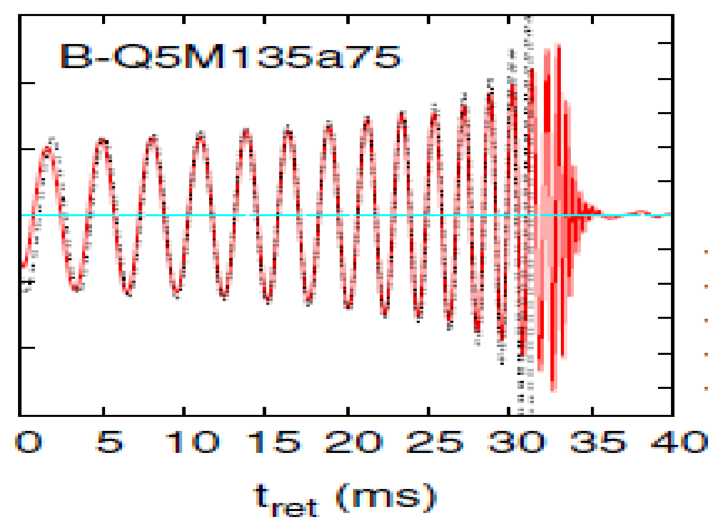

Key ingredients for tidal disruption in BH-NS

Tidal force > NS self gravity

⇒ $r \lesssim (M_{BH}/M_{NS})^{-2/3} (M_{NS}/R_{NS})^{-1} M_{BH} \equiv r_{tidal}$

If $r_{tidal} > r_{isco}$ ⇒ Tidal disruption

$r_{tidal} < r_{isco}$ ⇒ No tidal disruption

*ISCO = Inner Stable Circular Orbit

Key ingredients of the mass ejection in BH-NS are

- ▶ Spin of BH
- ▶ Mass ratio (M_{BH}/M_{NS})
- ▶ Compactness of NS (M_{NS}/R_{NS})

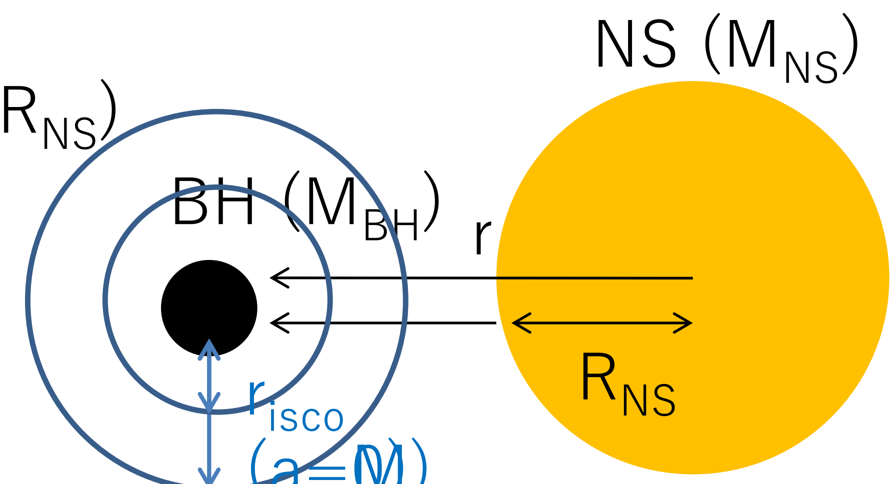

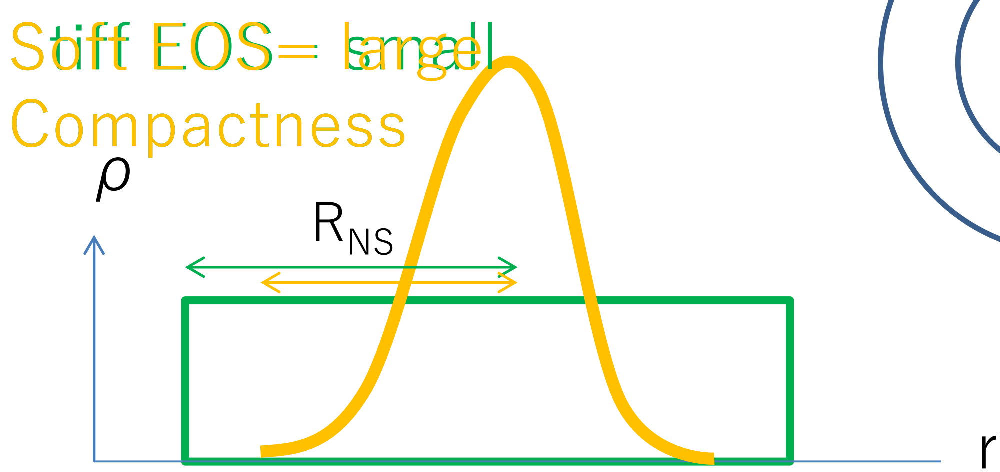

Key ingredients for tidal disruption

Lattimer & Prakash 06

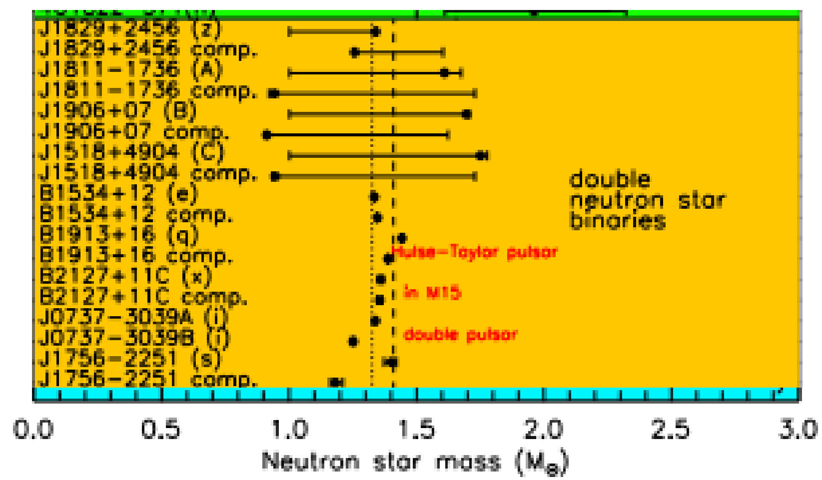

- ▶NS mass M_{NS} ⇒ 1.23-1.44$M_\odot$
- ▶Mass ratio ⇒ q ≳4-5
- ▶EOS ?
- ▶BH spin ?

<u>Systematic study in NR simulations</u>

⇒ Fitting formulae for the accretion torus (Foucart 12)

X-ray binary observation (Ozel+10)

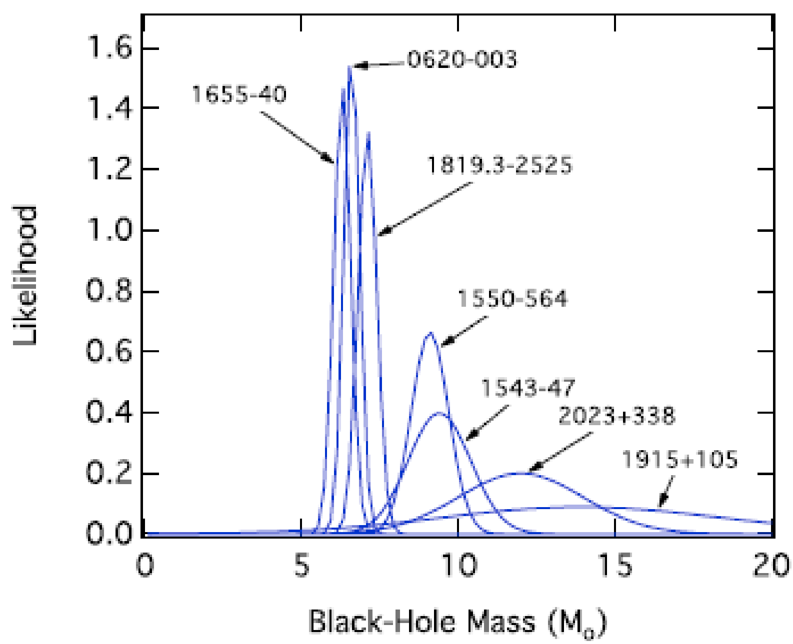

Disk Mass Prediction (Foucart 12)

Fitting formulae

$$M_{disk}/M_{NS}\,(q, C_{NS}, \chi) = \alpha\,(3q)^{1/3}(1-2C_{NS}) - \beta\, r_{isco}/R_{NS}$$

▶31 NR simulations (28models by Kyutoku+11, 7models by Caltech-Cornel 4 models by UIUC

Disk mass contour with q=7

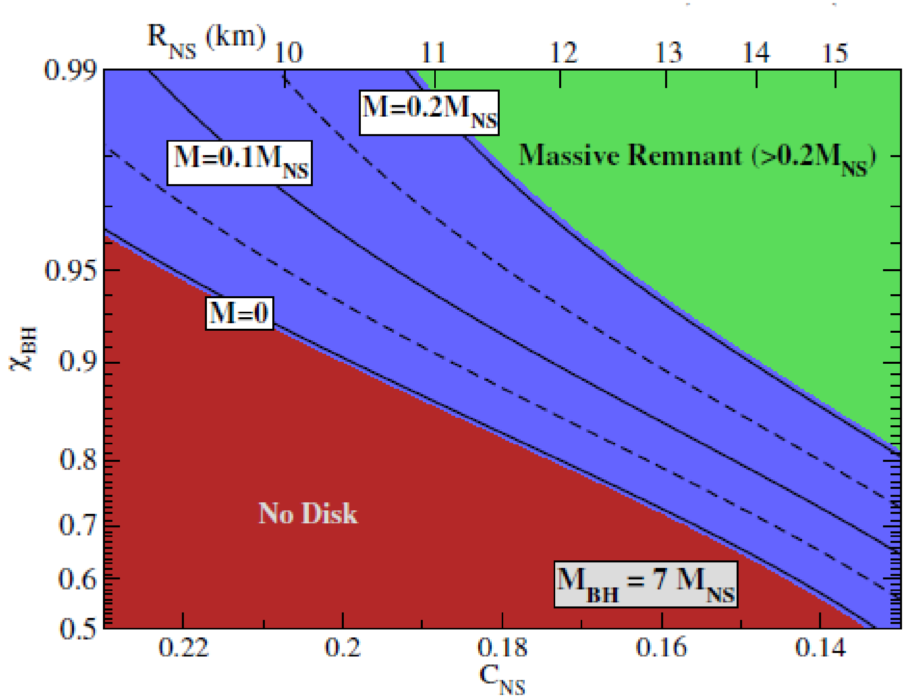

Spin contour with M_{disk}=0.1M_{NS}

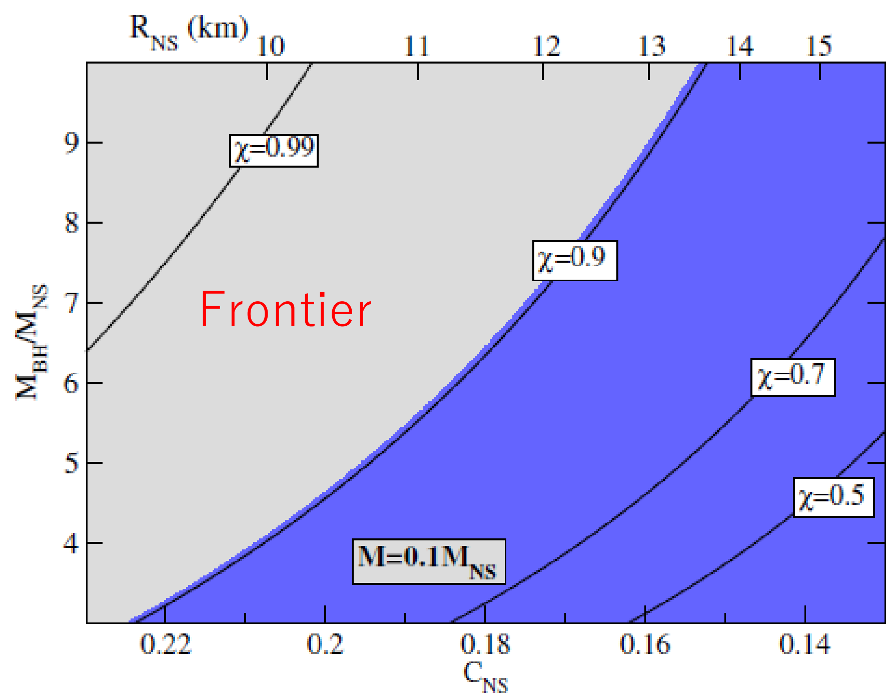

q=4-5, χ=0.75⇒Massive disk

Lovelace et al. q=3, C=0.144, χ=0.97, M_{disk}=0.6 M_{NS}

Tidal deformability of NSs

Lackey et al. 12, 14

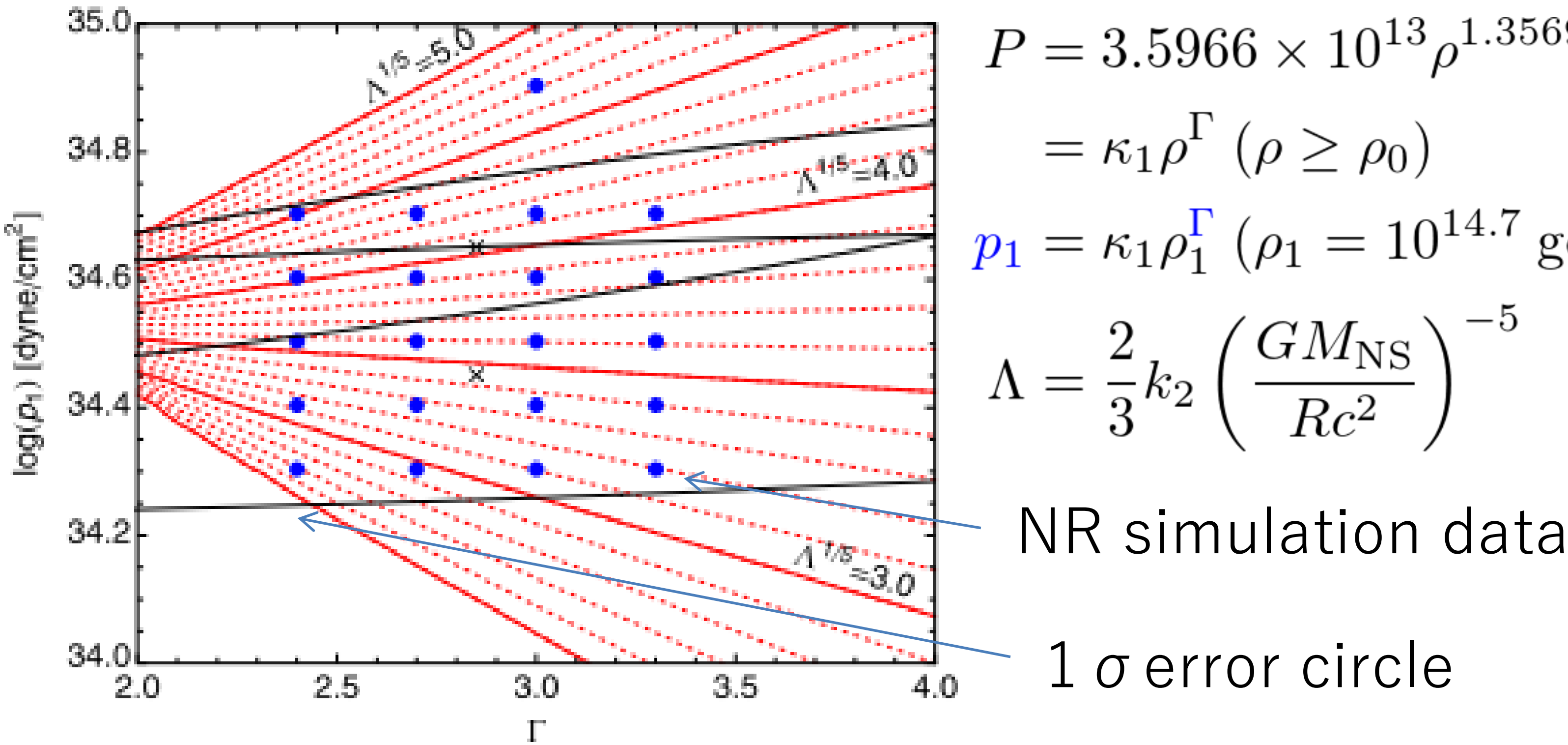

$$P = 3.5966 \times 10^{13} \rho^{1.3569} \ (\rho \leq \rho_0)$$

$$= \kappa_1 \rho^{\Gamma} \ (\rho \geq \rho_0)$$

$$p_1 = \kappa_1 \rho_1^{\Gamma} \ (\rho_1 = 10^{14.7} \ \mathrm{gcm}^{-3})$$

$$\Lambda = \frac{2}{3} k_2 \left(\frac{G M_{\mathrm{NS}}}{R c^2} \right)^{-5}$$

▶ Error contour for Advanced LIGO with D=100Mpc , $M_{BH}/M_{NS} = 2$, and $M_{NS}=1.35M_{\odot}$

Tidal deformability of NSs

Lackey et al. 12, 14

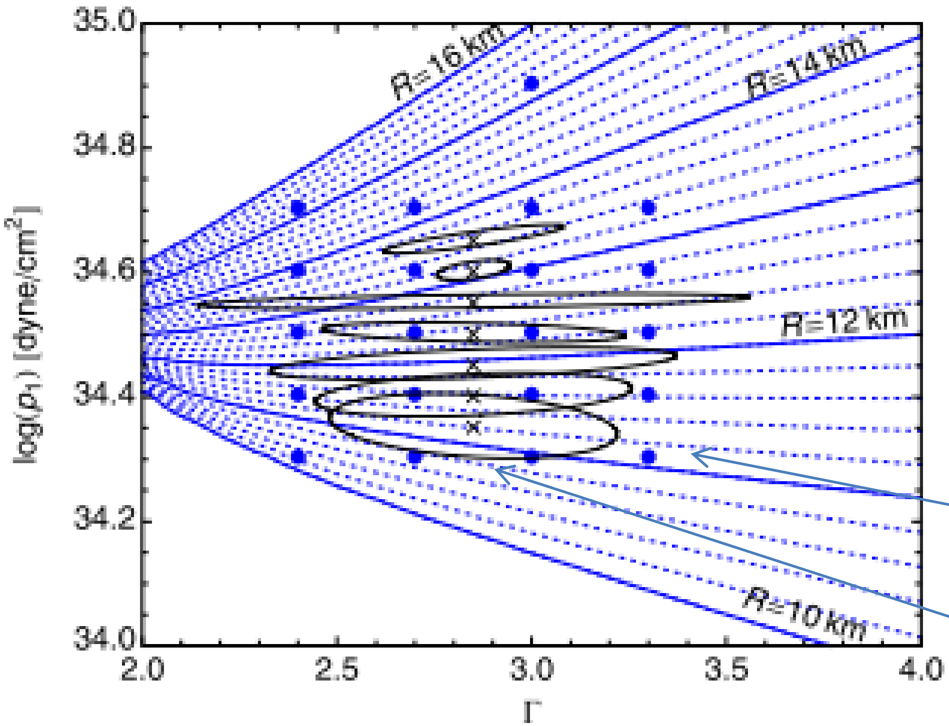

$$P = 3.5966 \times 10^{13} \rho^{1.3569} \ (\rho \le \rho_0)$$
$$= \kappa_1 \rho^{\Gamma} \ (\rho \ge \rho_0)$$
$$p_1 = \kappa_1 \rho_1^{\Gamma} \ (\rho_1 = 10^{14.7}\ \mathrm{gcm}^{-3})$$
$$\Lambda = \frac{2}{3} k_2 \left(\frac{G M_{\rm NS}}{R c^2} \right)^{-5}$$

NR simulation data

1 σ error circle

▶ Error circle of ET with D=100Mpc, $M_{BH}/M_{NS} = 2$, $M_{NS}=1.35M_{\odot}$

▶ Need high-precision GW waveforms and large parameter study(M_{BH}/M_{NS}, M_{NS}, EOS, BH spin(dir.,mag)

Mass ejection due to tidal torque (Kyutoku et al. 13, Kyutoku et al. 15)

A part of the tidal tail ⇒ Crescent like shape of the ejceta

ρ_{eje} on the orbital plane Log[ρ (g/cc)]

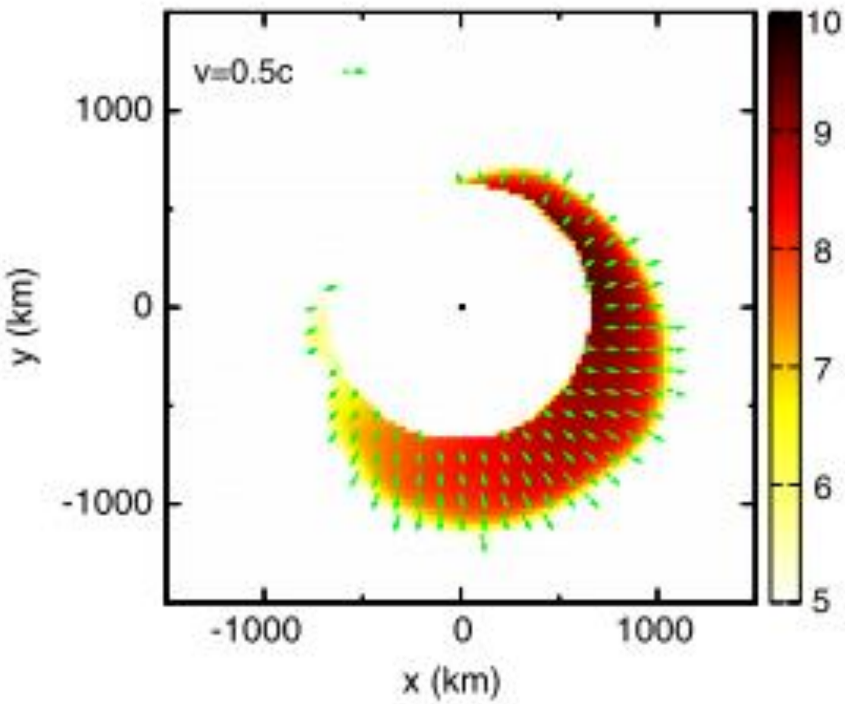

ρ_{eje} on the meridional plane

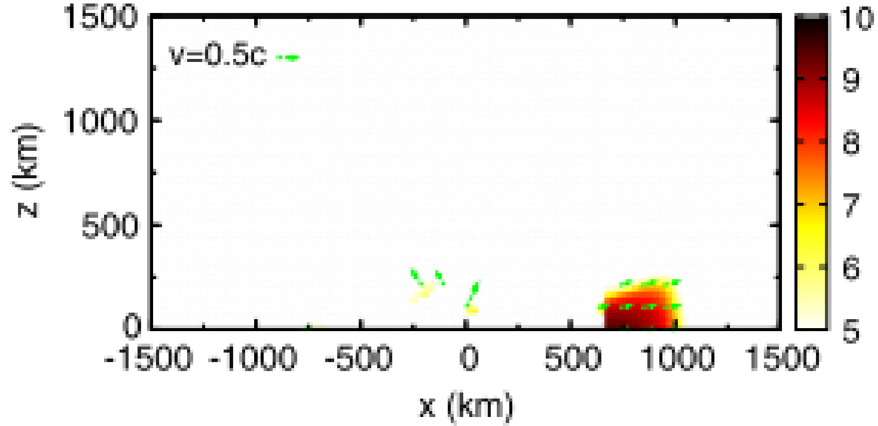

This dynamical ejecta is a primary component in BH-NS mergers (Tilted BH spin case ⇒ Kawaguchi kun's talk)

A macronova model of the BH-NS (Hotokezaka+13, Tanaka+13)

1st step : Numerical Relativity simulation of BH-NS merger => Amount and morphology of ejecta

2nd step : Photon radiation transfer in ejecta (heating due to the radioactive decay of the r-process element)

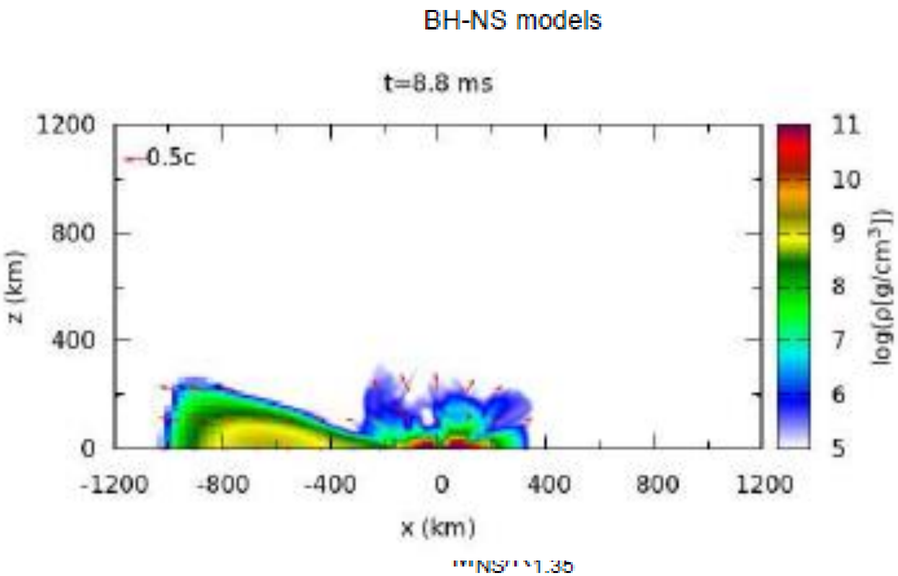

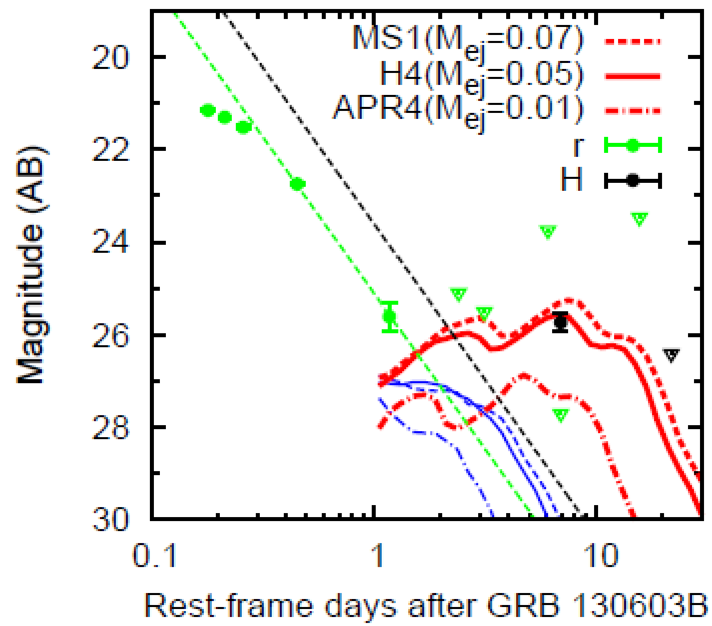

Hard Soft

BH-NS merger models suggest $0.02\ M_\odot < M_{ej} < 0.07\ M_\odot$ is needed to reproduce the light curve of GRB130603B. => It favors a “hard” EOS.

Note that you can see inverse trend in NS-NS case.

What's else ?

▶ Neutrino driven wind (Qian & Woosley 96)

$$\dot{M} \approx 4.5 \times 10^{-3} L_{\bar{\nu}_e,53}^{5/3} \epsilon_{\bar{\nu}_e,10}^{10/3} R_6^{5/3} M_{2.7}^{-2} M_\odot/\mathrm{s},$$

▶ Disk wind due to the nuclear recombination/viscous heating (Fernandez & Metzger 13)

$M_{ej} \sim 0.1 M_{disk}$ for the viscous timescale (e.g., O(1)s)

▶ Magnetic-field effect (e.g., Blandford & Payne 82)

BH-NS merger simulations with microphysics

(Deaton et al. 13, Fourcart et al. 14)

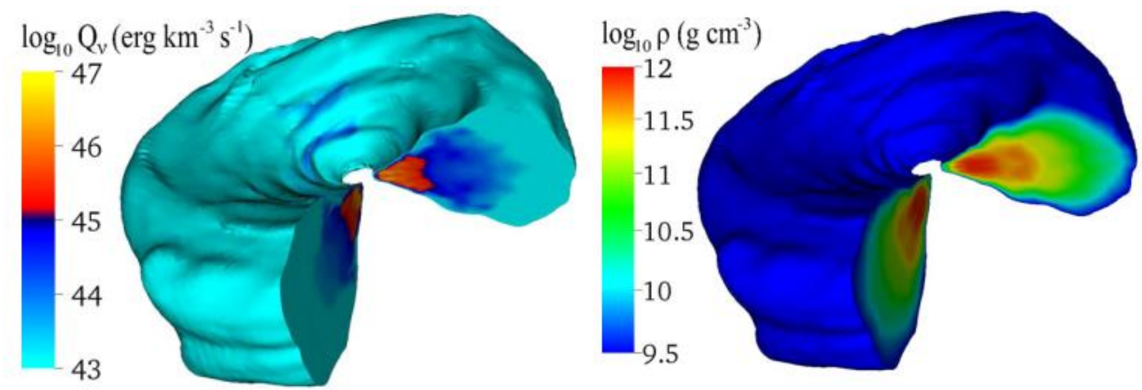

Ejecta mass evolution

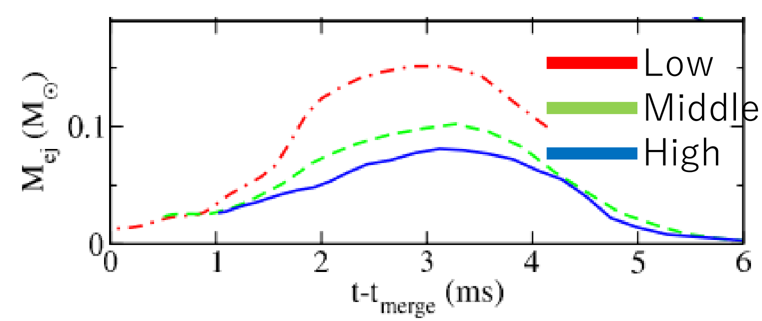

▶ Mentioning only the dynamical ejecta (no neutrino heating)

▶ $L_{\nu e} \sim 10^{53}$ erg/s

BH – torus systems

<u>A key ingredient = "viscosity"</u>

EOM : $\partial_t(\rho R^2 \Omega) + \partial_A(\rho R^2 \Omega v_A - \eta R^2 \partial_A \Omega) = 0$ (A=R, z)

ρ =density, Ω =angular velocity, η =dynamical viscosity

⇒ ▶ Angular momentum transfer by the viscous term.

▶ Energy dissipation due to the viscosity

Q. What is the "viscosity" in BH-torus systems ?

A. Magnetohydrodynamical turbulence ;

$q = q_{ave} + \delta q$ s.t. $\langle q \rangle = q_{ave}$ and $\langle \delta q \rangle = 0$ where $\langle \cdot \rangle$ denotes the time average.

EOM : $\partial_t \langle \rho R^2 \Omega \rangle + \partial_A (\langle \rho R^2 \Omega v_A \rangle + \rho R W_{A\phi}) = 0$ (A=R, z)

$W_{A\phi} = \langle \delta v_A \delta v_\phi - B_A B_\phi / 4\pi \rho \rangle$: Reynolds+Maxwell stress

BH – torus systems

Q. What produces the turbulence ?
A. Magnetohydrodynamical instability ; The magnetorotational intability (MRI) is a powerful amplification mechanism (Balbus & Hawley 91) . Unstable for $\nabla \Omega < 0$ and growth rate $\propto \Omega$

Q. Does magnetic field exist in BH-NS binaries ?
A. Yes . The presence of the magnetic fields is one of the most characteristic properties of NSs.

Therefore, it is mandatory to perform BH-magnetized NS merger simulations.

The BH-magnetized NS simulations by Illinois group

(Liu et al. 08, Etienne et al. 12a, 12b, Paschalidis et al 14)

- q=3, M_{NS}/R_{NS}=0.145, χ =0.75
- AMR Algorithm, $\Delta x_{fin} \approx$260m, $L_{fin} \approx$ 20km

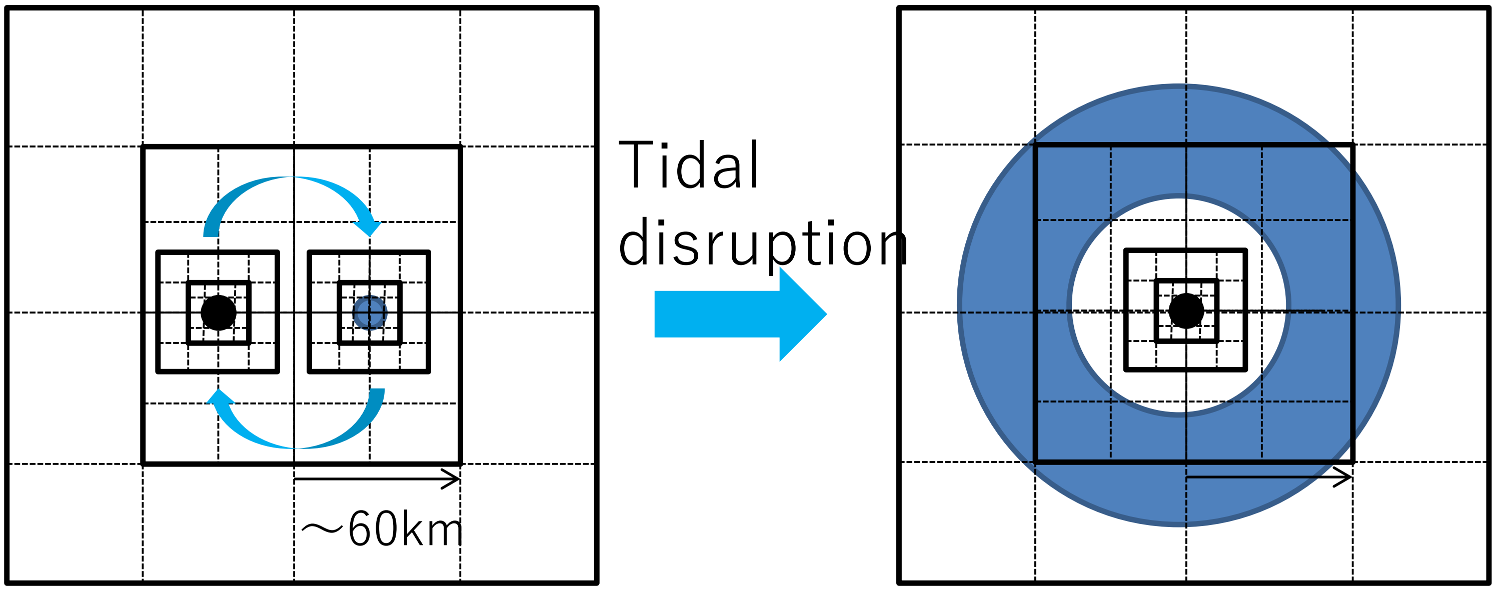

The BH-magnetized NS simulations by Illinois group

(Liu et al. 08, Etienne et al. 12a, 12b, Paschalidis et al 14)

Magnetic field evolution

Unit(Vertical axis) 9.3×10^{53}erg, (Horizontal) 26 μs

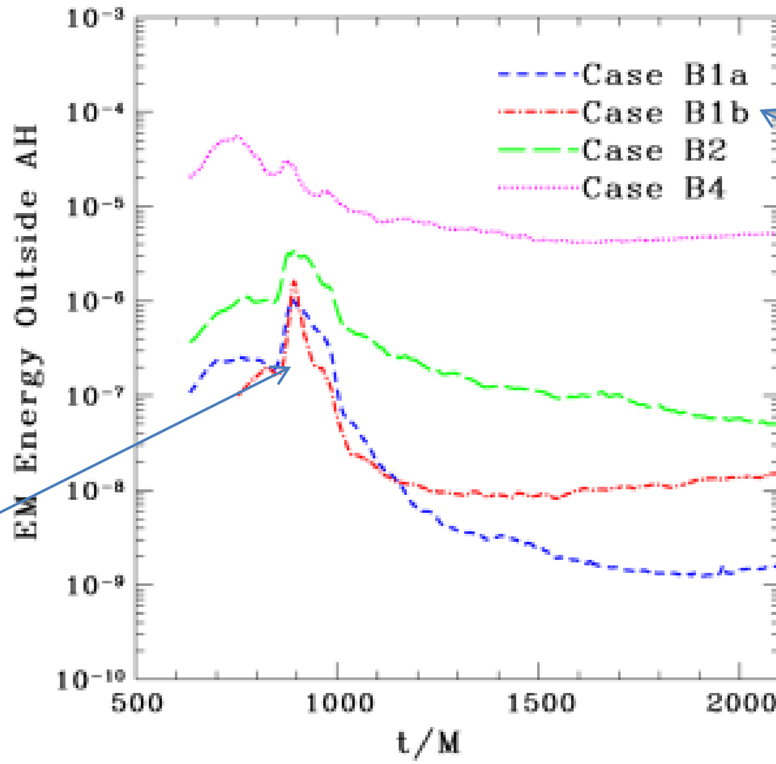

Tidal disruption

Different initial B strengt
and/or configuration

- ▶ No magnetic field amplification inside the torus
- ▶ No discussion on the outflow except Paschalidis et al. 14

Difficulty in MHD simulation

▶ A short wavelength mode has a high growth rate
▶ Turbulence is killed by a numerical viscosity.
Mandatory to do an in-depth resolution study, which is lacking in a bunch of the simulations .

▶ Δx = 120m, $N=1024^3$ (K ; 32,768 cores)
▶ Δx = 160m, $N=756^3$ (XC30 ; 4,096 cores)
▶ Δx = 202m, $N=614^3$ (XC30 ; 4,096 cores)
▶ Δx = 270m, $N=464^3$ (FX10 ; 3,456 cores)
c.f. highest-res. in BH-magnetized NS simulation is
$\Delta x \approx 260$m, $N = 140^3$

<u>Fiducial model</u>

▶ EOS : APR4 ($M_{max} \approx 2.2 M_\odot$), $M_{NS} = 1.35\ M_\odot$
▶ M_{BH}/M_{NS} : 4
▶ BH spin : 0.75
▶ B_{max} : 10^{15}G

Outline of numerical relativity-MHD code (Kiuchi et al. 12, 14)

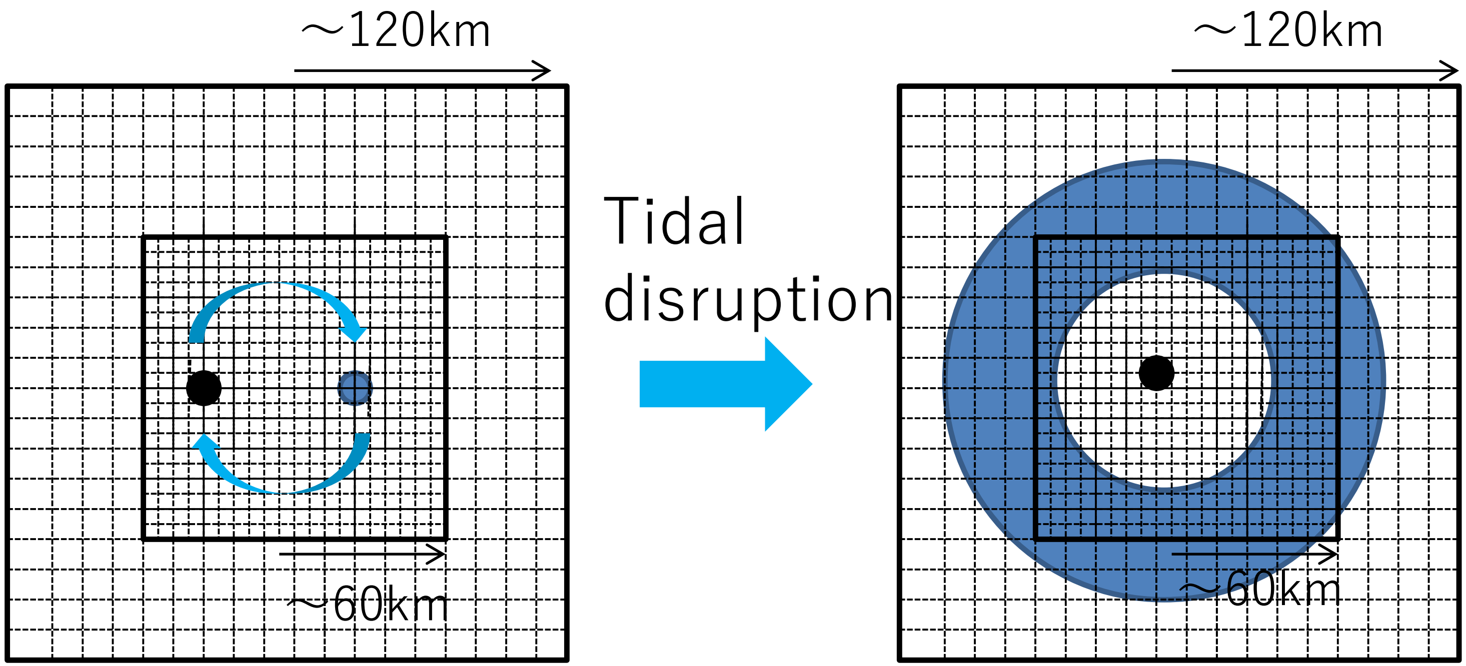

▶With the FMR algorithm, the accretion torus is covered by finer grid points than those used in the AMR algorithm.

▶ But, the computational cost is much higher than the AMR simulations.

Mass ejection

Ejecta mass evolution

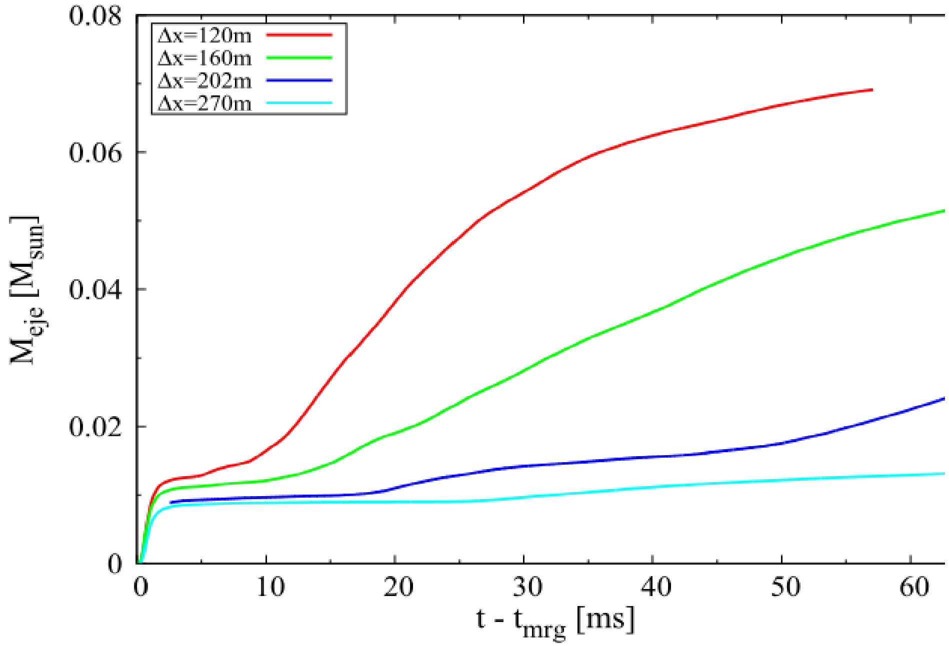

Plasma beta on meridional plane

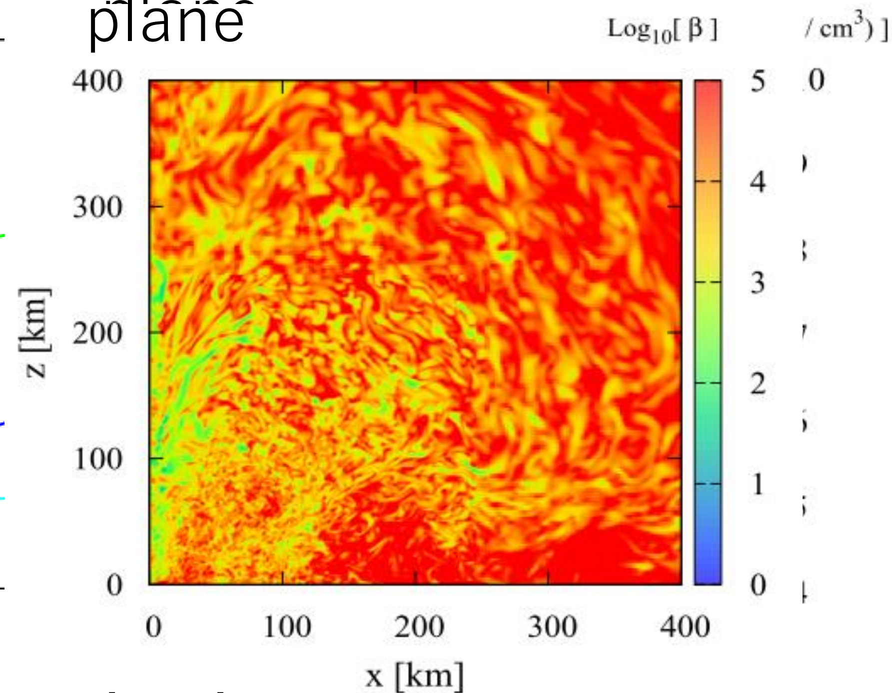

- ▶ t ≲10ms ⇒ Dynamical mass ejection (Kyutoku et al. 15)
- ▶ 10ms ≲ t ⇒ New component : Disk wind
- ▶ Magnetic pressure would not be a main agent
- ▶ The well resolved turbulent eddies are likely to play an important role
- ▶ Linear growth rates are approximately converged; 0.07-0.08 Ω (Non-axisymetric MRI, $\lambda_{\text{MRI, fastest}}/\Delta x \gtrsim 10$)

Energy of the turbulent flow

▶ Energy transport mechanism = MHD turbulent eddies (Reynolds+Maxwell stress)

▶ The higher the resolution is, the larger the amount of the disk wind

<u>Energy spectrum of the turbulent flow</u>

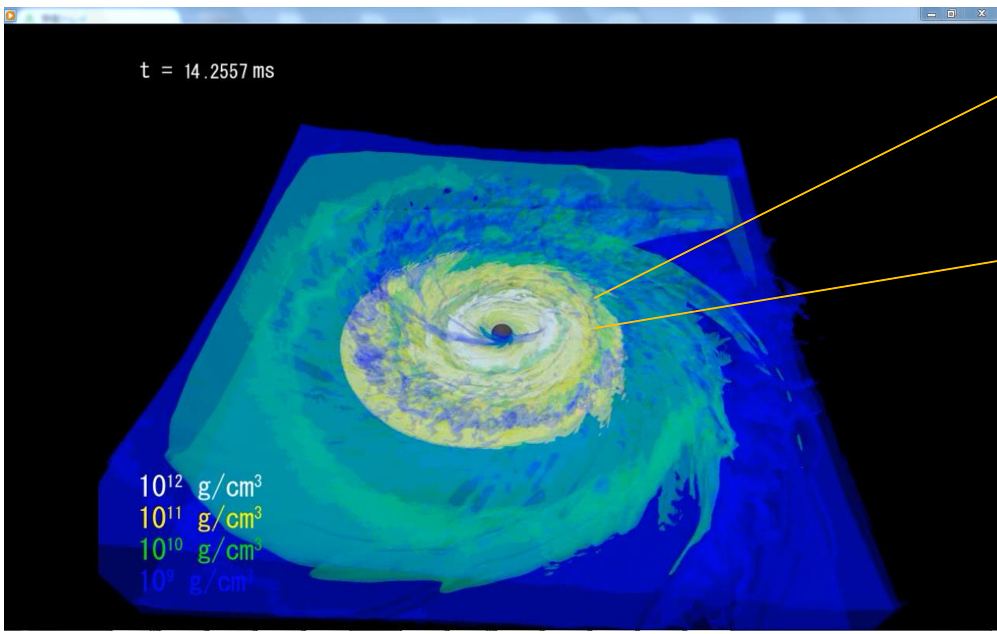

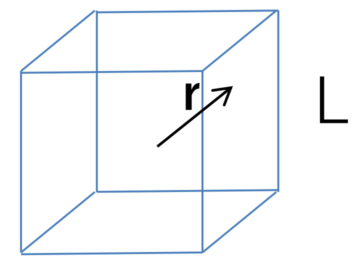

Step 1. Choose a cubic region

Step 2. $\delta v^i = v^i - \langle v^i \rangle$

$\langle\rangle$ Time average

Step 3. $R_{ij}(\mathbf{r}) = \langle \delta v^i(\mathbf{x}+\mathbf{r})\, \delta v^i(\mathbf{x}) \rangle$

Step 4. $\phi_{ij}(\mathbf{k}) = \iiint R_{ij}(\mathbf{r})\, d\mathbf{k}$

Step 5. $E(k) = \iint \phi_{ij}(\mathbf{k})\, d\Omega_k$

$k = |\mathbf{k}|$

Energy spectrum the turbulent flow

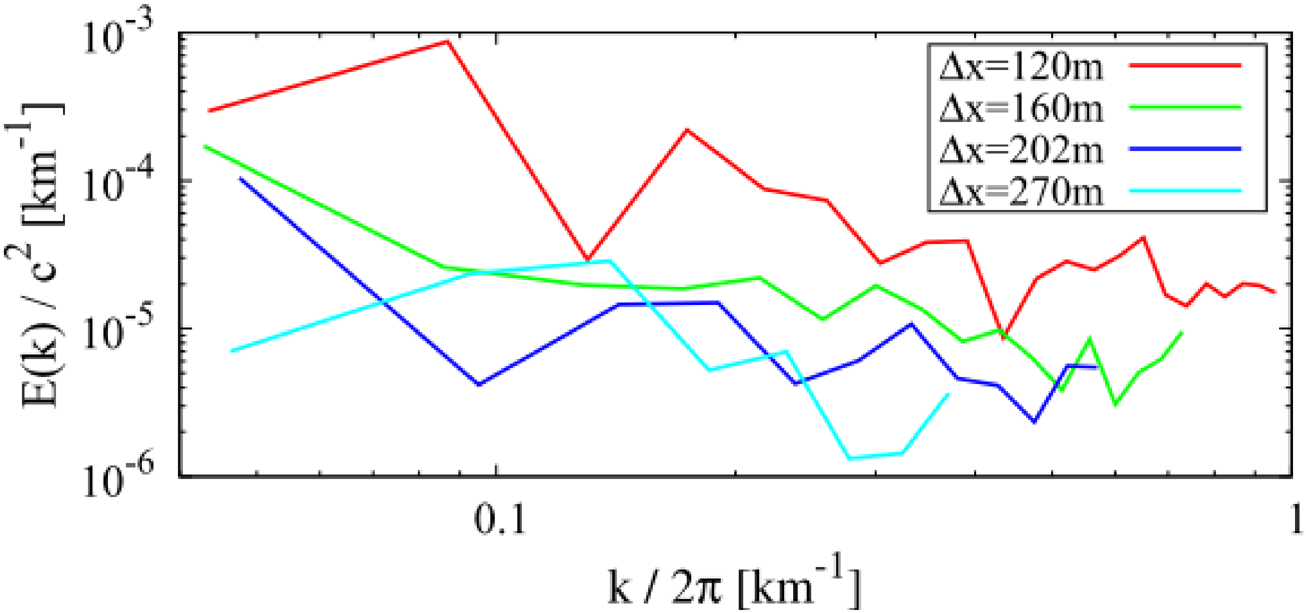

▶x ϵ [50km:70km], y ϵ [-10km:10km], z ϵ [-10km:10km], T=10-20ms

▶The turbulent energy is injected at a smaller scale for the higher resolution run.

▶The amplitude of the spectrum is higher in the higher resolution run ⇒ The turbulent eddies have a larger energy.

Is the energy transferred outward and thermalized ?

Reynolds+Maxwell stress

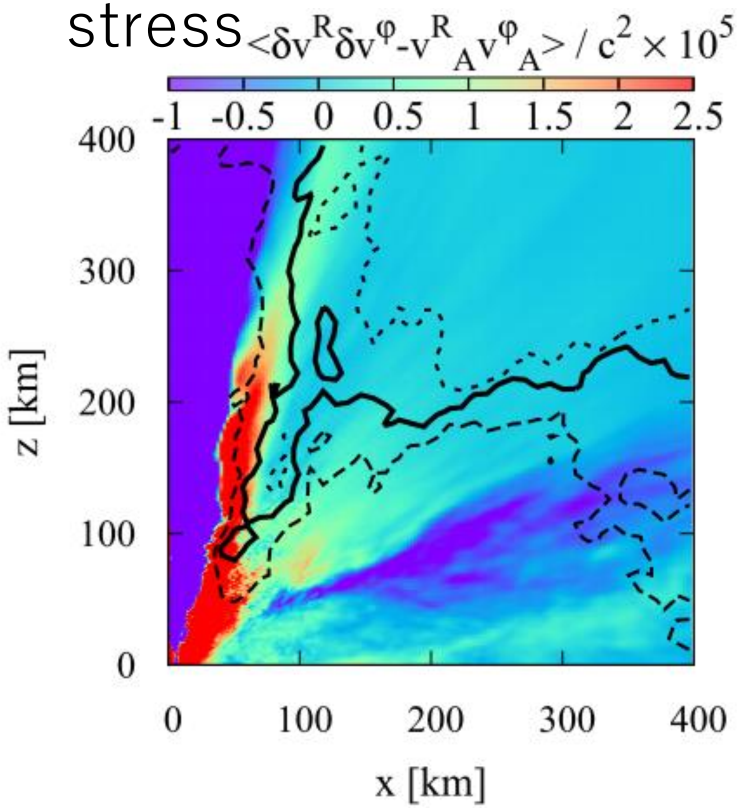

Thermal component of specific internal energy

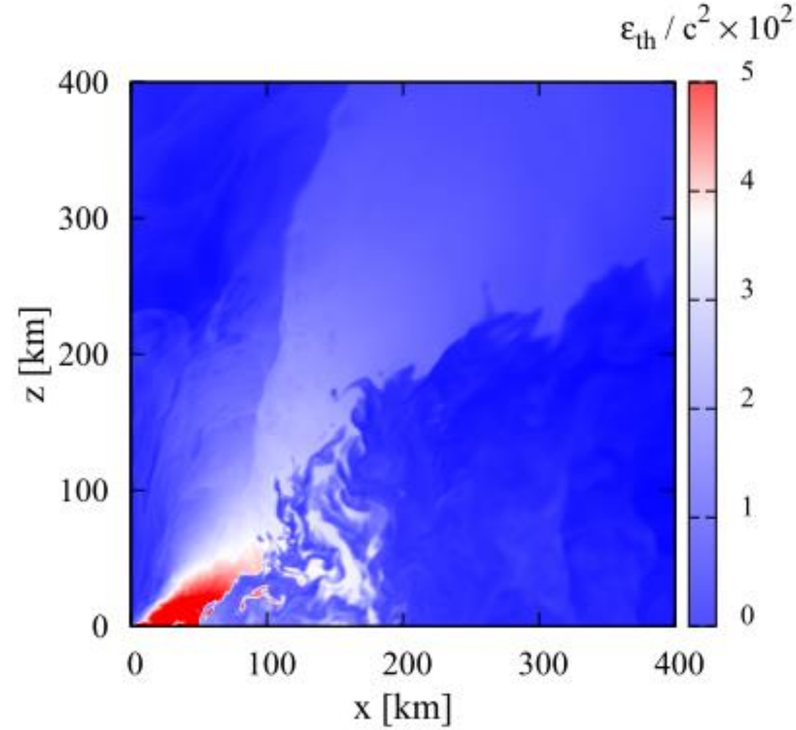

Yes.

▶The energy is transferred outward.

▶Efficient energy conversion to the thermal energy is realized in the vicinity of the inner edge of the torus.

Mechanism of turbulence driven torus wind

▶The realistic high viscosity enhances the mass accretion inside the torus and converts the mass accretion energy to thermal energy efficiently.

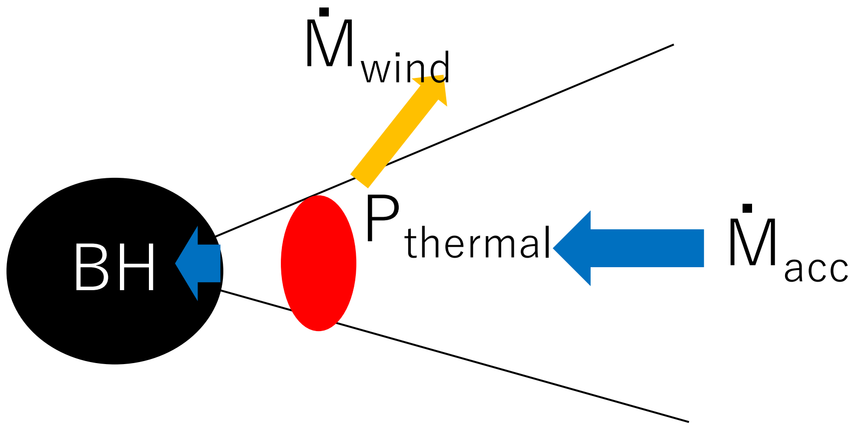

In the absence of the effective turbulent viscosity,

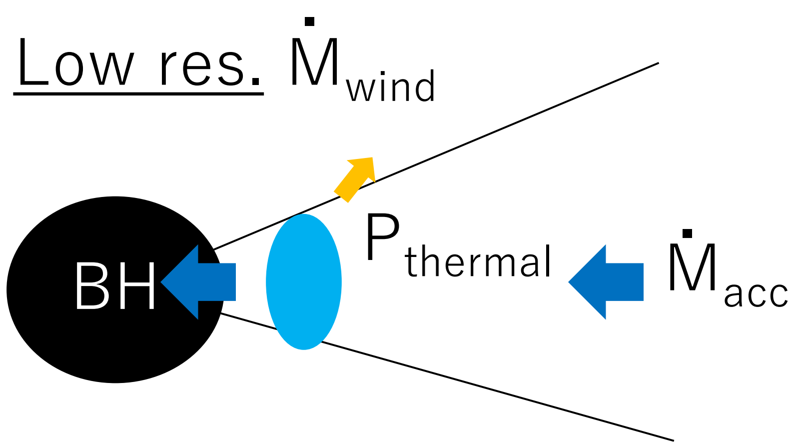

Key ingredients for the disk wind

▶ High spin BH

BH is spun up to $\chi \approx 0.85$-0.9 after the merger

$R_{ISCO}(\chi=0.9) = 2.32M_{BH}$ cf. $R_{ISCO}(\chi=0.0) = 6M_{BH}$

If you consider the "realistic" value of the mass ratio $q \gtrsim 7$, the high spin is necessary for the tidal disruption as well.

▶ Energy source of the wind = Mass accretion energy

▶ Transport agent = Turbulent eddies

▶$\approx$50% of the accretion torus at t = 10ms is ejected as the torus wind

Implication of this new mass ejection (i)

▶ Formation of the low plasma beta region ($\beta \sim 10^{-2}$)
The wind facilitates the poloidal motion ⇒ Coherent poloildal magnetic field

β on the meriodinal plane

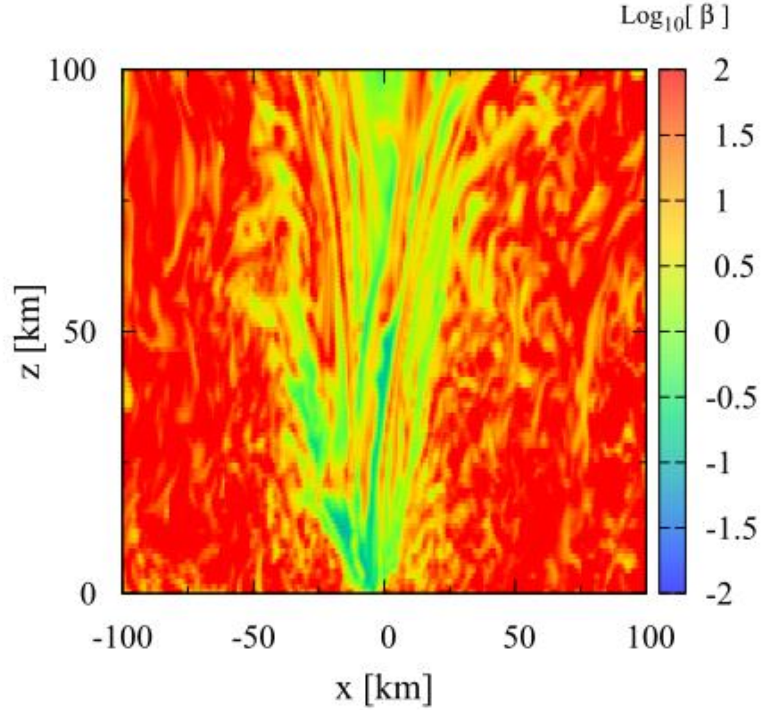

BZ luminosity evolution

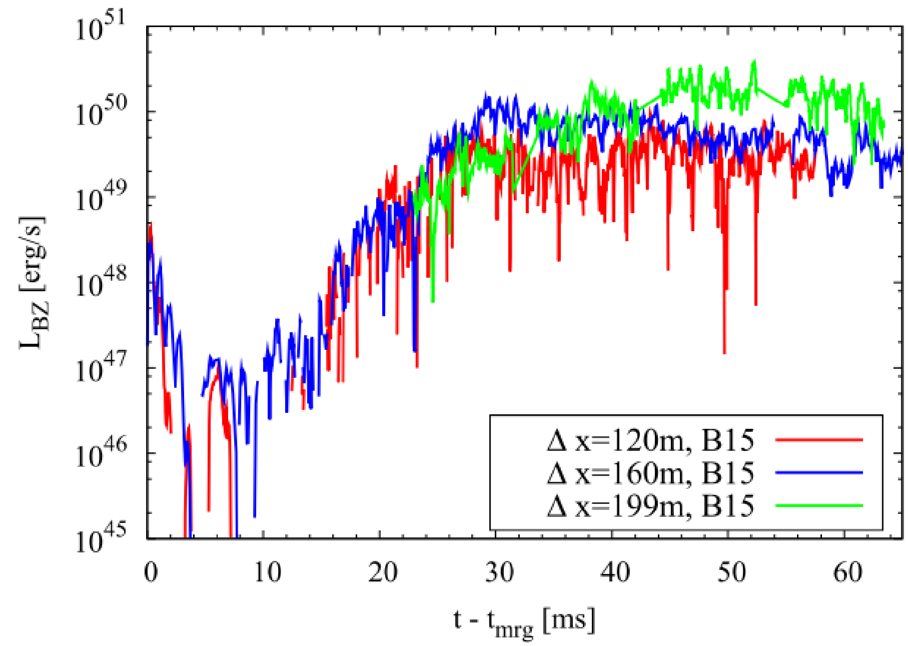

▶ Enhancement of the BZ luminosity (Brandford & Znajek 77)
$L_{BZ} \approx 2 \times 10^{49}$ erg/s ⇒ Central engine candidate of the SGRBs with low luminosity (Lee & Ramirez-Ruiz 07)

Implication of this new mass ejection (ii)

▶ Collimation of the relativistic jet

Dynamical ejecta is concentrated on the orbital plane.

On the other hand, for the NS-NS merger case ⇒ The ejecta expands quasi-spherically. (Hotokezaka et al. 13, Sekiguchi et al. 15)

Jet propagation simulation in the NS-NS ejecta (Nagakura et al. 14)

Z

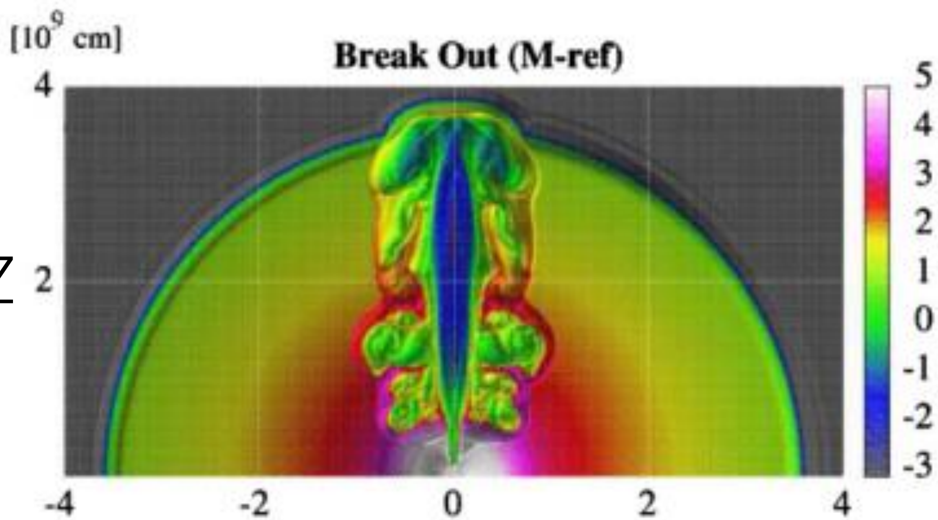

X

Ejecta density

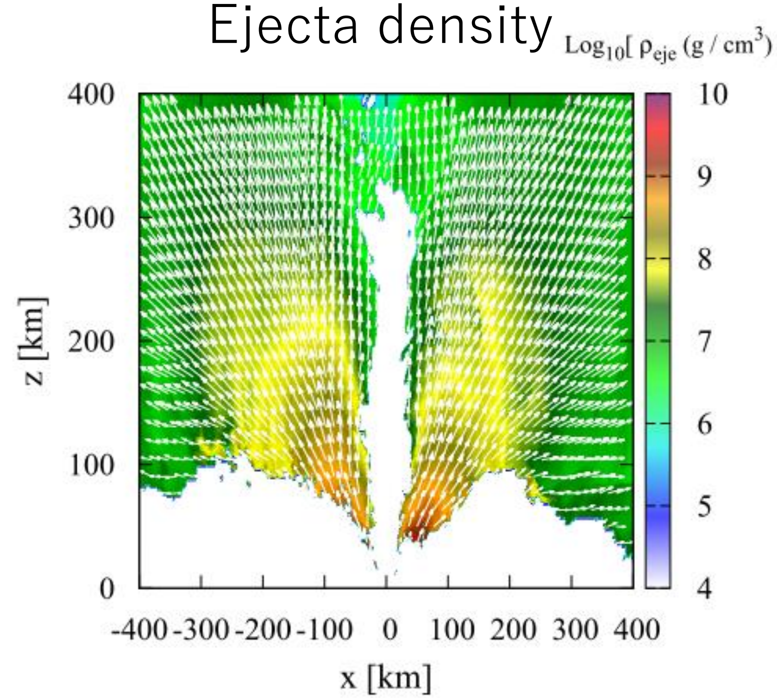

▶Disk wind would help the collimation of the relativistic jet

Implication of this new mass ejection (iii)

▶ Nucleosynthesis in the BH-NS merger

Electron fraction of the dynamical ejecta is ≲ 0.1

⇒ Reproduce the third peak of the solar abundance

On the other hand, for the NS-NS mergers, Ye of the ejecta has a broad distribution. (Sekiguchi et al. 15, Wanajo et al. 14)

Bauwsein et al. 14

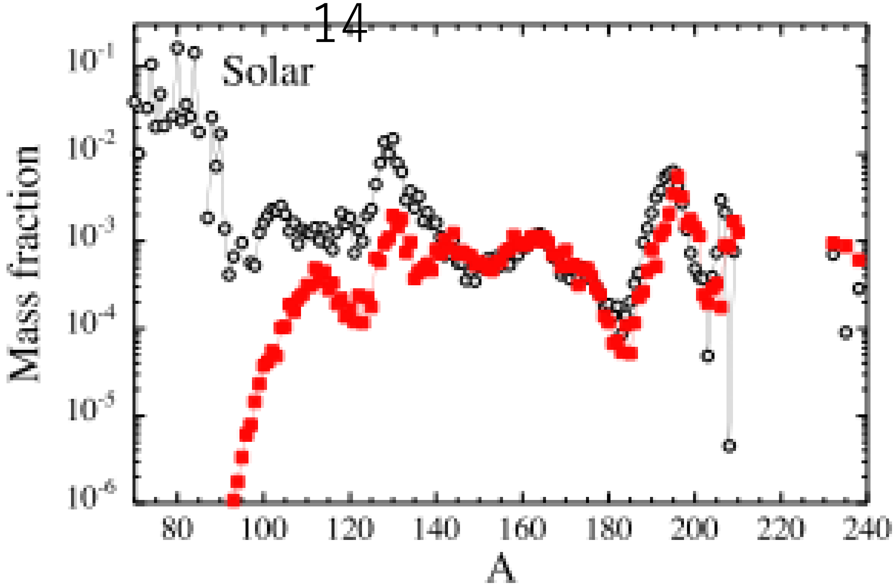

Wanajo et al. 14

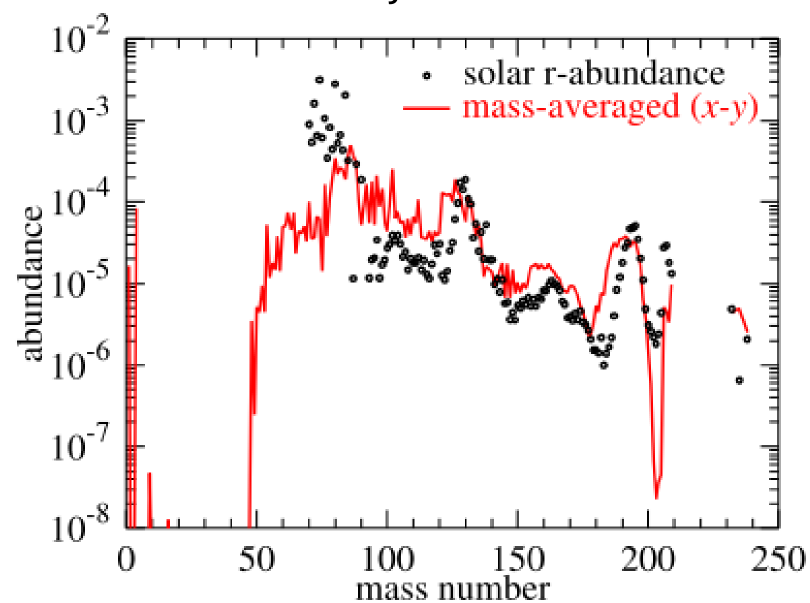

▶Disk wind launches in the vicinity of the torus surface. The fluid elements experience shock heating. ⇒ Different Ye distribution from that for the dynamical component.

Implication of this new mass ejection (iv)

<u>Macronova/kilonova model in the BH-NS merger</u> (Li-Paczynski 98)

▶ Dynamical ejecta$\sim 10^{-6}$-$10^{-1}M_\odot$ (Hotokezaka et al. 13, Kyutoku et al. 15)

▶ Disk wind due to the nuclear recombination/viscous heating (Fernandez & Metzger 13)

$M_{ej} \sim 0.1M_{disk}$ for the viscous timescale (e.g., O(1)s)

▶ Disk wind due to the MHD turbulence

$M_{ej} \sim 0.06M_\odot$ ($\sim 0.5M_{disk}$), but only one point in the parameter spaces

Systematic studies have to be done.

Caveat and summary

▶ Self consistent modeling is important ; if you start from an equilibrium torus and BH, you cannot get a disk wind we found in this study.
▶ Resolution study is essential as well.

NR simulations of the BH-magnetized NS mergers on K.
▶ Disk wind driven by the MHD-turbulence

<u>Implications</u>
▶ Central engine of the SGRBs
▶ The nucleosynthesis of the r-process elements
▶ The radioactively-powered transient emission

High-res. simulation of the tilted BH-NS mergers

▶ Simulation set up

BH – magnetized NS binary merger ; tilted BH spin case

Tilted spin

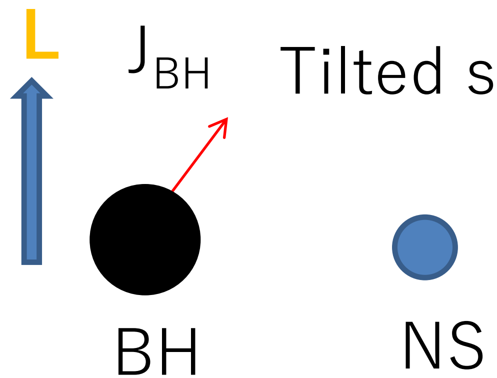

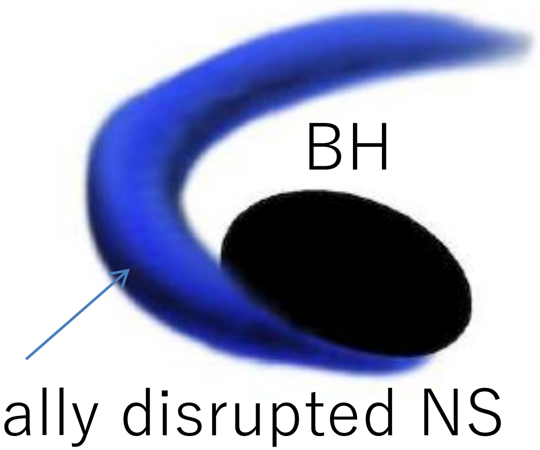

(Foucart+11,12, Kawaguchi et al. 1

▶ Simulation size

Nested grid structure ; N*level=$1{,}118^3$*10, Δx_{fine}=120m

(cf. previous simulation : N*level=100^3*10, Δx_{fine}=150m)

Summary

We are figuring out the realistic picture of BHNS mergers.

▶High-precision GW forms in inspiral and late inspiral phase ⇒ Template bank

▶ Evolution in post merger phase (B-field)
Remnant massive NS is strongly magnetized ⇒ Angular momentum transport due to MRI.

▶ Evolution in post merger phase (Neutrino)
▶ $L_\nu \sim 10^{53}$ erg/s
▶ Could explain the solar abundance of the r-process elements.
▶ Neutrino driven wind ?

Science target of compact binary mergers
Compact binary merger as a candidate of SGRBs central engine (Nakar 07, Berger 13)

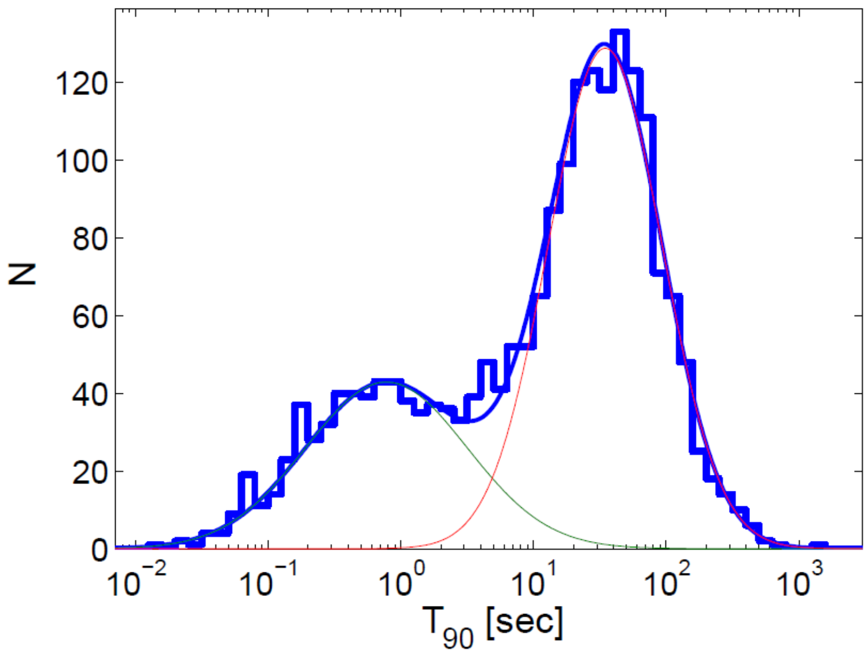

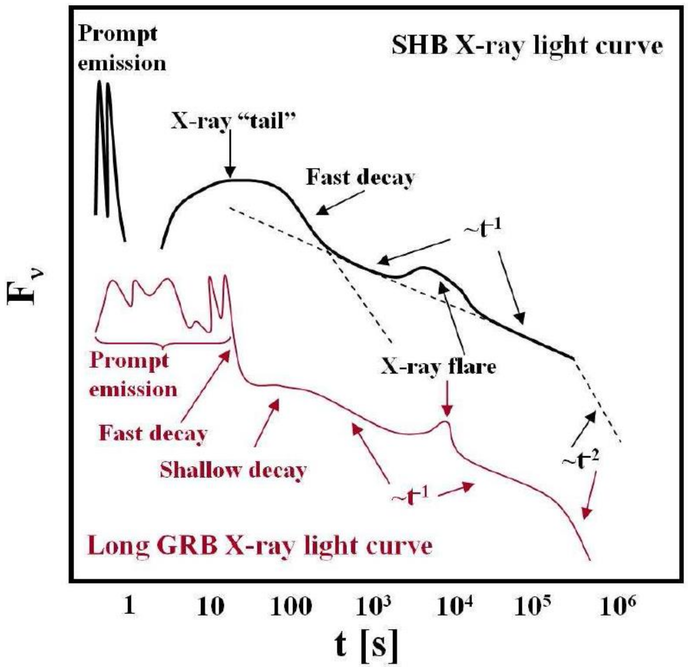

- ▶ Bimodal distribution of T_{90}
- ▶ Prompt emission w/wo Extended emission

Compact binary merger as a candidate of SGRBs central engine (Nakar 07, Berger 13)

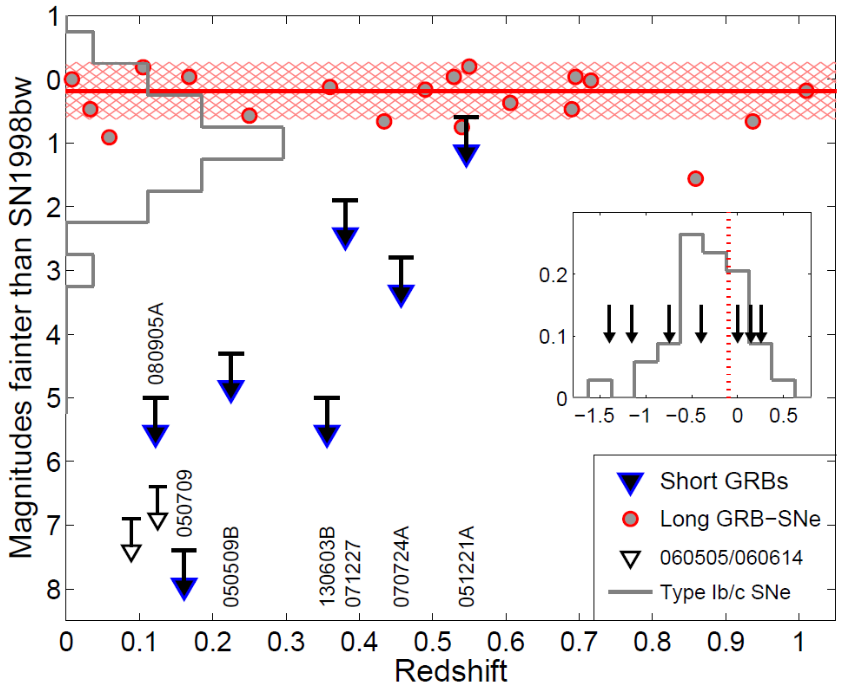

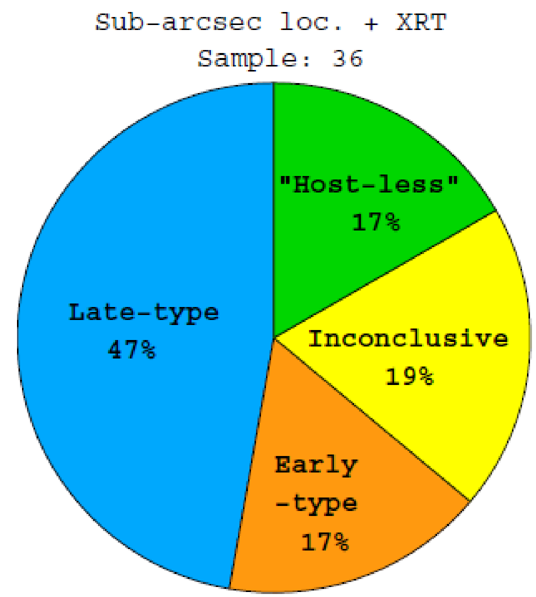

▶ Lack of SN associations ⇔ LGRB-SN associations

▶ Host galaxy type = A mix of Elliptical and Spirals

⇔ Star forming galaxy (LGRB)

⇒ Progenitors belong to older stellar population.

Compact binary merger as a candidate of SGRBs central engine (Nakar 07, Berger 13)

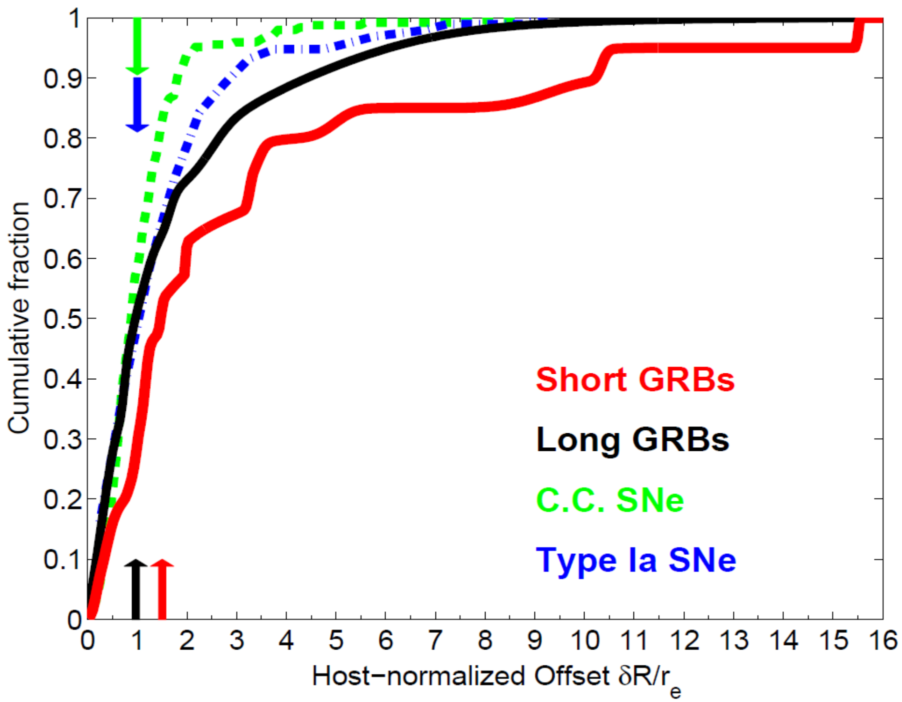

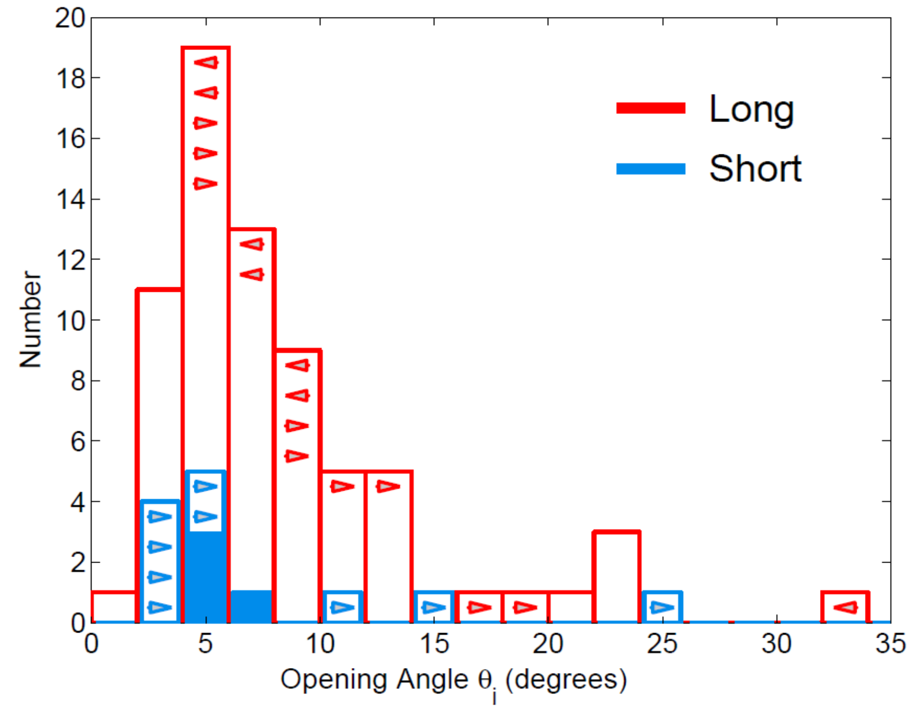

▶ Locations of SGRBs have an offset relative to the host centers. ⇒ Progenitors may have a kick.

▶ Beaming-corrected event rate density ⇒ 270^{+1580}_{-180} $\mathrm{Gpc}^{-3}\ \mathrm{yr}^{-1}$ ⇒ Consistent with BNS merger rate density

Compact binary merger may drive SGRBs